ISSN 2782-2192 (Print)
ISSN 2782-2206 (Online)

Journal of Advanced Materials and Technologies

J·A·M·T

Vol. 9, No. 2.
2024

TSTU Publishing

ISSN 2782-2192 (Print)
ISSN 2782-2206 (Online)
DOI: 10.17277/issn.2782-2192

Journal of Advanced Materials and Technologies

Vol. 9, No. 2.
2024

Том 9, № 2
2024

16+

Journal of Advanced Materials and Technologies

Scientific Journal

"Journal of Advanced Materials and Technologies" is a peer-reviewed scientific journal of research in materials science and related issues in materials physics and mechanics.

"Journal of Advanced Materials and Technologies" publishes original articles, reviews, short reports written by both renowned scientists and young researchers that contribute to the development of modern materials science.

The journal promotes research and exchange of information in the field of theoretical and practical research into materials science, modeling of processes involved in the creation of new materials, including nanomaterials, their properties and application.

The journal papers and metadata are available at Chemical Abstracts, CAS (American Chemical Society), Google Scholar, WorldCat, ROAR (Registry of Open Access Repositories), OpenAIRE (OpenAIRE - Open Access Infrastructure for Research in Europe), BASE (Bielefeld Academic Search Engine), RePEc: Research Papers in Economics, EBSCO.

ISSN 2782-2192 (Print), ISSN 2782-2206 (Online)

Rename information	Advanced materials & technologies (2016-2021) Print ISSN 2414-4606, Online ISSN 2541-8513
The journal was founded	2016
Publication frequency	Quarterly
Founders	Tambov State Technical University (TSTU), Merzhanov Institute of Structural Macrokinetics and Materials Sciences of Russian Academy of Sciences (ISMAN)
Postal address	TSTU: Bld. 2, 106/5, Sovetskaya St., Tambov, 392000 ISMAN: 8, Academician Osipyan St., Moscow region, Chernogolovka, 142432
Editorial office address	Bld. 2, 106/5, Sovetskaya St., Tambov, 392000
Contacts	Phone + 7 4752 63 03 91; amt.journal@yandex.ru
Printing House	TSTU Publishing, 112A, Michurinskaya St., Tambov, 392032 Phone + 7 4752 63 03 91; + 7 4752 63 07 46
Website ***E-mail*** ***Phone***	http://amt.tstu.ru/ amt.journal@yandex.ru +7 4752 63 92 93
Subscription	The electronic version of the Journal is freely available on the journal's website, as well as in open access databases. The subscription index for the Journal printed version in the unified catalog "Press of Russia" is 80453
Editor-in-Chief	Mikhail I. Alymov, D. Sc. (Engineering), Professor, Corresponding Member of the Russian Academy of Sciences

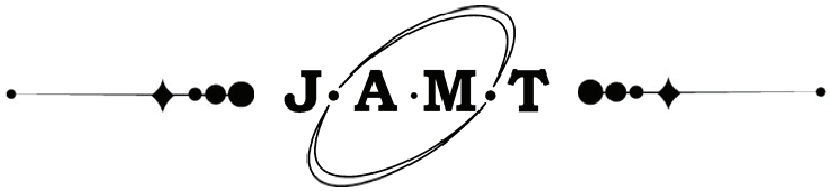

Journal of Advanced Materials and Technologies

Научный журнал

«Journal of Advanced Materials and Technologies» – научный рецензируемый журнал, посвященный исследованиям в области материаловедения и примыкающих вопросов физики и механики материалов.

Журнал «Journal of Advanced Materials and Technologies» публикует оригинальные статьи, обзоры, краткие сообщения, содействующие развитию современной науки о материалах, подготовленные как известными учеными, так и молодыми специалистами.

Миссия журнала – обмен актуальной научной информацией в области теоретических и практических исследований и моделирования процессов, связанных с получением, определением свойств новых материалов, в том числе наноразмерных, и их применения.

Средство массовой информации периодическое печатное издание, журнал «Journal of Advanced Materials and Technologies» зарегистрировано Федеральной службой по надзору в сфере связи, информационных технологий и массовых коммуникаций. Регистрационный номер СМИ ПИ № ФС 77-74804 от 25.01.2019.

Журнал входит в перечень рецензируемых научных изданий (перечень ВАК Минобрнауки РФ) от 16 декабря 2021 г. по научным специальностям: 1.4.15 – Химия твердого тела; 2.6.6 – Нанотехнологии и наноматериалы; 2.6.13 – Процессы и аппараты химических технологий; 2.6.17 – Материаловедение.

Материалы журнала размещены в РИНЦ, Chemical Abstracts, CAS (American Chemical Society), Академия Google (Google Scholar), WorldCat, СОЦИОНЕТ, ROAR (Registry of Open Access Repositories), OpenAIRE (OpenAIRE - Open Access Infrastructure for Research in Europe), BASE (Bielefeld Academic Search Engine), RePEc: Research Papers in Economics, EBSCO.

ISSN 2782-2192 (Print), ISSN 2782-2206 (Online)

Сведения о переименовании	«Advanced materials & technologies» (2016–2021) Print ISSN 2414-4606, Online ISSN 2541-8513
Журнал основан	2016 г.
Периодичность	4 раза в год
Учредители	Федеральное государственное бюджетное образовательное учреждение высшего образования «Тамбовский государственный технический университет» (ФГБОУ ВО «ТГТУ»), Федеральное государственное бюджетное учреждение науки Институт структурной макрокинетики и проблем материаловедения им. А. Г. Мержанова Российской академии наук (ИСМАН)
Адреса учредителей	ФГБОУ ВО «ТГТУ»: 392000, Тамбовская область, г.о. город Тамбов, г. Тамбов, ул. Советская, д. 106/5, помещ. 2, ИСМАН: 142432, Московская область, г. Черноголовка, ул. Академика Осипьяна, д. 8
Адрес издателя	ФГБОУ ВО «ТГТУ»: 392000, Тамбовская область, г.о. город Тамбов, г. Тамбов, ул. Советская, д. 106/5, помещ. 2
Адрес редакции ***Контакты***	392000, Тамбовская область, г.о. город Тамбов, г. Тамбов, ул. Советская, д. 106/5, помещ. 2 Тел.: + 7 4752 63 03 91; amt.journal@yandex.ru
Адрес типографии	392032, Тамбовская обл., г. Тамбов, ул. Мичуринская, д. 112А Тел.: + 7 4752 63 03 91; + 7 4752 63 07 46
Сайт	http://amt.tstu.ru/
E-mail	amt.journal@yandex.ru
Телефон	+7 4752 63 92 93
Подписка	Подписку на печатную версию журнала можно оформить по объединенному каталогу «Пресса России». Подписной индекс – 80453
Главный редактор	Алымов Михаил Иванович, д. т. н., профессор, член-корреспондент РАН

EDITORS

СОВЕТ РЕДАКТОРОВ

CONTENTS

Original papers

Nanostructured, nanoscale materials and nanodevices

Advanced structural materials, materials for extreme conditions

Materials for energy and environment, next-generation photovoltaics, and green technologies

Reviews

Nanostructured, nanoscale materials and nanodevices

СОДЕРЖАНИЕ

Оригинальные статьи

Наноструктурированные, наномасштабные материалы и наноустройства

Передовые конструкционные материалы, материалы для экстремальных условий

Материалы для энергетики и окружающей среды, фотоэлектрическая энергия следующего поколения и зеленые технологии

Обзор

Наноструктурированные, наномасштабные материалы и наноустройства

Original papers
Nanostructured, nanoscale materials and nanodevices

УДК 546.26-162 DOI: 10.17277/jamt.2024.02.pp.084-090

Estimation of graphene layers number and defectiveness of few-layered graphene particles by Raman spectroscopy

© Nataliya N. Goncharova[a], Vladimir M. Samoilov[a]✉, Viktoriya A. Elchaninova[a], Anastasiya V. Nakhodnova[a], Egor A. Danilov[a], Konstantin A. Tarasov[a]

[a] *NIIgraphite – Research and Development Institute of Graphite-Based Structural Materials, 2, Electrodnaya St., Moscow, 111524, Russian Federation*

✉ VMSamoylov@rosatom.ru

Abstract: The purpose of the present work is to develop methods for assessing the quality of aqueous suspensions of few-layered graphenes using Raman spectroscopy technique. Aqueous suspensions of few-layered graphene particles were manufactured by direct exfoliation of natural graphite under with ultrasound in the presence of surfactants. An experimental assessment of the effectiveness of different methods of Raman spectroscopy data analysis in order to determine the average number of graphene layers and the defectiveness of few-layered graphene particles was carried out. It is concluded that it is possible to determine the average number of graphene layers in aqueous suspensions of few-layer graphene particles based on the ratio of integral intensities and the position of the *G* and 2*D* peaks. Additionally, it is proposed to use the ratio of the peaks of the integrated intensities of peaks *D* and *G* as a parameter characterizing the defectiveness of particles of few-layered graphenes. Examples are given of using this approach to assess the quality of graphene samples obtained using various technologies via averaged distribution functions of the number of layers in particles and the I_D/I_G ratio. It was shown that samples with minimal amount of layers had minimal particle size and high defectivity, while samples with higher number of layers had larger particle size with low defectivity.

Keywords: graphene; graphene suspensions; few-layered graphene; Raman spectroscopy; colloidal solutions; graphene structure.

For citation: Goncharova NN, Samoilov VM, Elchaninova VA, Nakhodnova AV, Danilov EA, Tarasov KA. Estimation of graphene layers number and defectiveness of few-layered graphene particle by Raman spectroscopy. *Journal of Advanced Materials and Technologies*. 2024;9(2):084-090. DOI: 10.17277/jamt.2024.02.pp.084-090

Определение количества графеновых слоев и дефектности частиц малослойных графенов методом рамановской спектроскопии

© Н. Н. Гончарова[a], В. М. Самойлов[a]✉, В. А. Ельчанинова[a], А. В. Находнова[a], Е. А. Данилов[a], К. А. Тарасов[a]

[a] *Научно-исследовательский институт конструкционных материалов на основе графита «НИИграфит», ул. Электродная, 2, Москва, 111524, Российская Федерация*

✉ VMSamoylov@rosatom.ru

Аннотация: Цель работы – разработка способов оценки качества водных суспензий малослойных графенов с применением метода рамановской спектроскопии. Водные суспензии частиц малослойных графенов получены путем прямой эксфолиации природного графита под воздействием ультразвука в присутствии поверхностно-активных веществ. Проведена экспериментальная оценка эффективности некоторых методик анализа данных рамановской спектроскопии для определения среднего количества слоев графена и дефектности частиц малослойных графенов. Сделан вывод о возможности определения среднего количества слоев графена в водных суспензиях частиц малослойных графенов по соотношению интегральных интенсивностей и положению пиков *G* и 2*D*. Дополнительно предложено использовать параметр соотношения интегральных интенсивностей пиков *D* и *G* в качестве параметра, характеризующего дефектность частиц малослойных графенов. Приведены примеры использования данного подхода для оценки качества графеновых препаратов, полученных по различным технологиям с использованием усредненных функций распределения количества слоев в частицах и соотношения

I_D/I_G. Показано, что препараты с минимальным количеством слоев имели минимальный размер частиц и высокую дефектность, в то время как препараты с более высоким количеством слоев – больший размер частиц при низкой дефектности.

Ключевые слова: графен; графеновые суспензии; малослойный графен; рамановская спектроскопия; коллоидные растворы; структура графена.

Для цитирования: Goncharova NN, Samoilov VM, Elchaninova VA, Nakhodnova AV, Danilov EA, Tarasov KA. Estimation of graphene layers number and defectiveness of few-layered graphene particle by Raman spectroscopy. *Journal of Advanced Materials and Technologies*. 2024;9(2):084-090. DOI: 10.17277/jamt.2024.02.pp.084-090

1. Introduction

50 years ago, the British researchers Tuinstra and Koenig first linked the parameters of Raman spectroscopy of soot and pyrocarbon with the diameter of crystallites [1], as determined by X-ray diffraction. This marked the beginning of the development of Raman spectroscopy as a structure-sensitive method in relation to all classes of carbon materials without exception. Among the "pioneers" one cannot fail to mention the Brazilian researcher Luis Conchado, who established the relationship between the parameters of Raman spectroscopy and the parameters of the crystal structure of graphite-like materials determined by X-ray phase analysis [2].

Back in the 2000s, European scientists undertook extensive research into a wide variety of classes of carbon materials. In the studies by Ferrari and his coworkers, the data from [1, 2] were confirmed and refined, and the possibility of determining not only the size of crystallites, but also the concentration of defects in graphene layers was established [3, 4]. Raman spectroscopy has become one of the main methods for identifying graphene [3–11], and a recognized method for studying carbon nanostructures such as fullerenes [12, 13] and carbon nanotubes [14, 15].

However, the main advantage of Raman spectroscopy remains the possibility of non-destructive testing of two-dimensional nanomaterials and in particular graphenes, while intensive research is aimed at finding ways to use Raman spectroscopy for quality control of ready-to-use structures [3–10].

The most important figure of merit for the quality of graphene structures, in addition to defectiveness, is the number of graphene layers. The aim of this study was to develop methods for estimating the number of layers in particles of few-layer graphenes using Raman spectroscopy.

2. Materials and Methods

2.1. Materials preparation

In order to develop a technique for determining the number of layers in particles of few-layer graphenes and studying them, liquid-phase exfoliated samples were used. The initial raw material was natural graphite of the GSM-2 or GE-2 grades, which had previously undergone gas-thermal refining in a Freon atmosphere at a temperature of 2000 °C and processing on a cup vibrating grinder for 30–240 min. An aqueous suspension was prepared from a sample of natural graphite (300 mg), distilled water (50 mL) and a surfactant (polyglycidyl ether 1H,1H,11H-eicosofluoro-1-undecanol with a gross formula of $C_{26}H_{34}O_{11}F_{20}$) (30 mg).

The resulting suspension in a container was treated with ultrasound with a submersible (horn-type) concentrator on a MELFIZ MEF 391 installation with a frequency of 22.5 kHz and an acoustic power of 200 W for 6 hours.

After removing the container from the ultrasonic unit, a sample (at least 0.1 mL) was taken and placed in liquid form on a single-crystalline silicon wafer, then dried with hot air and submitted for Raman assessment (series 1). Series 2 was obtained in a similar way, with a sonication time of 4 hours.

Series 3 and 4 of suspension samples of few-layered graphenes were obtained using a similar method, however, before ultrasonic treatment, the samples were crushed on a roller vibrating grinder with a predominant abrasion-crushing action for 30 minutes (series 3) and 2 hours (series 4).

Samples of series 5 and 6, provided by GoldKG, Bishkek (Kyrgyzstan), were obtained by circulating a water-alcohol graphite-containing suspension in a disintegrator with a rotor diameter of 200 mm, at different speeds and process durations.

2.2. Raman spectroscopy

Raman spectroscopy is based on inelastic scattering of photons. Light scattering occurs when an electromagnetic wave interacts as it passes through a crystal lattice. When a light wave interacts with the surface of a material, the vast majority of photons (> 99.999 %) are elastically scattered without changing wavelength (Rayleigh scattering), but a small fraction of photons (< 0.001 %) undergo

inelastic (Raman) scattering with respective change in energy and wavelength photons. The resulting photon spectrum is passed through a filter that separates the inelastically scattered photons. Said scattered photons are amplified and directed to a detector, which records their frequency change with respect to incident photons (Raman shift) [16].

A Renishaw inVia Reflex confocal Raman microspectrometer was used to study samples of aqueous graphene suspensions. Suspensions were applied onto a silicon wafer substrate with 300 nm thermal oxide layer. The microspectrometer is equipped with an optical microscope and a cooled CCD detector. The laser radiation power did not exceed 1 mW, and the laser spot had a diameter of approximately 0.55 μm.

3. Results and Discussion

Figure 1 shows optical microphotographs and Raman spectra of the studied samples of suspensions of few-layered graphenes. It is obvious that the applied coatings were very heterogeneous in their particle size distributions (see Figs. 1*a*–*e*). The Raman spectra of few-layered graphene samples contained three main lines: *D*, *G* and 2*D* (see Figs. 1*f*–*l*). In addition, the intense line (1000 cm^{-1}) inherent to silicon was clearly visible in the spectra. The intensity of this line varied, decreasing as the amount of graphene in the applied coating increased. In this case (see Figs. 1*f*–*l*), it is obvious that the high variation of the line intensity (1000 cm^{-1}) indicated the inhomogeneity of the applied coating.

As a rule, two characteristic bands are observed in graphene, like many other carbon materials, in the first-order Raman spectrum (1000–2000 cm^{-1}) (see Fig. 1). One of them is the Raman-allowed band at 1580 cm^{-1}, corresponding to the ideal graphite vibrational mode with E_{2g} symmetry, often referred to as the *G*-mode or *G* band, which is determined by the vibrations of carbon atoms in the plane of the "graphene" layers and is associated with carbon atoms in the state of sp^2 hybridization [2–4]. Another active Raman band at 1360 cm^{-1} is induced by disordered carbon atoms, corresponds to lattice vibrations with A_{1g} symmetry, and is called the *D*-mode. Band *D* is associated with carbon atoms also in the state of both sp^2 and sp^3 hybridization, localized in the area of defects and the periphery of "graphene" layers [2–8]. The *D* band may be absent in highly perfect graphites: single-crystalline graphite, highly oriented samples of pyrolytic graphite (HOPG), some samples of natural graphite, and an increase in its intensity is considered to be the result of an increase in the amount of disordered carbon or peripheral atoms [2–6].

In this regard, discussions continue on the origin of the main second-order spectrum feature, the 2*D* line [4], since it was initially assumed that it is a 2nd order mode with respect to the *D* line. However, recent theoretical research has indicated a different nature of the generation of this line associated with the crystal structure of the material under study, in particular with the influence of graphene layers located under the main layer [3–5].

According to the results of numerous works [2–10], the ratio of the integral intensities of these bands, the I_D/I_G parameter is determined by the average distances between defects in the case of amorphized, in particular irradiated, graphene-like structures, and the sizes of L_a crystallites for natural graphites and various carbon materials after high-temperature processing at the graphitization stage [3–5]. For graphitized materials, the parameters of Raman spectroscopy can be used to determine other parameters of the crystal structure, such as the interlayer distance d_{002} and the height of crystallites L_c [2]. Numerous studies have shown the applicability of Raman spectroscopy for determining the number of graphene layers in various graphene like structures [3–11].

The most sensitive to the number of graphene layers is the I_{2D}/I_G parameter. This parameter that was used in works [4–11] for demonstrating the spectral differences between graphite and graphene. Figure 2 shows experimental data obtained by Holmi [10], who performed more than 2000 measurements on graphene samples (see Fig. 1*a*) obtained by the CVD method, and the calibration dependence for determining the average number of layers, *n*, proposed based on the results of work [10], is as follows (see Fig. 2*b*):

$$n = \sqrt{\frac{b}{(I_{2D}/I_G) - a}},$$

where $b = 1.667$, $a = 0.238$. Subsequently, this dependence was used to determine the number of graphene layers on samples of dried suspensions.

Figure 3 shows the distribution functions by the number of graphene layers for the studied suspensions of few-layered graphenes, calculated using the I_{2D}/I_G ratio.

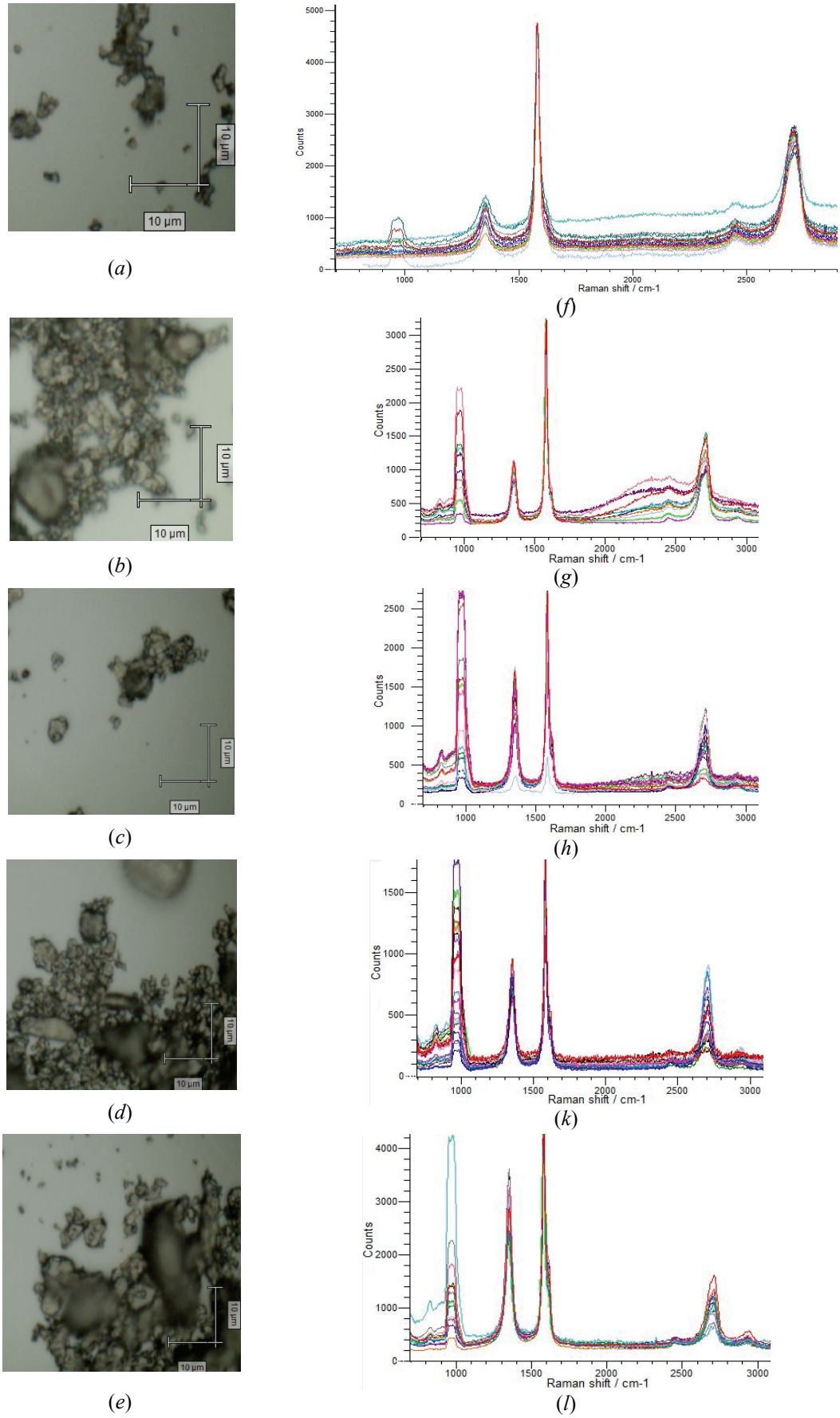

Fig. 1. Optical micrographs (*a–e*) and Raman spectra (*f–l*) of the studied few-layered graphenes suspensions

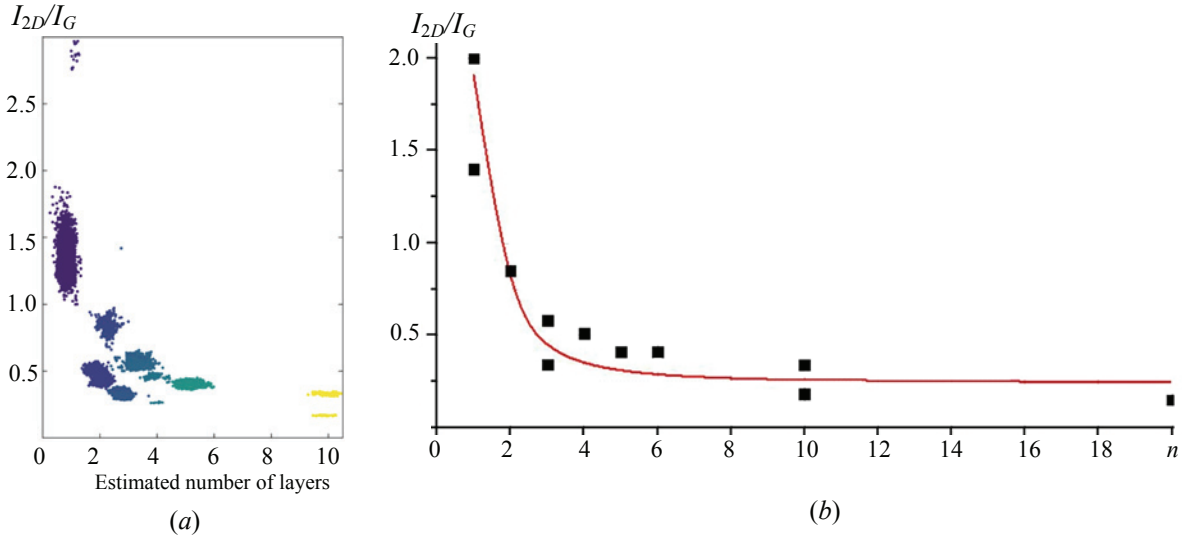

Fig. 2. Experimental data from [10] (*a*) and approximation of the I_{2D}/I_G parameter dependence on graphene layers number of low-layer graphene according to experimental data from [10] (*b*)

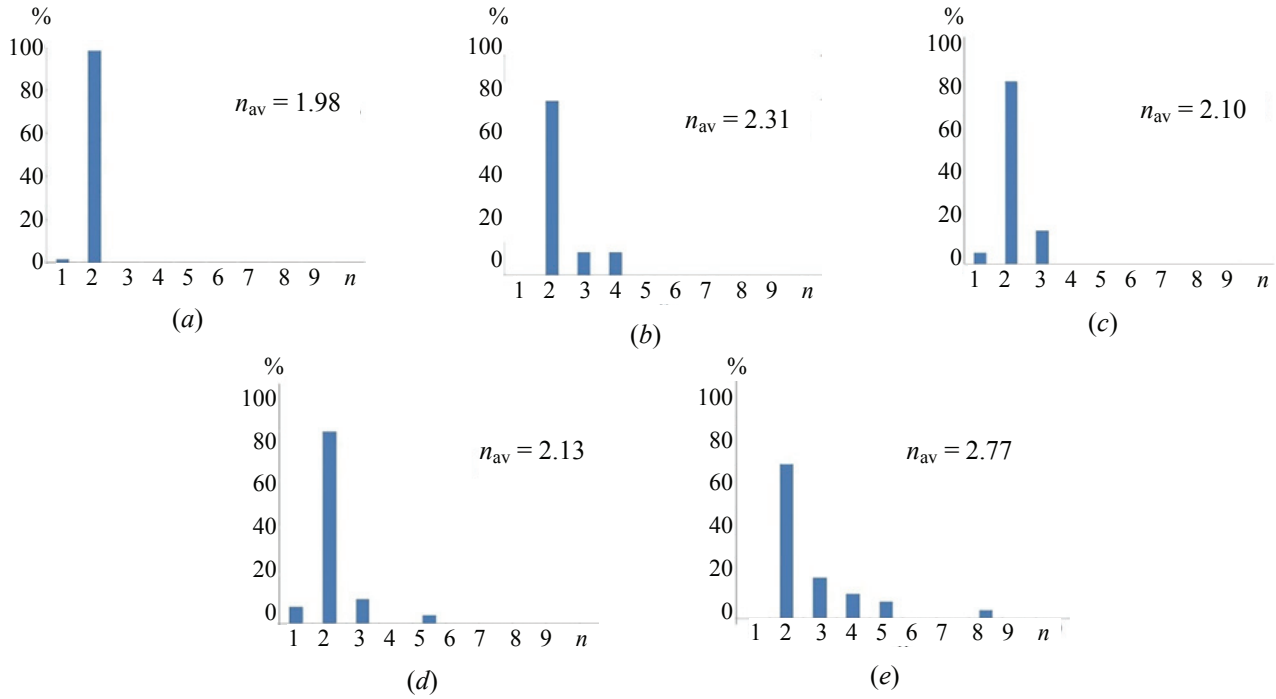

Fig. 3. Distribution functions by the graphene layers number for studied few-layered graphene suspensions calculated using the I_{2D}/I_G parameter

Additionally, the I_D/I_G parameter was used to characterize the quality of suspensions. Since the degree of graphitization of all starting materials – natural graphites – is almost the same, an increase in the intensity of the I_D peak relative to the intensity of the I_G peak shows a change in the degree of defectiveness of the material during the exfoliation process. The results representing the distribution functions of the I_D/I_G parameter for the studied suspensions are presented in Fig. 4.

4. Conclusion

Based on the data obtained, it should be concluded that exfoliation under the effect of ultrasound in the presence of a surfactant makes it possible to obtain suspensions of few-layered graphenes with a minimum number of layers, while the graphene layers have minimal defects. Reducing the ultrasonic treatment time leads to an increase in the average number of layers. The use of preliminary mechanical treatment does not lead to a decrease in the number of layers in the resulting suspensions, but the defectiveness of the layers greatly increases.

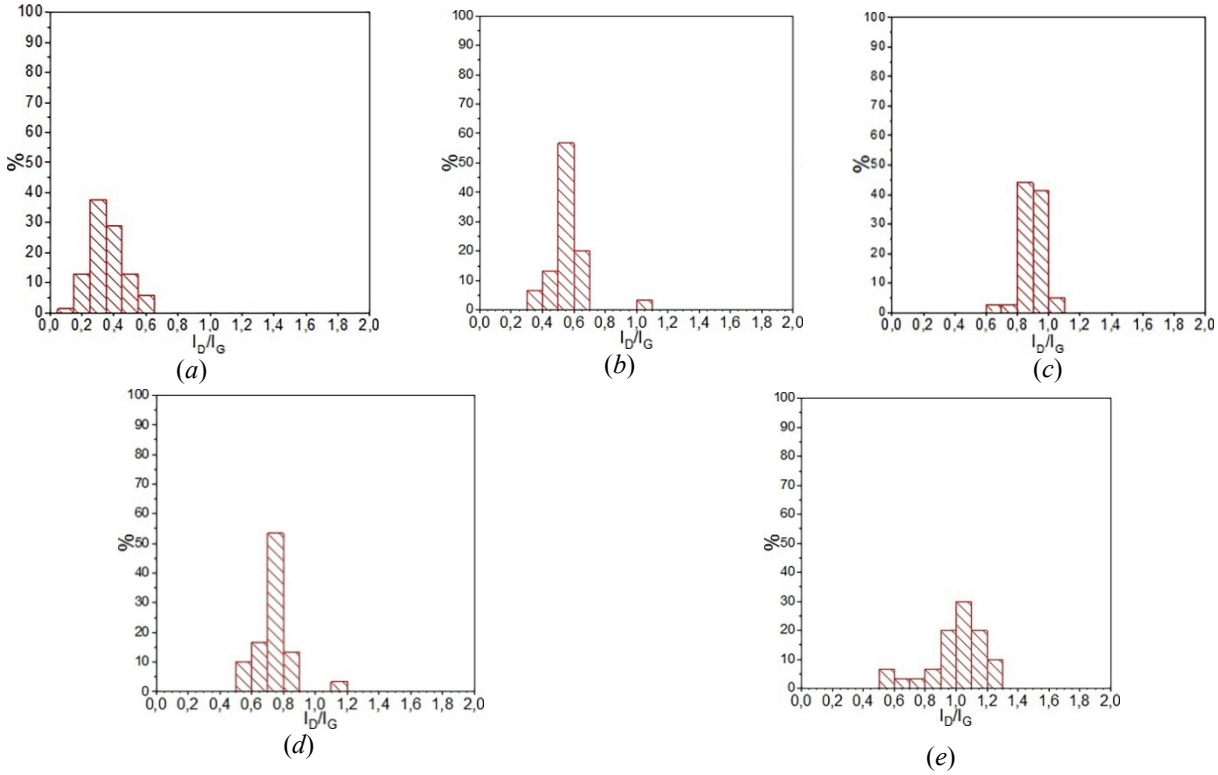

Fig. 4. I_D/I_G distribution functions for investigated suspensions

When using a disintegrator, it was not possible to obtain suspensions with very few graphene layers, but the defectiveness of graphene layers in the suspensions remained quite low. It should be noted that the latter method for producing few-layered graphenes has an undoubted advantage, since it has a productivity of about 0.5–1.0 kg of dry powder of few-layer graphene per hour, while the productivity of an ultrasonic installation, even at a power of 1 kW, does not exceed 0. 3–0.5 $g \cdot h^{-1}$.

In general, the study results are consistent with the results of the extensive study of various commercial graphene samples performed by the authors of [17], where a general trend was established: samples with a minimal number of layers had a minimal particle size and maximum defectiveness, while preparations with a higher number of layers had a larger particle size with low defectiveness.

Thus, the results obtained will allow further research in the development of effective technologies for producing few-layered graphenes in the form of suspensions using Raman spectroscopy parameters, striving to obtain materials with maximum valuesof the I_{2D}/I_G parameter and minimum values of the I_D/I_G parameter, in parallel using other developed we previously described control methods.

5. Funding

This study received no external funding.

6. Conflict of interests

The authors declare no conflict of interest.

References

1. Tuinstra F, Koenig JL. Raman spectrum of graphite. *Journal of Chemical Physics*. 1970;53(3):1126-1130. DOI:10.1063/1.1674108

2. Cançado LG, Takai K, Enoki T, Endo M, et al. Measuring the degree of stacking order in graphite by Raman spectroscopy. *Carbon.* 2008;46(2):272-275. DOI:10.1016/j.carbon.2007.11.015

3. Ferrari AC, Robertson J. Interpretation of Raman spectra of disordered and amorphous carbon. *Physical Review B.* 2000;61(20):14095-14107. DOI:10.1103/PhysRevB.61.14095

4. Ferrari AC, Meyer JC, Scardaci V, Casiraghi C, et al. Raman spectrum of graphene and graphene layers. *Physical Review Letters.* 2006;97(18). DOI:10.1103/PhysRevLett.97.187401

5. Wu JB, Lin ML, Cong X, Liu HN, Tan PH. Raman spectroscopy of graphene-based materials and its applications in related devices. *Chemical Society Reviews.* 2018;47(5):1822-1873. DOI:10.1039/C6CS00915H

6. Das A, Chakraborty B, Sood AK. Raman spectroscopy of graphene on different substrates and influence of defects. *Bulletin of Materials Science.* 2008;31(3):579-584. DOI:10.1007/s12034-008-0090-5

7. Gupta A, Chen G, Joshi P, Tadigadapa S, Eklund PC. Raman scattering from high-frequency phonons in supported *n*-graphene layer films. *Nano Letters*. 2006;6(12):2667-2673. DOI:10.1021/nl061420a

8. Zhu W, Dimitrakopoulos C, Freitag M, Avouris P. Layer number determination and thickness-dependent properties of graphene grown on SiC. *IEEE Transactions on Nanotechnology*. 2011;10(5):1196-1201. DOI:10.1109/TNANO.2011.2130536

9. Graf D, Molitor F, Ensslin K, Stampfer C, et al. Spatially resolved Raman spectroscopy of single- and few-layer graphene. *Nano Letters.* 2007;7(2):238-242. DOI:10.1021/nl061702a

10. Holmi J. *Determining the number of graphene layers by Raman-based Si-peak analysis.* Available from: https://core.ac.uk/download/pdf/80719206.pdf [Accessed 11 March 2024]

11. Kumar V, Kumar A, Lee DJ, Park SS. Estimation of number of graphene layers using different methods: a focused review. *Materials*. 2021;14. DOI:10.3390/ma14164590

12. Dresselhaus MS, Dresselhaus G, Eklund PC. Raman scattering in fullerenes. *Journal of Raman Spectroscopy.* 1996;27(3-4):351-371. DOI:10.1002/(SICI)1097-4555(199603)27:3/4<351::AID-JRS969>3.0.CO;2-N

13. Kuzmany H, Pfeiffer R, Hulman M, Kramberger C. Raman spectroscopy of fullerenes and fullerene-nanotube composites. *Philosophical Transactions of the Royal Society of London. Series A: Mathematical, Physical and Engineering Sciences.* 2004;362(1824):2375-2406. DOI:10.1098/rsta.2004.1446

14. Dresselhaus MS, Dresselhaus G, Jorio A, Souza Filho AG, Saito R. Raman spectroscopy on isolated single wall carbon nanotubes. *Carbon.* 2002;40(12):2043-2061. DOI:10.1016/S0008-6223(02)00066-0

15. Wang Y, Vasileva D, Zustiak SP, Kuljanishvili I. Raman spectroscopy enabled investigation of carbon nanotubes quality upon dispersion in aqueous environments. *Biointerphases.* 2017;12(1). DOI:10.1116/1.4978922

16. El-Mashtoly SF. 2nd ed. *Confocal Raman Microscopy*. In: Toporski J, Dieing Th, Hollricher O. (eds.) New York: Springer; 2018. 596 p. DOI:10.1017/S1431927619014880

17. Kovtun A, Treossi E, Mirotta N, Scida A, et al. Benchmarking of graphene-based materials: real commercial products vs. ideal graphene. *2D Materials.* 2019;6:025006. DOI:10.1088/2053-1583/aafc6e

Information about the authors / Информация об авторах

Nataliya N. Goncharova, Head of the Laboratory, NIIgraphite – Research and Development Institute of Graphite-Based Structural Materials, Moscow, Russian Federation, Moscow, Russian Federation; ORCID 0009-0003-6722-1246; e-mail: NNiGoncharova@rosatom.ru

Vladimir M. Samoilov, D. Sc. (Eng.), Professor, Chief Researcher, NIIGraphite, Moscow, Russian Federation, Moscow, Russian Federation; ORCID: 0000-0002-9861-905X; e-mail: VMSamoylov@rosatom.ru

Viktoriya A. Elchaninova, Researcher, NIIGraphite, Moscow, Russian Federation; ORCID: 0009-0006-3167-8924; e-mail: viaelchaninova@rosatom.ru

Anastasiya V. Nakhodnova, Cand. Sc. (Eng.), Head of the Testing Center, NIIGraphite, Moscow, Russian Federation; ORCID 0000-0006-3167-8924; e-mail AVNakhodnova@rosatom.ru

Egor A. Danilov, Cand. Sc. (Chem.), Head of the Laboratory, NIIGraphite, Moscow, Russian Federation; ORCID 0000-0002-1986-3936; e-mail: egadanilov@rosatom.ru

Konstantin A. Tarasov, Engineer, NIIGraphite, Moscow, Russian Federation; ORCID 0009-0006-2942-6365; e-mail: KoATarasov@rosatom.ru

Гончарова Наталия Николаевна, начальник отдела, Научно-исследовательский институт конструкционных материалов на основе графита «НИИГрафит», Москва, Российская Федерация; ORCID 0009-0003-6722-1246; e-mail: NNiGoncharova@rosatom.ru

Самойлов Владимир Маркович, доктор технических наук, профессор, главный научный сотрудник, НИИГрафит, Москва, Российская Федерация; ORCID: 0000-0002-9861-905X; e-mail: VMSamoylov@rosatom.ru

Ельчанинова Виктория Андреевна, научный сотрудник, НИИГрафит, Москва, Российская Федерация; ORCID: 0009-0006-3167-8924; e-mail: viaelchaninova@rosatom.ru

Находнова Анастасия Васильевна, кандидат технических наук, начальник испытательного центра, НИИГрафит, Москва, Российская Федерация; ORCID 0000-0006-3167-8924; e-mail: AVNakhodnova@rosatom.ru

Данилов Егор Андреевич, кандидат химических наук, руководитель лаборатории, НИИГрафит, Москва, Российская Федерация; ORCID 0000-0002-1986-3936; e-mail: egadanilov@rosatom.ru

Тарасов Константин Александрович, инженер, НИИГрафит, Москва, Российская Федерация; ORCID 0009-0006-2942-6365; e-mail: KoATarasov@rosatom.ru

Received 12 April 2024; Accepted 28 May 2024; Published 04 July 2024

Original papers
Advanced structural materials, materials for extreme conditions

УДК 691.3:539.2 DOI: 10.17277/jamt.2024.02.pp.091-099

Modification of fine-grained concrete with carbon nanotubes

© Dmitry A. Lyashenko[a]✉, Vladimir A. Perfilov[a]

[a] *Volgograd State Technical University,*
1, Akademicheskaya St., Volgograd, 400074, Russian Federation

✉ Dmitiry.lyashenko@yandex.ru

Abstract: The article considers the possibility of using nanotechnology in the production of concrete. Special attention is paid to the method of administration of nano-sized additives, due to their low concentration in the composition of concrete, as well as their tendency to form aggregates. Experimental data on the selection of a type of plasticizing additive to obtain optimum plastic properties of a concrete mix are presented. Thus, on the basis of the experimental data, the plasticizer SP-3 was selected, which allowed to reduce the water-cement ratio from 0.48 to 0.36 without losing the plasticity of the mixture. Data on the development of the composition of nanomodified fine-grained concrete by introducing Taunit-M carbon nanotubes in the amount of 0.01–0.001 % by weight of the binder are also presented. Two methods of introducing carbon nanotubes are considered, namely the technology of ultrasonic dispersion and the use of a vortex layer apparatus. The possibility of combining the two technologies to introduce a complex additive into concrete is considered. The greatest increase in strength (up to 26 %) was achieved when nanotubes were introduced into the mix using a linear induction rotator together with the introduction of a plasticizer into the water using an ultrasonic disperser.

Keywords: nanomodified concrete; carbon nanotubes; linear induction rotator; ultrasonic dispersion; superplasticizer; compressive strength; bending strength.

For citation: Lyashenko DA, Perfilov VA. Modification of fine-grained concrete with carbon nanotubes. *Journal of Advanced Materials and Technologies*. 2024;9(2):091-099. DOI: 10.17277/jamt.2024.02.pp.091-099

Модифицирование мелкозернистого бетона углеродными нанотрубками

© Д. А. Ляшенко[a]✉, В. А. Перфилов[a]

[a] *Волгоградский государственный технический университет,*
ул. Академическая, 1, Волгоград, 400074, Российская Федерация

✉ Dmitiry.lyashenko@yandex.ru

Аннотация: Рассмотрена возможность использования нанотехнологий в производстве бетона. Особое внимание уделено способу введения наноразмерных добавок, из-за их малой концентрации в составе бетона, а также их склонности к образованию агрегатов. Представлены экспериментальные данные по подбору вида пластифицирующей добавки для получения оптимальных пластических свойств бетонной смеси. На основе экспериментальных данных подобран пластификатор СП-3, который позволил понизить водоцементное отношение от 0,48 до 0,36 без потери пластичности смеси. Показаны данные по разработке состава наномодифицированного мелкозернистого бетона путем введения углеродных нанотрубок Таунит-М в количестве 0,01…0,001 % по массе вяжущего. Рассмотрено два метода внесения углеродных нанотрубок, а именно технология ультразвукового диспергирования, применение аппарата вихревого слоя и совместное применение двух технологий для комплексной добавки в бетон. Наибольшее повышение прочности (до 26 %) достигалось при введении в смесь нанотрубок с помощью линейно индукционного вращателя, совместно с введением в воду затворения пластификатора с помощью ультразвукового диспергатора.

Ключевые слова: наномодифицированный бетон; углеродные нанотрубки; линейно индукционный вращатель; ультразвуковое диспергирование; суперпластификатор; прочность при сжатии; прочность при изгибе.

Для цитирования: Lyashenko DA, Perfilov VA. Modification of fine-grained concrete with carbon nanotubes. *Journal of Advanced Materials and Technologies*. 2024;9(2):091-099. DOI: 10.17277/jamt.2024.02.pp.091-099

1. Introduction

Active mineral additives and superplasticizers occupy a special place among the available additives for concrete preparation. The analysis of literature data [1, 2] shows that the most effective additives are cement stone modifiers, which have a similar crystallo-chemical structure to inorganic nanoparticles (e.g. SiO_2). However, modification with such nanoparticles is difficult to apply as it is difficult to distribute the additive uniformly throughout the material. For this purpose, such additives can be used as a suspension with water for binder hydration [3–5]. In addition, there is the problem of distributing nanoscale additives uniformly throughout the volume of the mix. This is due to the fact that such additives are introduced in tenths and hundredths of a percent by weight of other components of the mix. In this context, the search for the most efficient and at the same time cost-effective methods of nanomodified concrete is an urgent task. The development of technologies for obtaining nanomaterials with different properties dictates the need to study the effect of introduced nanoparticles on the properties of silicate systems [6–9]. Problems related to the controlled improvement of structural concrete properties such as compressive and flexural strength, waterproofing, frost resistance, etc. [10, 11], as well as the effect on the performance of other building materials including binders (cement, gypsum, lime) are of considerable interest. There are experimental data on the use of fullerenes in the production of cinder and aerated concrete blocks, according to which the strength of conventional blocks increases by 16-18% and their density decreases by 8–10 % at a concentration of fullerene-like compounds equal to 1-10 g per ton of concrete. It also leads to a reduction in the production cycle [12].

Strotsky et al. [13] showed that in concrete production, the introduction of carbon nanoparticles with sizes ranging from 10 to 50 nm in the amount of 0.004 wt. % with respect to cement improved the effect of silica microadditive (8 wt. %) and increased the compressive strength of concrete up to 104.5 MPa. It also resulted in a significant increase in Young's modulus, Poisson's ratio, density and decrease in water permeability of concrete. The increase in concrete shrinkage, which was up to 30% with a single microsilica additive, disappeared.

Nanomodified concretes are essentially composed of the same materials as conventional concrete mixes, but their composition is chosen to ensure durability through the formation of new structural properties of the material. Concretes with improved performance characteristics are called high-performance concretes. Research in this direction is being carried out in Germany, Japan, Norway and Switzerland [15–19].

In Galinovsky et al. [20] the introduction of carbon structures into concrete mixing water is considered. Carbon nanotubes (CNTs) are an example of such additives. They are layers of graphene coiled into cylinders with lengths from 1 to 100 μm and different diameters. CNTs have improved mechanical properties [21, 22]. Depending on the number of graphene layers, there are both single-walled carbon nanotubes (SWCNTs) and multi-walled carbon nanotubes (MWCNTs). SWCNTs are strips of graphene sheets and have a diameter of 6–13 nm. MWCNTs have a larger number of these layers and their inner diameter varies between 6–16 nm, while their outer diameter is up to 100 nm. Due to their very small size, CNTs are subject to van der Waals forces, which cause them to agglomerate. This disadvantage of nanoscale additives requires methods to introduce them into the material composition. The most common methods are ultrasonic dispersion of such particles (ultrasonic dispersers, cavitators and ultrasonic baths), mechanical grinding and the combination of these technologies with the use of superplasticisers. There are many examples of the use of these methods in the scientific literature [23, 24]. We also previously considered the possibility of using nanomodifying additives, namely carbon nanotubes, where an increase in strength of over 15 % was observed [25, 26].

The aim of the present work is to study the effect of the introduced complex admixture in concrete containing carbon nanotubes and superplasticiser on the physical and mechanical properties of concrete and concrete mix.

2. Materials and Methods

2.1. Initial materials

For all conducted experiments the test beams of 40×40×160 mm size were made. The following materials were used for laboratory tests: cement Eurocement of M500D0 grade (JSC Cemros, Moscow); quartz sand with a grain size modulus of 1.9; plasticising additives: superplasticisers under trade mark “Linamix SP-180”, “Polyplast Premium”, “Aeroplast”, “Relamix T2”, “C-3”, “Polyplast SP-3”, “PFM NLK”, “POLYPLAST SP-4”, “Polyplast SP Sub”. All additives were introduced into the concrete mix in the form of suspension together with mixing water, in the amount of 0.5 wt. % of cement weight.

CNTs "Taunit-M" (NanoTechCenter LLC, Tambov, Russia) were used as a nanomodifier. CNTs are hollow carbon tubes with an outer diameter of 10–30 nm, inner diameter of 5–15 nm and length up to 2 μm.

2.2. Equipment for making and examining concrete samples

To investigate the mechanism of additives influence on the performance characteristics of fine-grained concrete, laboratory studies were carried out using the following equipment:

– ultrasonic device with visualization "Pulsar-1.2" (Interpribor LLC, Russia). It was used for the determination of strength characteristics by non-destructive method, including the early hardening of concrete;

– scanning electron microscope (SEM) "Versa 3d" (FEICompany, USA) was used to study the structure of nanomodified concrete;

– ultrasonic dispersant "UZG13-0,1/22" (Techcentre, Russia) was used for the introduction of additives into the mixing water;

– linear induction rotator "LIV-2" (Manufacturer – Russia) was used for introduction of carbon nanoadditives into dry mix, as well as for the activation of cement binder.

2.3. Preparation of the samples

One of the most important properties of a concrete mix is its mobility or plasticity, as this factor affects the technical and economic characteristics of the concrete works. This parameter is directly influenced by the amount of water added to the mix. Concrete mixes have their own water-holding capacity, which is determined by experimentation. It is well known that the introduction of more water leads to an increase in the porosity of the material and therefore a decrease in strength. In order to maintain strength with the same amount of water, different plasticizer additives are used. A group of plasticizers was selected for this study. The effect of each plasticizer was determined by Suttard viscometer tests. In order to study the strength properties, test beams of 40×40×160 mm were prepared with the following composition C – 500 g; sand – 1500 g; W/C – 0.36; plasticizer – 0.5 % by weight of the binder; CNT – 0.01–0.001 % by weight of the binder. The strength properties of the test specimens after 7, 14 and 28 days were investigated using the "Pulsar 1.2" device. The flexural strength of the 28-day samples was determined in accordance with Russian Standard 10180.

3. Results and Discussion

3.1. Selection of a plasticizer

The first part of the study aimed to determine the optimum performance characteristics of the concrete mix. Plasticizers were selected for the development of complex modifying additives in concrete. The results show that plasticizers have selective effects on different types of cement, due to the mineral and chemical composition of the binder on water-soluble additives. In this work, the water-cement ratio was determined experimentally in order to obtain a mix with optimum mobility. Samples were taken from each mix under normal curing conditions.

After 28 days, each sample of fine-grained concrete was tested for compressive and bending strength using a non-destructive control method with the ultrasonic device "Pulsar 1.2". The results of the research are presented in Table 1.

Table 1. Characteristics of the studied compositions using various plasticisers

Plasticiser	W/C	The blurring of the cone, mm	Density, kg·m^{-3}	Compressive strength, MPa
–	0.48	106	2220.7	53.7
SP-4	0.36	108	2277.3	68.1
PolyplastSP-3	0.36	113	2235.6	67.8
C-3	0.36	106	2281.3	64.5
PFM NLK	0.36	107	2250	62.9
Linamix SP-180	0.36	110	2286.3	65.4
Polyplast Premium	0.36	111	2264.5	66.4
Aeroplast	0.36	109	2234.4	60.7
Relamix 2T	0.36	107	2217.6	68.7
Polyplast SP Sub	0.36	109	2235.6	65.9

The standard cone blur method was used to determine the plasticizing effect of the additives on the mix. The best effect was shown by the plasticizer "Polyplast SP-3". At the same time, the fine-grained concrete samples with the superplasticizers "Relamix 2T", "SP-4" and "Polyplast SP-3" had higher strength. The increase in strength in comparison with the reference composition was 22, 21.3 and 20.6 %, respectively.

The obtained results of experimental studies confirm that the most effective plasticizers are those based on polycarboxylates at the same quantity of the added additive. Such plasticizers are less sensitive to the composition of the concrete and the type of cement binder.

The study of the obtained compositions shows a positive plasticizing effect. It should be noted that the additive "Polyplast SP-3" showed the best performance. Thus, the introduction of 0.5 % of the additive by weight of cement made it possible to reduce the water-cement ratio by 25 %, which ultimately led to an increase in strength.

3.2. Determining the efficiency of CNT introduction by ultrasonic dispersion

After selecting the superplasticizer, it was decided to use additional modifying additives, namely CNTs "Taunit-M" in small quantities (0.001–0.0001 wt. % by weight of the binder).

A staged series of tests was prepared for the research. The composition of fine-grained concrete including cement, sand and water was chosen as a control composition. The proportions of the components were chosen on the basis of optimum mobility of the mix. For additional analysis, a mix containing the plasticizer "Polyplast SP-3" was also prepared. The plasticizer was introduced in two ways: by mechanical stirring in the mixing water and by ultrasonic dispersion using the USG13-0.1/22 device. In this case, the use of ultrasonic treatment allowed the amount of plasticizer to be reduced from 0.6 to 0.5 wt. % by weight of the binder in the same mixes. On the basis of the literature data, it was decided to prepare three other mixtures with the use of plasticizer together with carbon nanotubes "Taunit-M" in the amount of 0.003, 0.004, 0.005 wt. % by weight of cement. The plasticizer and carbon nanotubes were introduced together into the mixing water under ultrasonic action for 5 minutes. Table 2 below shows the composition of the samples tested.

Table 2. Compositions of the studied mixes

Composition	Polyplast SP-3, g	CNTs Taunit-M, g	R_{com}, MPa	R_{bend}, MPa
1 (control)	–	–	27.4	5.53
2	3.0	–	35.6	5.86
3	2.5	–	35.2	6.43
4	2.5	0.003	37.4	6.53
5	2.5	0.004	39.7	6.63
6	2.5	0.005	40.2	6.80

Based on the laboratory test done, results were also obtained for the strength characteristics of the samples for each composition at 28 days of age (Figs. 1 and 2). It was found that the use of plasticizer increased the strength by 16 % both in compression (R_{com}) and in bending (R_{bend}). At the same time, however, the ultrasonic influence during the introduction of the plasticizer made it possible to reduce the amount of plasticizer additive without losing the strength properties (Compositions 2, 3).

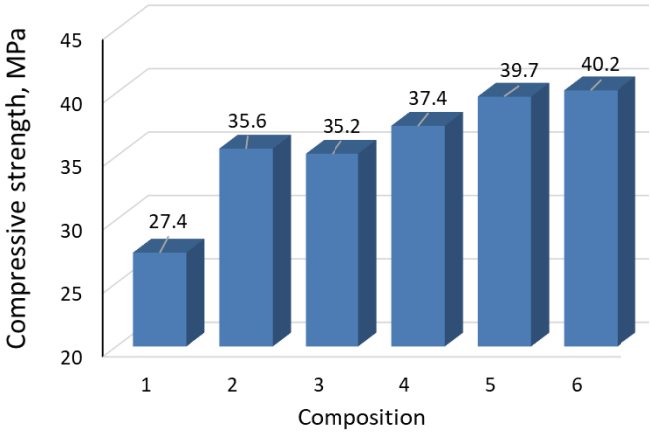

Fig. 1. Compressive strength test

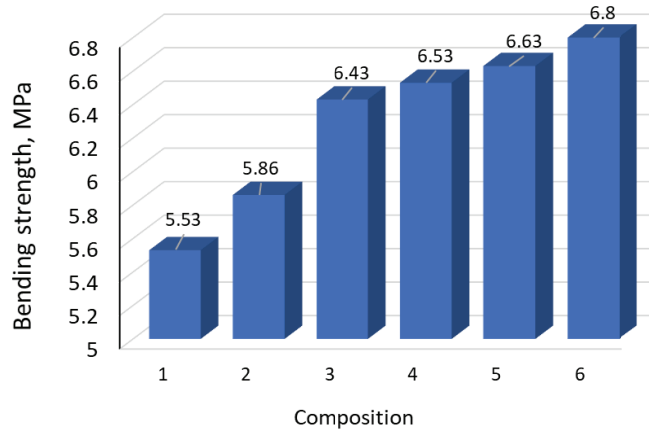

Fig. 2. Bending strength test

Table 3. The studied compositions and strength characteristics

Composition	SP-3, g	CNTs, wt. % by weight of cement	R_{com}, MPa		
			7 days	14 days	28 days
1 (control)	2.5	–	36.5	39.0	40.8
2	2.5	0.001	39.3	40.8	45.5
3	2.5	0.002	40.0	40.8	43.6
4	2.5	0.003	39.7	42.5	47.2
5	2.5	0.004	41.1	42.7	45.8
6	2.5	0.005	41.8	43.6	47.6
7	2.5	0.006	41.4	44.5	46.7
8	2.5	0.007	41.7	44.0	47.6
9	2.5	0.008	41.2	43.4	47.2
10	2.5	0.009	40.8	43.4	47.1
11	2.5	0.01	43.2	44.3	48.4

The use of a complex additive of plasticizer and CNTs increased the strength as the concentration of nanotubes increased. The introduction of carbon nanotubes increased the strength in the range of 26 to 31 %. It can be concluded that further tests are needed to determine the rational amount of additive with increasing concentration of the introduced additive.

Further, to study the effect of CNTs nanoadditive on the strength characteristics of fine-grained concrete, another series of tests was prepared from 11 compositions of C:S – 1:3, W/C – 0.36, SP-3 – 0.5 wt. % by weight of binder and different concentration of CNTs. Carbon nanotubes were introduced in the amount from 0.001 to 0.01 wt. % by weight of cement. The control samples (composition 1) did not include the nanoadditive. The investigated compositions are presented in the table below. For each composition the compressive strength was determined using non-destructive method of control with the device "Pulsar 1,2" at the age of 7, 14, 28 days. The results of the obtained data are given in Table 3.

As can be seen from the data obtained, the introduction of CNTs leads to an increase in the strength of fine-grained concrete. For example, the minimum amount of nanoadditive increased the compressive strength by 10 %. The maximum increase in strength is characteristic of Composition 11 and was 16 %. However, due to the insignificant difference in the strength values, it can be concluded that the introduction of nanotubes "Taunit-M" in the amount of 0.005–0.01 wt. % by weight of the binder has almost the same effect.

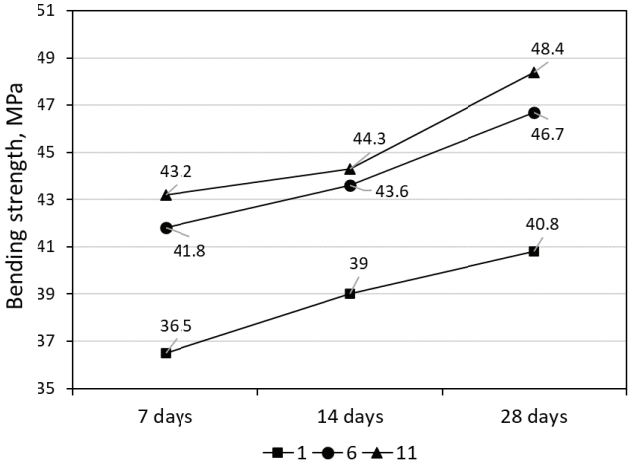

Fig. 3. The character of the strength gain of the fine-grained concrete

It should be noted that the increase in strength is already observed on the 7th day. Thus, for the composition with the maximum concentration of CNTs, the increase was 15 %. It is known that the increase in strength in the early curing period has a positive effect on the production processes associated with the manufacture of concrete products.

As can be seen in Fig. 3, the samples modified with nanoadditives showed an accelerated intensity of strength increase compared to the control composition.

3.3. Study of the method of CNTs introduction using a linear-induction rotator

In this work, the method of introduction of carbon nanostructures using a vortex layer apparatus was also investigated. A series of samples were prepared in which carbon nanotubes were introduced

into the cement binder using a linear induction rotator (LIR). For comparison, one series was prepared by ultrasonic dispersion technique. The preparation technology was as follows: cement binder and sand (C:S – 1:3) were jointly loaded into the LIR chamber, together with CNTs and ferromagnetic grinding bodies. The components were processed in the apparatus for 2 min. Plasticizer was introduced into the mixing water. All components were mixed to obtain a homogeneous mixture and samples were molded. Thus, four compositions were prepared including a control one without CNTs and three compositions with inclusion of nanoadditive in different concentrations. The compositions with the obtained characteristics are shown below in Table 4.

According to the data in the table, it is clear that the introduction of CNTs by LIR technology allows obtaining an insignificant increase in strength. The compressive strength increased in the case of ultrasound by 14 %, and when using LIR – by 15 %. This is explained by an additional effect of vortex influence, namely, activation of concrete mix components by grinding with grinding bodies.

3.4. Method of introduction of the complex additive

The last stage of the research was the joint application of the two technologies. The introduction of the complex additive was carried out sequentially in two stages: 1) introduction of a plasticiser by dispersion in mixing water; 2) introduction of CNTs into cement binder in LIR chamber. After treatment, all components were mixed for further moulding of the samples. After 28 days, the compressive and flexural strength limits were determined for each sample (Table 5).

3.5. Study of the structure of nanomodified concrete

In order to study the morphology of the nanomodified concrete, the samples destroyed during the tests were crushed to a powdery state, and a small amount of them were placed in a microscope chamber.

As shown in the images (Fig. 4*a*, *b*), the carbon nanotubes have a stable diameter value along the length of the fiber. This provides good conditions for the growth of cement stone around the carbon inclusions. Concrete modification at the nanoscale is evidenced by the discrete reinforcement of the cement matrix, where ettringite minerals together with nanotubes (Fig. 4*a*) allow the new formations to be combined into a single structure. The nanotube modified concrete has a dense arrangement of particles, resulting in an increase in strength properties.

Table 4. Compositions of the studied mixtures of fine-grained concrete

Composition	CNTs, wt. % per g	SP-3, g	LIR R_{com}, MPa	Ultrasound R_{com}, MPa
1	–	3	40.8	40.8
2	0.004/0.020		45.9	47.9
3	0.005/0.025		47.7	48.1
4	0.006/0.030		46.8	47.2

Table 5. Strength characteristics of the studied samples

Composition	CNTs, wt. %	R_{com}, MPa	R_{bend}, MPa
1	–	53.6	6.8
2	0.0001	65.0	8.1
3	0.0002	65.8	8.2
4	0.0003	67.0	8.2
5	0.0004	66.1	8.6
6	0.0005	68.2	9.0
7	0.0006	67.0	8.7
8	0.0007	66.2	8.4
9	0.0008	67.1	8.6
10	0.0009	67.4	8.7
11	0.0010	68.6	9.0

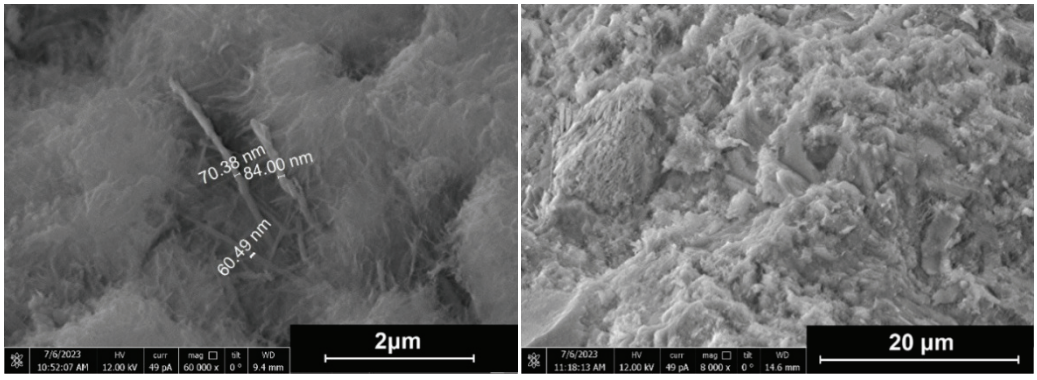

(*a*) (*b*)

Fig. 4. SEM-images of nanomodified concrete: *a* – magnification 60.000×; *b* – magnification 8.000×

The experimental data show that the maximum increase in strength is achieved at the maximum concentration of CNTs (Composition 11). This was 27 %. It should be noted that a slight difference in strength increase was achieved in composition 6 (26 %). From this it can be concluded that it would be more rational to use a lower amount of additive when selecting the concrete composition.

The microscope was also used to study the structure of samples obtained from the destruction of beams on presses. These are particles of fine-grained concrete (up to 5 mm in size).

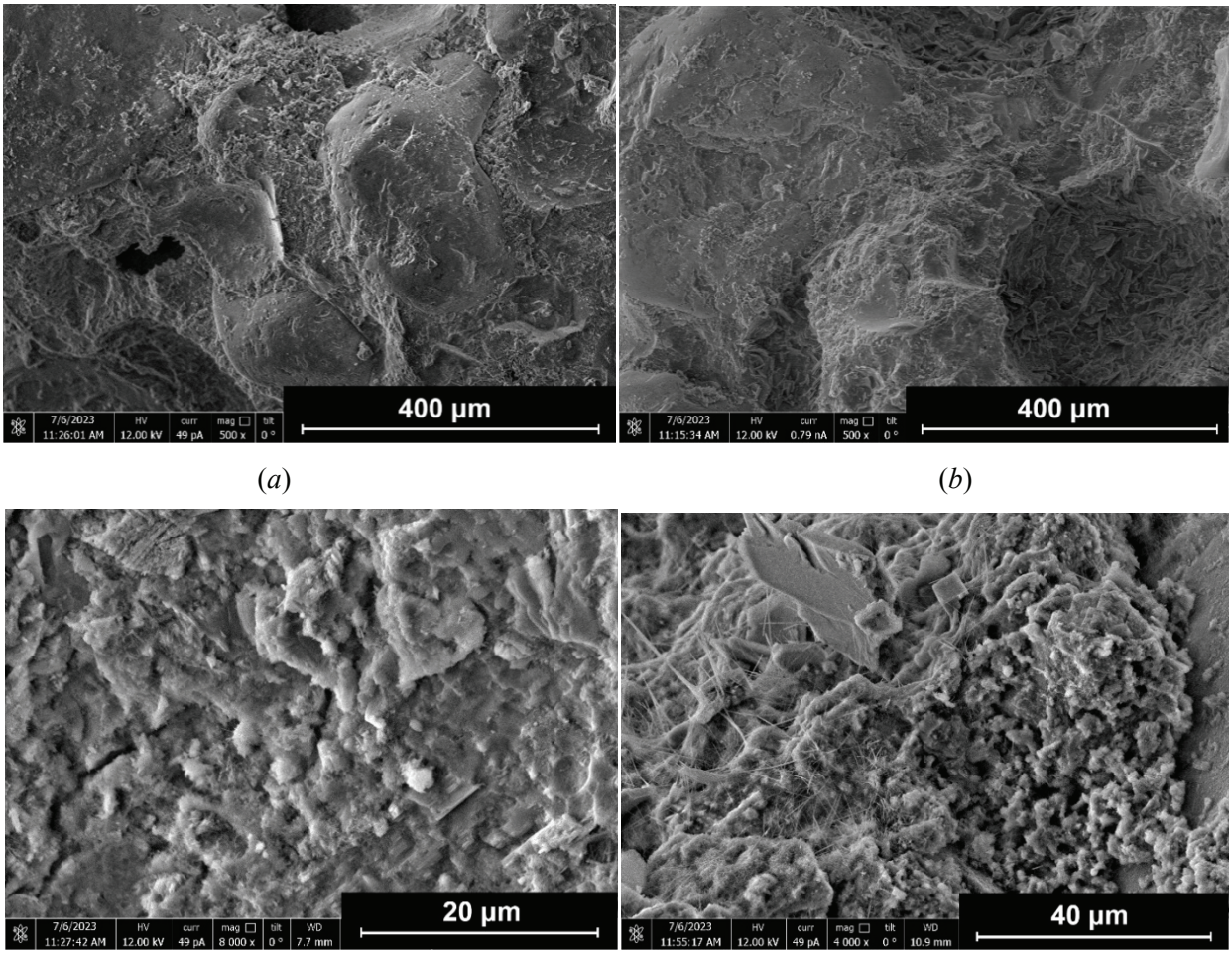

(*a*) (*b*)

(*c*) (*d*)

Fig. 5. SEM-images of the nanomodified samples:
a, *b* – control sample; *c*, *d* – nanomodified sample

The use of the nanostructured CNTs “Taunit-M” additive results in a denser and stronger concrete structure (Fig. 5), which is the reason for the increase in strength properties.

4. Conclusion

According to experimental studies, the introduction of carbon nanotubes “Taunit-M” leads to an increase in compressive and bending strength. An insignificant amount of the introduced additive (0.0001 wt. % by weight of the binder and higher) together with the plasticizer allows to noticeably increase the strength properties. It should be noted that there is an insignificant difference in the increase of strength characteristics when using from 0.0005 to 0.001 wt. % of CNTs by weight of cement. On this basis, it can be concluded that there is an optimal amount of the additive, regardless of the method of its introduction into the concrete composition. At the same time, it should be noted that the use of LIR allows slightly higher strength values to be obtained due to the additional grinding of the dry components. The study of the morphology of the interpore partitions of concrete using electron microscopy shows that the samples modified with nanotubes have a denser structure, which increases the strength properties. The micrographs show the inclusions of nanotubes, whose reinforcement can reduce the formation of nanoscale cracks and increase the durability of modified fine-grained concrete.

5. Funding

This study received no external funding.

6. Conflict of interests

The authors declare no conflict of interests.

References

1. Palamarchuk AA, Shishkina OA, Kochurov DV, Tarakan AG. Polymer concretes – promising building materials. *Mezhdunarodnyy studencheskiy nauchnyy vestnik*. 2018;6:105. (In Russ.)

2. Yendzhievskaya IG, Demina AV, Yendzhievsky AS, Dubrovskaya SD. Evaluation of the interaction of additives in concrete. *Vestnik Tomskogo gosudarstvennogo arkhitekturno-stroitel'nogo universiteta = Vestnik of Tomsk State University of Architecture and Building*. 2022;24(3):128-137. DOI:10.31675/1607-1859-2022-24-3-128-137 (In Russ.)

3. Moiseeva VI, Pirogova YaV, Tyumentsev ME, Pankov PA. Nanotechnology in the field of production of building materials. *Innovatsii i investitsii*. 2019;11:293-297. (In Russ.)

4. Dahlan AS. Impact of nanotechnology on high performance cement and concrete. *Journal of Molecular Structure*. 2021;1223:128896. DOI:10.1016/j.molstruc.2020.128896

5. Fakhratov MA, Evdokimov VO, Borodin AS. Prospects for the use of nanostructured concrete in construction. *Inzhenernyy vestnik Dona*. 2018;3:124. (In Russ.)

6. Lin Y, Zheng W, Liu S, Yuan M, Qin X. Multi-ion erosion test and molecular dynamics simulation of carbon nanotube concrete under stray current and salt brine environment. *Developments in the Built Environment*. 2024;17:100335. DOI:10.1016/j.dibe.2024.100335

7. Bhatta DP, Singla S, Garg R. Microstructural and strength parameters of Nano-SiO_2 based cement composites. *Materials Today: Proceedings*. 2021;46(15):6743-6747. DOI:10.1016/j.matpr.2021.04.276

8. Ashwini RM, Potharaju M, Srinivas V, Durga KS, et al. Compressive and flexural strength of concrete with different nanomaterials: A Critical Review. *Journal of Nanomaterials.* 2023;2023(1):1004597. DOI:10.1155/2023/1004597

9. Sun H, Amin MN, Qadir MT, Arifeen SU, et al. Investigating the effectiveness of carbon nanotubes for the compressive strength of concrete using AI-aided tools. *Case Studies in Construction Materials*. 2024;20: e03083. DOI:10.1016/j.cscm.2024.e03083

10. Askari KOA, Singh VP, Dalezios NR, Crusberg TC. Polymer concrete. *International Journal of Hydrology*. 2018;2(5):630-635. DOI:10.15406/ijh.2018.02.00135

11. Cherednichenko TF, Tambovtsev AM, Chesnokova VD, Zhurbenko MD. Technological and economic aspects of the development of lightweight concrete for structural purposes. *Inzhenernyy vestnik Dona*. 2021;9(81):1-7. (In Russ.)

12. Lhasaranov SA, Urkhanova LA, Buyantuev SL. Investigation of the phase composition of cement stone with carbon nanomaterials. *Stroitel'nyye materialy*. 2018;1(2):23-25. (In Russ.)

13. Strotsky VN, Gordeeva EV, Vaskin VM, Shitikov ES, Fedorov EV. Investigation of the physico-mechanical properties of high-strength concrete with the addition of microsilicon and an ultrafine carbon additive with nanoparticles 10-50 nm in size. In: *Scientific works of JSC TSNIIS.* Moscow: TSNIIS Publ. House; 2008. p. 33-40. (In Russ.)

14. Nurtdinov MR, Solovyov VG, Buryanov AF. Fine-grained concretes, modified nanofibers AlOOH and Al_2O_3. *Stroitel'nyye materialy*. 2015;2:68-71. (In Russ.)

15. Raveendran N, Vasugi K. Synergistic effect of nano silica and metakaolin on mechanical and microstructural properties of concrete: An approach of response surface methodology. *Case Studies in Construction Materials*. 2024;20:e03196. DOI:10.1016/j.cscm.2024.e03196

16. Raj RS, Arulraj GP, Anand N, Kanagaraj B, Lubloy E. Nano-bentonite as a sustainable enhancer for alkali activated nano concrete: Assessing mechanical, microstructural, and sustainable properties. *Case Studies in Construction Materials*. 2024;20:e03213. DOI:10.1016/j.cscm.2024.e03213

17. Venkata Rao M, Sivagamasundari R, Vamsi Nagaraju T. Achieving strength and sustainability in ternary blended concrete: Leveraging industrial and agricultural by-products with controlled nano-SiO_2 content. *Cleaner Materials*. 2023;9:100198. DOI:10.1016/j.clema.2023.100198

18. Syamsunur D, Wei L, Hisyam MN, Memon ZA, Sultan B. Research on performance monitoring of binary nano modified concrete based on temperature variation. *Case Studies in Construction Materials*. 2023;19:e02373. DOI:10.1016/j.cscm.2023.e02373

19. Hwangbo D, Son D-H, Suh H, Sung J, et al. Effect of nanomaterials (carbon nanotubes, nano-silica, graphene oxide) on bond behavior between concrete and reinforcing bars. *Case Studies in Construction Materials*. 2023;18:e02206. DOI:10.1016/j.cscm.2023.e02206

20. Galinovsky AL, Moiseev VA, Provotorov AS, Osipkov AS, Yakovlev GI. Development of ultra-jet technology for obtaining suspensions with carbon nanotubes. *Uprochnyayushchie tekhnologii i pokrytiya*. 2016;11(143):37-43. (In Russ.)

21. Pyrkin AA, Lukuttsova NP, Kostyuchenko GV. On the issue of improving the properties of fine-grained concrete with micro- and nanodisperse additives based on shungite. *Vestnik belgorodskogo gosudarstvennogo tekhnologicheskogo universiteta im. V.G. Shukhova*. 2011;2:16-20. (In Russ.)

22. Yakovlev GI, Grakhov VP, Gordina AF, Shaibadullina AV, et al. Influence of carbon black dispersions on the properties of fine-grained concrete. *Stroitel'nyye materialy*. 2018;8:89-92. (In Russ.)

23. Kozhukhova MI, Chulkova IL, Harhardin AN, Sobolev GK. Evaluation of the effectiveness of the use of hydrophobic aqueous emulsions containing nano - and micro-sized particles for the modification of fine-grained concrete. *Stroitel'nyye materialy*. 2017;5:92-97. DOI:10.31659/0585-430X-2017-748-5-92-97 (In Russ.)

24. Jung M, Park J, Hong S-g, Moon J. The critical incorporation concentration (CIC) of dispersed carbon nanotubes for tailoring multifunctional properties of ultra-high performance concrete (UHPC). *Journal of Materials Research and Technology*. 2022;17:3361-3370. DOI:10.1016/j.jmrt.2022.02.103

25. Lyashenko DA, Perfilov VA, Nikolaev ME, Lukyanitsa SV, Burkhanova RA. Increasing the strength of fine-grained concrete using carbon nanotubes and mechanical activation of the mixture. *Stroitel'nyye materialy*. 2023;12:49-54. DOI:10.31659/0585-430X-2023-820-12-49-54 (In Russ.)

26. Lyashenko DA, Perfilov VA, Nikolaev ME, Kozlovtseva EY. Modification of fine concrete with carbon nanotubes. *ICCATS 2023: Proceedings of the 7th International Conference on Construction, Architecture and Technosphere Safety, 10-16 September 2023, Sochi, Russia.* Moscow: Springer Science and Business Media Deutschland GmbH; 2024. p. 132-142. DOI:10.1007/978-3-031-47810-9_13

Information about the authors / Информация об авторах

Dmitry A. Lyashenko, Postgraduate, Volgograd State Technical University, Volgograd, Russian Federation; ORCID 0009-0002-6688-0293; e-mail: Dmitiry.lyashenko@yandex.ru

Ляшенко Дмитрий Александрович, аспирант, Волгоградский государственный технический университет, Волгоград, Российская Федерация; ORCID 0009-0002-6688-0293; e-mail: Dmitiry.lyashenko@yandex.ru

Vladimir A. Perfilov, D. Sc. (Eng.), Professor, Volgograd State Technical University, Volgograd, Russian Federation; ORCID 0009-0002-6688-0293; e-mail: vladimirperfilov@mail.ru

Перфилов Владимир Александрович, доктор технических наук, профессор, Волгоградский государственный технический университет, Волгоград, Российская Федерация; ORCID 0009-0002-6688-0293; e-mail: vladimirperfilov@mail.ru

Received 09 April 2024; Accepted 14 May 2024; Published 04 July 2024

Original papers
Advanced structural materials, materials for extreme conditions

УДК 678.019.391 DOI: 10.17277/jamt.2024.02.pp.100-109

The influence of hollow iron oxide microspheres on polyethylene climate aging

© Dmitrii A. Metlenkin[a]✉, Nikolay V. Kiselev[a, b], Bekzod B. Khaydarov[a, b], Dmitrii S. Suvorov[a, b], Elena A. Boychenko[a, b, c], Vasily A. Ovchinnikov[a], Zubarzhat R. Abushakhmanova[a], Evgeniy A. Kolesnikov[b], Igor N. Burmistrov[a, b]

[a] *Plekhanov Russian University of Economics, 36, Stremyanny Ln., Moscow, 117997, Russian Federation,*
[b] *National University of Science & Technology "MISIS", 4, Leninsky Pr., Moscow, 119049, Russian Federation,*
[c] *N.N. Semenov Federal Research Center for Chemical Physics, Russian Academy of Sciences, 4, Kosygin St., Moscow, 119334, Russian Federation*

✉ dametl@mail.ru

Abstract: Creation of biodegradable polymers is one of the most prospective trends aimed at solving problems of polymer waste accumulation and processing, and the development of effective oxo-additives for polyolefin raw materials. It is considered to be one of the most promising ways to ensure accelerated degradation of polymer waste in natural conditions. The present research work studies the effect of nanostructured iron oxide microspheres produced with ultrasonic aerosols pyrolysis on accelerated atmospheric aging of polyethylene. Two types of microspheres were used to modify polyethylene microspheres consisting of X-ray amorphous Fe_2O_3 (initial microspheres after synthesis) and microspheres, consisting of crystalline Fe_2O_3 (heat-treated). Samples of polyethylene modified with microspheres were aged by simulating cyclic climatic effects (temperature, UV, moisture). After the aging of polyethylene modified with microspheres, a higher degree of surface oxidation was discovered using the method of infrared spectroscopy. A strong surface erosion of polyethylene was observed with the addition of microspheres after aging at the same time, untreated polyethylene was preserved almost unchanged. The present study has shown that modification of polyethylene with iron oxide microspheres beyond the end of materials useful life provides its accelerated decomposition under the influence of the main components of atmospheric impact: light, temperature and humidity. At the same time, the complex of mechanical and technological properties of modified polyethylene remained at the acceptable level, which allows using the developed material for the production of packaging, agricultural and landscape films, which will decompose in natural conditions after the end of their lifetime.

Keywords: composites; microspheres; climatic aging; X-ray phase analysis; infrared spectroscopy; thermogravimetric analysis.

For citation: Metlenkin DA, Kiselev NV, Khaidarov BB, Suvorov DS, Boychenko EA, Ovchinnikov VA, Abushakhmanova ZR, Kolesnikov EA, Burmistrov IN. Influence of hollow iron oxide microspheres on polyethylene climate aging. *Journal of Advanced Materials and Technologies*. 2024;9(2):100-109. DOI: 10.17277/jamt.2024.02.pp.100-109

Влияние полых микросфер оксида железа на климатическое старение полиэтилена

© Д. А. Метленкин[a]✉, Н. В. Киселев[a,b], Б. Б. Хайдаров[a,b], Д. С. Суворов[a,b], Е. А. Бойченко[a,b,c], В. А. Овчинников[a], З. Р. Абушахманова[a], Е. А. Колесников[b], И. Н. Бурмистров[a,b]

[a] *Российский экономический университет имени Г. В. Плеханова, Стремянный пер., 36, Москва, 117997, Российская Федерация,*
[b] *Национальный исследовательский технологический университет «МИСИС», Ленинский пр., 4, Москва, 119049, Российская Федерация,*
[c] *Федеральный исследовательский центр химической физики имени Н. Н. Семёнова РАН, ул. Косыгина, 4, Москва, 119334, Российская Федерация*

✉ dametl@mail.ru

Аннотация: Создание биоразлагаемых полимеров – одно из актуальных направлений в решении проблем накопления и переработки полимерных отходов. Разработка эффективных оксодобавок к полиолефиновому сырью рассматривается как один из наиболее перспективных способов обеспечения ускоренной деструкции

полимерных отходов в природных условиях. Исследовано влияние наноструктурированных микросфер оксида железа, полученных методом пиролиза ультразвуковых аэрозолей, на ускоренное атмосферное старение полиэтилена. Для модификации полиэтилена были использованы микросферы двух типов: первый тип на основе рентгеноаморфного Fe_2O_3 (исходные микросферы после синтеза), второй тип на основе кристаллического Fe_2O_3 (термообработанные). Образцы полиэтилена, модифицированного микросферами, состаривали путем моделирования циклических климатических воздействий (температура, УФ, влажность). После ускоренного старения модифицированного микросферами полиэтилена методом инфракрасной спектроскопии обнаружена более высокая степень окисления поверхности. Показана сильная поверхностная эрозия полиэтилена с добавлением микросфер после старения, при этом необработанный полиэтилен сохранялся практически в неизменном виде. Представленное исследование показало, что модификация полиэтилена микросферами оксида железа после окончания срока службы материалов обеспечивает его ускоренное разложение под действием основных компонентов атмосферного воздействия: света, температуры и влажности. При модификации микросферами комплекс механических и технологических свойств полиэтилена остался на приемлемом уровне, что позволяет использовать разработанный материал для производства упаковочных, сельскохозяйственных и ландшафтных пленок, которые после окончания срока службы будут разлагаться в естественных условиях.

Ключевые слова: композиты; микросферы; климатическое старение; рентгенофазовый анализ; инфракрасная спектроскопия; термогравиметрический анализ.

Для цитирования: Metlenkin DA, Kiselev NV, Khaidarov BB, Suvorov DS, Boychenko EA, Ovchinnikov VA, Abushakhmanova ZR, Kolesnikov EA, Burmistrov IN. Influence of hollow iron oxide microspheres on polyethylene climate aging. *Journal of Advanced Materials and Technologies*. 2024;9(2):100-109. DOI: 10.17277/jamt.2024.02.pp.100-109

1. Introduction

Over the past few decades, the demand for plastics has increased significantly due to their low cost, excellent durability and processability. According to *The Economist*, between 1950 and 2015 about 8.3 billion tonnes of different types of plastics was produced worldwide. Currently, only 9 % of plastic materials are recycled and approximately 12 % are incinerated, while 79 % are thrown away as garbage into the environment [1]. This fact creates problems of plastic waste accumulation, which causes enormous damage to various ecosystems. Plastic accumulation is caused by its inability to decompose in natural conditions due to the presence of antioxidants and stabilizers in its composition [2].

The use of degradable materials can be a solution to reduce the accumulation of waste in the environment. These materials can be divided into two groups: those that are inherently biodegradable, whose chemical structure allows direct action by biological enzymes (such as amylase and cellulase), and those that become biodegradable after one or more physical and/or chemical processes, such as hydrolysis, photolysis or pyrolysis [2]. The latter group includes polymeric materials containing prooxidants/degradants known as oxobiodegradable polymers. These materials require oxidative degradation under UV light and heat to reduce their molar mass and form groups that are more easily assimilated by microorganisms [3].

The development of materials that are able to decompose under the influence of environmental factors with the assistance of oxo-additives at the end of their lifetime is one of the promising industrial approaches to the problem of polymer waste accumulation in the environment. As usual, transition metal compounds: Fe, Mn, Co added in stearates form or other organic complexes are used as oxo-additives whose function is to assist the degradation of the material [4, 5]. Inclusion of polar groups and reduction of molecular weight in polymer chains promotes interaction with microorganisms in the environment, turning them into biodegradable materials [3, 4].

The paper by Francisco J. Arráez and colleagues [5] considered the oxidation process of impact resistant polystyrene with the addition of 1.5 and 3 wt. % oxidizable raw material d2w as a pro-oxidant. The active components of this additive are Fe and Mn stearates (metal content (56.71 ± 0.41) and (6500 ± 200) ppm respectively). The authors showed that compositions with 1.5 % oxo-additive exhibited faster degradation than samples with 3 % oxo-additive at temperatures of 50 and 55 °C. A complete loss of mechanical properties of the pro-oxidant samples was noted and the changes were faster with increasing temperature.

The paper [3] investigated the effect of the pro-oxidant additive PDQ-H containing manganese at a concentration of 0.8 wt. % on the accelerated degradation of linear low density polyethylene (LLDPE) and low density polyethylene (LDPE). It was found that for both accelerated degradation and

environmental degradation a complete loss of mechanical properties was obtained. Also, by FTIR spectroscopy it was found that due to the simultaneous presence of different degradation products containing carbonyl groups, the carbonyl band becomes wider with increasing degradation time, indicating a significant break in the polymer chains.

The analysis of the literature data shows that a common problem of using oxo-additives is the partial degradation during processing because of elevated temperatures [6, 7]. Thermal stability of samples with oxo additives, which in most studies / papers [8–10] was evaluated by TGA, naturally decreased due to oxodegradation processes leading to the formation of low molecular weight impurities. In this regard, the search for new materials that can perform the role of oxo-additives is an important scientific direction.

Not only the nature of the active metal and its compound, but also the dispersity and distribution of the additive as well as its morphology and specific surface area influence the effectiveness of oxo-degrading additives. In this case, hollow and porous oxide and metal microspheres are considered as a functional additive to various polymeric materials, characterized by a high specific surface area, processability and ease of creating composites with a uniform distribution in a wide range of concentrations and imparting a variety of functional properties [5, 11–16]. The introduction of microspheres based on metals and their compositions used as oxo-additives can provide a similar effect and reduce the period of natural decomposition of polymer composites.

In this regard, the purpose of this article is to investigate the effect of hollow iron oxide microspheres on the accelerated climatic aging processes and the basic mechanical properties of PE.

2. Materials and Methods

2.1. Sample production technology

LDPE in granules (LB7500N LP408294, LG Chem, South Korea) was used as a tested polymer matrix material.

Hollow iron oxide microspheres were obtained by ultrasonic spray pyrolysis at 900 °C. $Fe(NO_3)_3$-$9H_2O$ (chemical grade, RusChem, Moscow, Russia) was used to prepare a 20 % aqueous solution of iron nitrate. The solution was prepared and filtered using a paper filter, and then poured into the tank of a domestic ultrasonic atomizer. The flow rate of the dispersed solution through the steel tube reactor was maintained using an air compressor. A continuous supply of aerosol was carried out until the precursor in the tank was finished. After completion of the process and cooling down the plant elements, a dark red powder was extracted from the filter.

The resulting powder was divided into two equal parts for further removal of unreacted salt residues. The first part was placed in a muffle furnace for further afterburning of salts and recrystallization of microspheres. The second part of the powder was washed with distilled water; an ultrasonic homogenizer was used to better dissolve the iron nitrate in water. The resulting stable suspension was separated by centrifugation. Additionally, the powder was washed with acetone and air dried.

The compositions were prepared by rolling on the laboratory rollers UBL-6175-BL (PRC). The compositions of the tested samples are presented in Table 1.

The duration of mixing the composition was 15 min at roller temperatures of 150 and 140 °C and the gap between the rolls of 0.5–1.0 mm. Having mixed the composition, it was cooled and crushed on a rotary knife mill “Vibrotehnik” (Russia). Then the sample of the composition was dried in a drying cabinet for 30 min at t = 90 °C and pressed on a hand press RPA-12 at 180 °C and 150 MPa to obtain homogeneous films of thickness 1.2 mm. The samples of LDPE composites containing 1.25, 2.5, 5.0 wt. % of heat-treated and initial iron microspheres were prepared.

2.2. Analytic methods

The structure of microspheres and composite was studied by scanning electron microscope (SEM) Tescan Vega 3, TESCAN, Brno, Czech Republic with EDX analyzer.

In this paper, the X-ray phase analysis (XRD) was performed on an ARL X'TRA diffractometer (Thermo Scientific, Switzerland) using CuKα radiation ($\lambda CuK\alpha = 0.15412$ nm) in the 2θ angle range (5–60 degrees). Bregg-Brentano measurement

Table 1. LDPE-based composites modified with iron oxide microspheres

Microsphere type	Microsphere content, wt. %		
Initial	1.25	2.5	5.0
Heat-treated	1.25	2.5	5.0

Table 2. Physical and mechanical properties of composites

Tested materials	Microsphere content, wt. %	Relative elongation at the point F_{max} (ε_{max}), %	Yield strength σ_s, MPa	Modulus of elasticity E, MPa
Initial LDPE	0.00	576	8.00	128
LDPE filled with heat-treated microspheres Fe_2O_3	1.25	294	5.90	184
	2.50	267	5.86	200
	5.00	140	5.84	162
LDPE filled with initial microspheres Fe_2O_3	1.25	255	5.90	167
	2.50	376	5.90	139
	5.00	411	6.00	168

geometry, step scanning mode (0.02 degree step) at 1.2 was used. XRD based on CuKα radiation and Bregg-Brentano geometry is the most popular of the X-ray phase spectroscopy methods.

The accelerated weathering test was performed via three-factor climatic chamber ATLAS UV-Test (USA) according to ASTM D5208 (cycle B). The single 12-hours test cycle consisted of 4-hour condensation at 50 °C, and then irradiation with UV light for 8 hours at 70 °C. The wavelength of UV lamp was 340 nm and the irradiance was 1.35 $W \cdot m^{-2}$ with humidity of 90–100 %. The total time of weathering was 168 hours (14 cycles).

The IR spectra of the compositions and the initial LDPE before and after exposure in an environmental chamber were recorded using a Bruker Lumos FT-IR microscope macromodule in the spectral range of 4000–600 cm^{-1}.

The thermogravimetric analysis (TGA) was carried out using a synchronous thermal analysis device (TGA/DSC3+, Mettler Toledo, Greifensee, Switzerland) in the temperature range of (+25–+800) °C at a heating rate of 10 $deg \cdot min^{-1}$ in air (100.0 $mL \cdot min^{-1}$). For measurements, a 150 μL aluminum oxide crucible was used; the sample weight was 4–6 mg. The results were processed using the Star SW Lab Mettler software version 16.10 (Greifensee, Switzerland).

The processes of glass transition, cold crystallization, and melting of LDPE and composites were studied by a differential scanning calorimeter DSC 214 Polyma (NETZSCH-Geratebau GmbH, Selb, Germany) according to ISO 11357-3:2018. The heating of the samples was carried out in the temperature range of 20–200 °C at a scanning speed of 10 $°C \cdot min^{-1}$. The weight of the samples was (8 ± 0.5) mg. A temperature scale and an enthalpy of melting were calibrated against indium, zinc, and stannic standard samples.

The analysis of physical and mechanical properties of the compositions was carried out using a universal testing machine DVT (Devotrans, Turkey). For the tests on the pneumatic punching press GT-7016-AR (Gotech testing Machines Inc., Taiwan) the samples of compositions with size 100×10 mm were cut out. A total of 21 samples were prepared: 3 samples for each composition (n = 7). The results of relative elongation, yield strength and modulus of elasticity were obtained automatically from geometrical parameters of samples in Devotrans CKS v2.1.4 software system by a series of at least 5 measurements (samples) as shown in Table 2.

3. Results and Discussion

The phase composition and structure of microspheres powder was investigated with the X-ray diffraction technique (Fig. 1).

The diffractogram of microspheres without annealing does not contain sharp peaks (Fig. 1 – curve *a*), which indicates that the material of the microspheres is amorphous. The diffractogram of annealed microspheres shows high crystallinity of the material (Fig. 1 – curve *b*). The interpretation of the XRD data showed the presence of one phase – hematite Fe_2O_3.

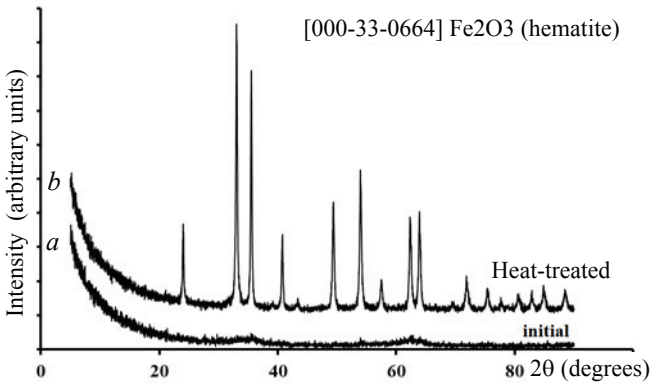

Fig. 1. Diffractograms of heat-treated and initial microspheres

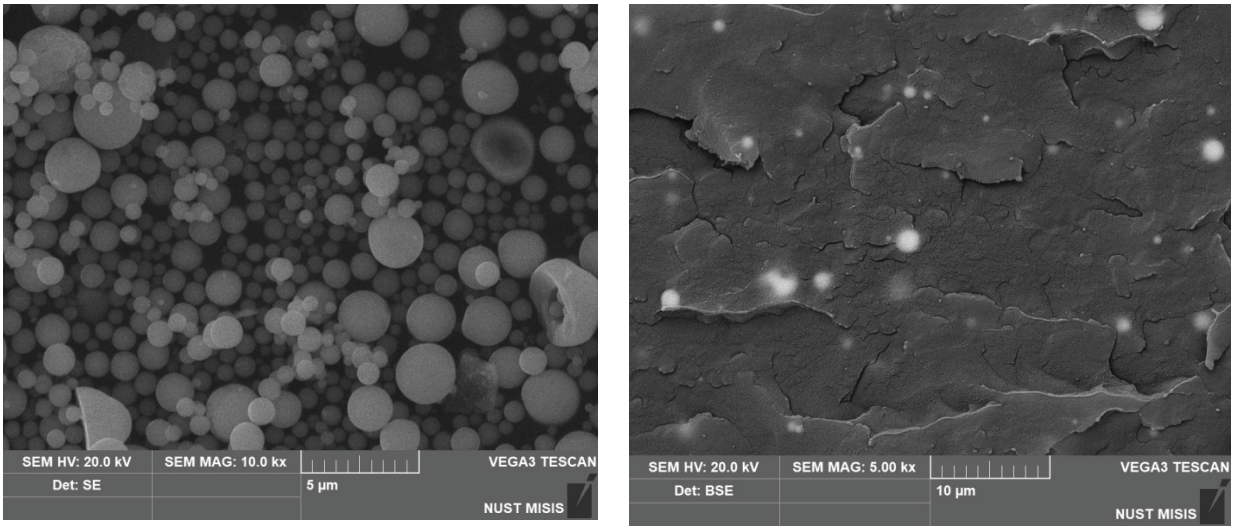

(*a*) (*b*)

Fig. 2. Structure of Fe_2O_3 microspheres (*a*) and LDPE-based composite (*b*) containing 5.0 wt. % Fe_2O_3 microspheres (brittle fracture)

The obtained microspheres had a hollow structure and an average size from 1 to 4 microns (Fig. 2*a*). In the composite, the spheres were well blended with the binder and, when examining the brittle chip surface (Fig. 2*b*), they cannot be practically detected on the surface. The analysis of the SEM data also did not reveal the presence of aggregates of microspheres. Individual particles are statistically distributed throughout the composite.

The introduction of functional fillers often leads to a decrease in the complex of mechanical properties, so the study of strength properties of the investigated composites was carried out (Table 2). According to the Table 2 it was found that the introduction of microspheres in the whole investigated range of concentrations (from 1.25 to 5 wt. %) does not significantly affect the strength characteristics of polyethylene. Considering the preservation of standard values of physical and mechanical properties when introducing microspheres into the composition of LDPE, as well as their small size and lack of aggregates, the obtained compositions can be used in the production of consumer goods, for example, packaging films, bags.

The main negative influence of traditionally used oxo additives is the reduction of properties and degradation at elevated temperatures during the processing of composites and manufacturing of products from them. Thus, the influence of microsphere-based additives on the heat resistance of polyethylene was investigated (Fig. 3).

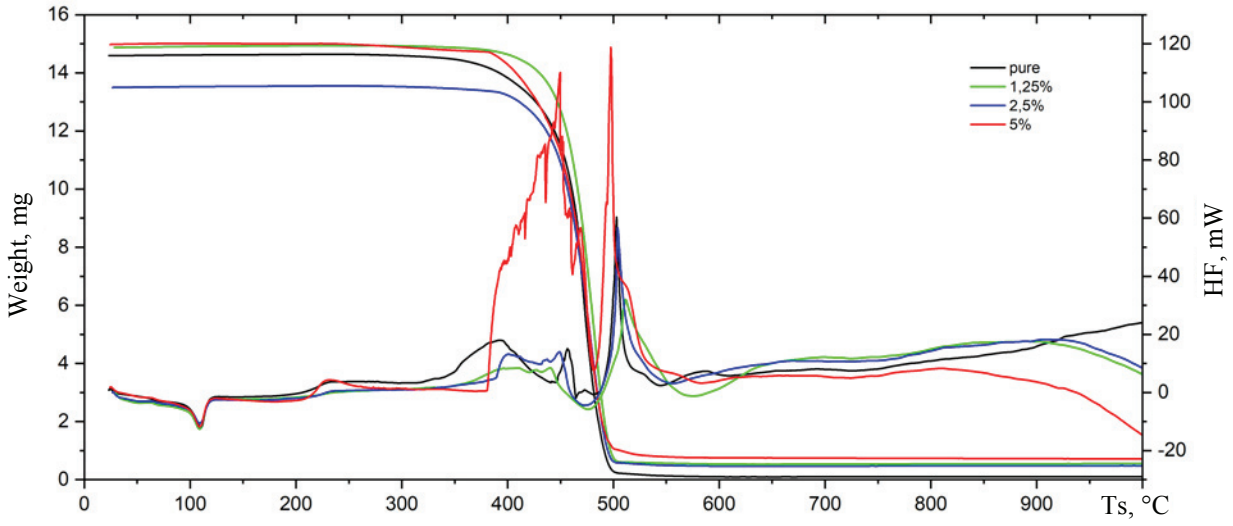

Fig. 3. TGA/DSC curves initial LDPE and LDPE filled with heat-treated microspheres Fe_2O_3

The comparison of mass loss and DSC curves of the investigated samples with the curve of the original LDPE is shown in Fig. 3. The onset temperatures of degradation of microsphere-filled composites, both according to the data of thermal effects and heat fluxes do not differ much from the pure polymer. The main degradation stages occur at temperatures (more than 350 °C), which are much higher than the processing temperature (180–210 °C). Thus, it can be concluded that there is no significant degradation during processing.

The study of DSC curves indicated that the destruction of the composite includes 2 stages: active combustion at temperatures of 330–480 °C, during which about 92–95 % of the mass of samples is lost and some amount of coke residue is formed, which is destroyed at the second stage at 480–550 °C (Figs. 3 and 4*a*). Increasing the content of microspheres leads to an increase in the proportion of coke residue even without considering the mass fraction of filler (Fig. 4*b*). Probably, microspheres play the role of substrate for carbon settling during degradation, and the higher the proportion of coke structures settled on microspheres, the earlier on the temperature scale the degradation process starts (Fig. 4*a*) and the higher the heat flux (Fig. 4*b*).

Composites with different content of heat-treated and initial microspheres were placed in a climatic chamber where they were subjected to cyclic exposure to UV irradiation, elevated temperature and humidity. After this testing for 168 hr. the samples were examined by FTIR spectroscopy (Fig. 5).

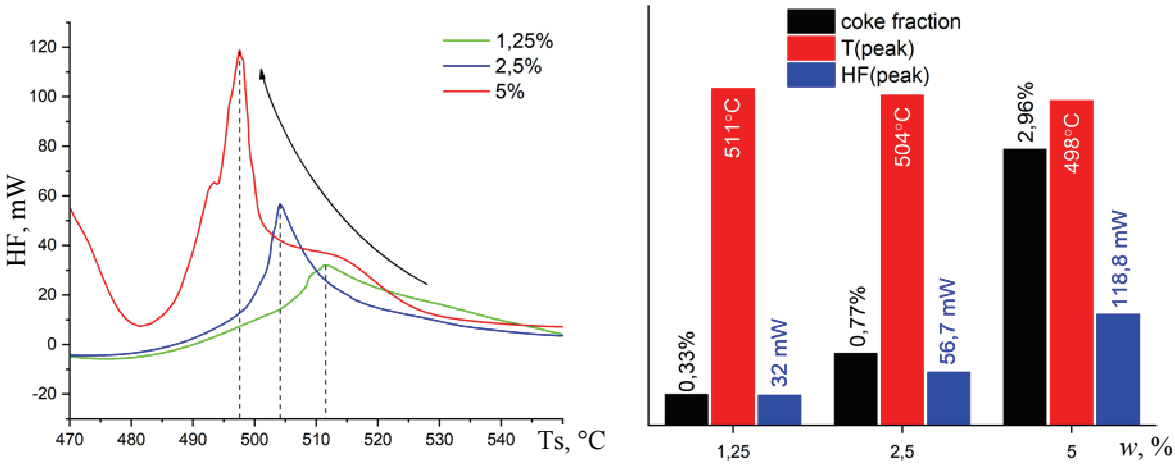

Fig. 4. TGA/DSC curves of LDPE filled with heat-treated microspheres Fe_2O_3

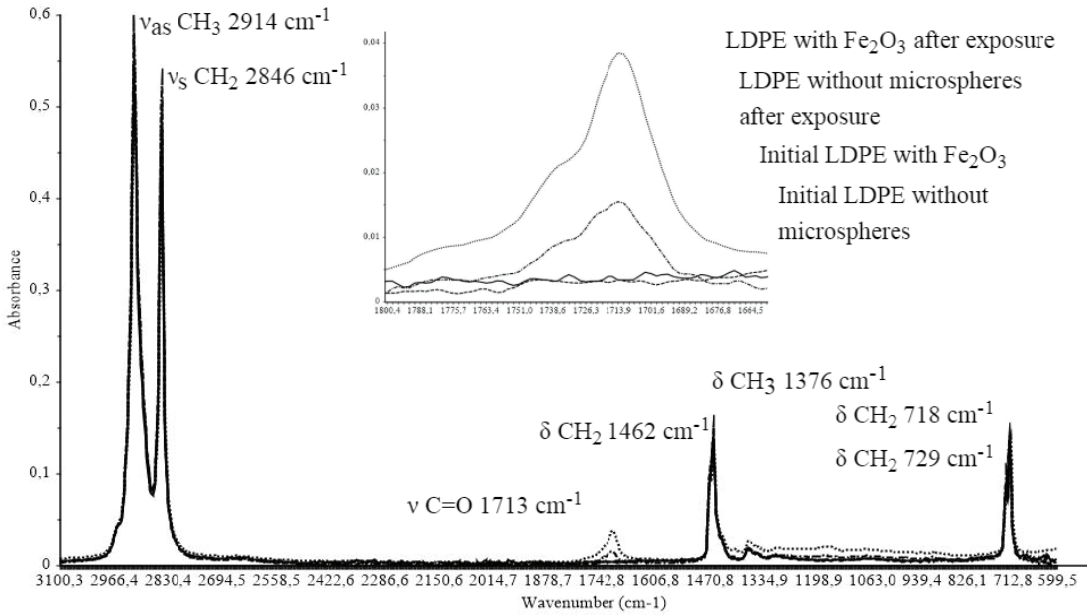

Fig. 5. FTIR spectra of initital LDPE and LDPE composite containing heat-treated Fe_2O_3 microspheres in the range 3100–600 cm^{-1}

The IR absorption peaks on the spectra of PE compositions containing heat-treated and initial microspheres correspond to the typical polyethylene functional groups present in the obtained compositions:

– 2914 cm^{-1} – asymmetric stretching vibrations of CH_2 groups [17];

– 2846 cm^{-1} – symmetric stretching vibrations of CH_2 groups [17];

– 1462 cm^{-1} – bending vibrations of CH_2 groups [18];

– 1376 cm^{-1} – bending vibrations of CH_2 groups [19];

– 729, 718 cm^{-1} – wagging bending vibrations of CH_3 groups.

Absorption peaks characteristic of the C=O bond were not observed on the spectrum of the original PE and the spectra of the composites before exposure.

After exposure in a climatic chamber for 168 hours, an increase in the intensity of the absorption band at 1713 cm^{-1}, corresponding to the C=O group, was observed in compositions with added microspheres. In the case of heat-treated microspheres, the observed effect was slightly higher from compositions with initial microspheres, which may be due to the higher catalytic activity of the heat-treated form.

The band at 1713 cm^{-1} belongs to stretching vibrations of C=O, the change in the intensity of which is traditionally associated with polymer degradation processes [20–22]. In particular, Pablos et al. [22] studied the effect of iron and calcium stearates on the degradation of PE under natural and artificial exposure using FTIR spectroscopy; it was found that PE containing stearates had a significant increase in the intensity of the carbonyl oxygen peak after photoaging. The increase in carbonyl group content leads to a decrease in the level of hydrophobicity of the material surface and promotes accessibility for further not only oxidative but also microbial degradation [21]. Zapata et al. [23] studied the effect of $CaCO_3$ nanoparticles on the photoaging of PENP. In the IR spectra of the photoaged LDPE / $CaCO_3$ composition, there is a strong peak at 1720 cm^{-1}, which is associated with the valence vibration of the C=O carbonyl group. The intensity of the carbonyl bands naturally increased with increasing exposure time of the composition [24, 25].

The study of samples before and after accelerated aging by the DSC method (Fig. 6)

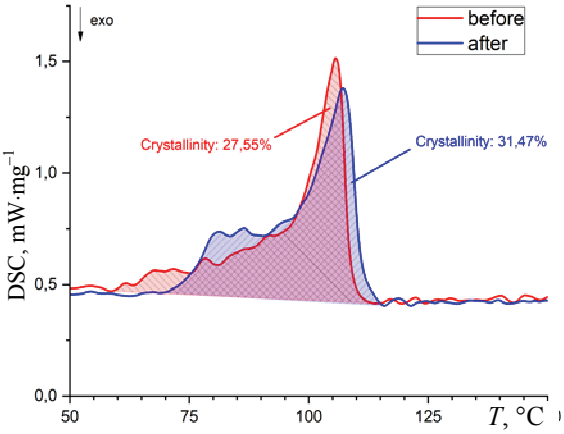

Fig. 6. DSC curves of LDPE composite containing heat-treated Fe_2O_3 before and after accelerated aging. The surface of the samples before and after aging was examined by optical microscopy (Fig. 7)

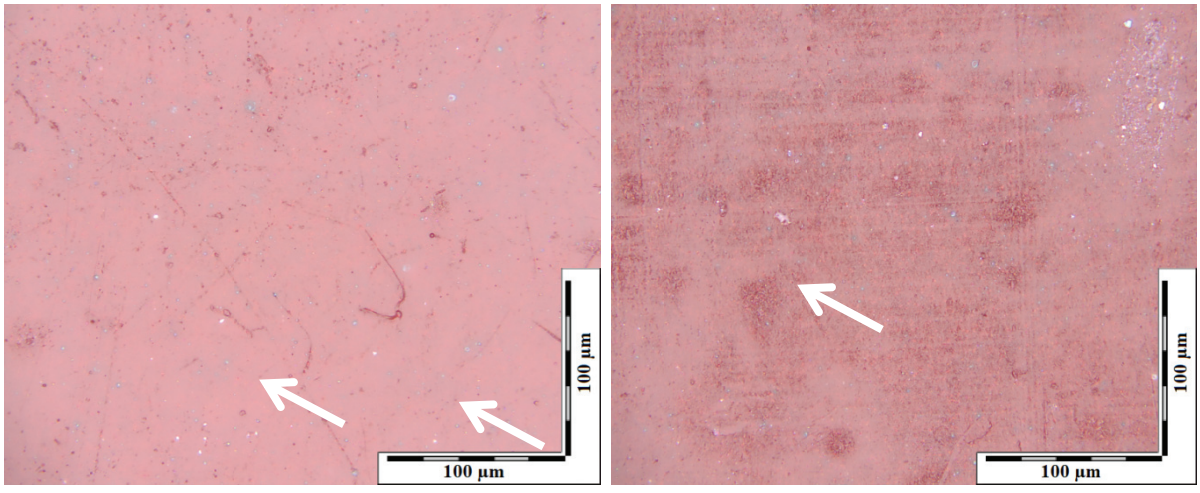

(*a*) (*b*)

Fig. 7. Surface micrographs of samples with 5 % Fe_2O_3 crystalline spheres (*a*) before climate chamber, (*b*) after exposure in the climate chamber (arrows highlight numerous areas of surface erosion)

showed that the degree of crystallinity slightly increased after exposure in the climatic chamber as a result of prolonged treatment at elevated temperature. At the same time, the melting range shows a peak at lower temperatures (76–85 °C), which may be responsible for the melting of partially destructed fragments of branched macromolecules with a lower degree of order and reduced molecular weight. At the same time, the main peak shifted slightly to higher temperatures, which may be due to both measurement error and the possible formation of cross-linked structures that hinder primary melting.

The surface of the samples before and after aging was examined by optical microscopy (Fig. 7).

Microphotographs (Fig. 6) show significant surface erosion after exposure in the climatic chamber. This erosion is presumably related to the oxidation of the polyethylene surface and the occurrence of microcracks and spalling of the oxidized material as a result of cyclic heating and cooling.

Comparing the results with similar approaches, it should be noted that introduction of various additives into the composite composition affects mechanical properties. The aging of polypropylene (PP) composites reinforced with date palm nanofiber was studied by Basheer A. Alshammari and colleagues [26]. In this study [26] the authors showed similar results: strain at break decreased in the modified composites. The paper [27] analyzed the use of the most common metal stearates as additives initiating oxidative degradation of polyolefins. The study found that calcium stearate is most susceptible to oxidative degradation in contrast to zinc and magnesium stearates. The effect of accelerated weathering on poly(3-hydroxybutyrate-co-3-hydroxyvalerate) (PHBV) and PHBV-based nanocomposites with rutile titanium (IV) dioxide (PHBV/TiO_2) was investigated in paper [28]. In this case the addition of TiO_2 enhanced the mechanical properties of the nanocomposites, the nucleation effect retarded the degradation process under photo and moisture exposure, shifting the degradation process to longer periods of time. Thus, addition of various modifiers to polymer compositions is relevant, and the properties of the developed composites may differ depending on the sphere of application of such material.

4. Conclusion

The present study showed a promising possibility of using nanostructured iron oxide microspheres obtained by spray-pyrolysis of ultrasonic aerosols as an additive accelerating atmospheric aging of polyethylene.

After climatic tests of the original polyethylene and polyethylene modified with microspheres, a higher degree of surface oxidation was observed in the case of the modified material.

The study of the influence of the crystalline structure of iron oxide in the composition of the synthesized filler on the rate of atmospheric aging of polyethylene showed that the use of heat-treated (crystalline) microspheres slightly more effectively increased the intensity of the C=O bond peak on the IR spectra of the composite after aging in the climatic chamber, compared to the X-ray amorphous (initial) spheres.

Optical microscopy of the surface of polyethylene samples before and after aging showed strong surface erosion for polyethylene modified with microspheres, which may contribute to the active reproduction of microorganisms, provoking more intensive biodegradation compared to the original polymer.

The introduction of up to 5 wt. % of microspheres into PE did not lead to a significant change in the properties of the material, as shown by our studies, in connection with which it can be assumed that the developed material can find a wide application for the manufacture of packaging, agricultural and landscape films, which will decompose in natural conditions after the end of the service life.

5. Funding

This research received no external funding.

6. Conflict of interests

The authors declare no conflict of interests.

References

1. The Economist. *The Known Unknowns of Plastic Pollution*. Available from: https://www.economist.com/international/2018/03/03/the-known-unknowns-of-plastic-pollution [Accessed 4 March 2024]

2. Jakubowicz I. Evaluation of degradability of biodegradable polyethylene (PE). *Polymer Degradation and Stability*. 2003;80(1):39-43. DOI:10.1016/S0141-3910(02)00380-4

3. Chiellini E, Corti A, D'Antone S, Baciu R. Oxo-biodegradable carbon backbone polymers – Oxidative degradation of polyethylene under accelerated test conditions. *Polymer Degradation and Stability*. 2006;91(11):2739-2747. DOI:10.1016/j.polymdegradstab.2006.03.022

4. Ammala AJ, Bateman S, Dean KM, Petinakis E, et al. An overview of degradable and biodegradable

polyolefins. *Progress in Polymer Science*. 2011;36:1015-1049. DOI: 10.1016/j.progpolymsci.2010.12.002

5. Arráez FJ, María Luisa Arnal, Müller AJ. Thermal degradation of high-impact polystyrene with pro-oxidant additives. *Polymer Bulletin*. 2018;76(3):1489-1515. DOI:10.1007/s00289-018-2453-4

6. Cowie JMG, Arrighi V. *Polymers*. CRC Press; 2007. 520 p.

7. Contat-Rodrigo L. Thermal characterization of the oxo-degradation of polypropylene containing a pro-oxidant/pro-degradant additive. *Polymer Degradation and Stability*. 2013;98(11):2117-2124. DOI:10.1016/j.polymdegradstab.2013.09.011

8. Al-Salem SM, Al-Hazza'a A, Karam HJ, Al-Wadi MH, et al. Insights into the evaluation of the abiotic and biotic degradation rate of commercial pro-oxidant filled polyethylene (PE) thin films. *Journal of Environmental Management*. 2019;250:109475. DOI:10.1016/j.jenvman.2019.109475

9. Corti A, Muniyasamy S, Vitali M, Imam SH, Chiellini E. Oxidation and biodegradation of polyethylene films containing pro-oxidant additives: Synergistic effects of sunlight exposure, thermal aging and fungal biodegradation. *Polymer Degradation and Stability*. 2010;95(6):1106-1114. DOI:10.1016/j.polymdegradstab.2010.02.018

10. Kyrikou I, Briassoulis D, Hiskakis M, Babou E. Analysis of photo-chemical degradation behaviour of polyethylene mulching film with pro-oxidants. *Polymer Degradation and Stability*. 2011;96(12):2237-2252. DOI:10.1016/j.polymdegradstab.2011.09.001

11. Gusain R, Gupta K, Joshi P, Khatri OP. Adsorptive removal and photocatalytic degradation of organic pollutants using metal oxides and their composites: A comprehensive review. *Advances in Colloid and Interface Science*. 2019;272:102009. DOI:10.1016/j.cis.2019.102009

12. Arshady R. Microspheres for biomedical applications: preparation of reactive and labelled microspheres. *Biomaterials*. 1993;14(1):5-15. DOI:10.1016/0142-9612(93)90015-T

13. Paulose R, Mohan R, Parihar V. Nanostructured nickel oxide and its electrochemical behavior – A brief review. *Nano-Structures & Nano-Objects*. 2017;11:102-111. DOI:10.1016/j.nanoso.2017.07.003

14. Overcash JW, Suslick KS. High surface area iron oxide microspheres via ultrasonic spray pyrolysis of ferritin core analogues. *Chemistry of Materials*. 2015;27(10):3564-3567 DOI:. 10.1021/acs.chemmater.5b00766

15. Jakubowicz I, Yarahmadi N, Arthurson V. Kinetics of abiotic and biotic degradability of lowdensity polyethylene containing prodegradant additives and its efect on the growth of microbial communities. *Polymer Degradation and Stability*. 2011;96(5):919-928. DOI:10.1016/j.polymdegradstab.2011.01.031

16. Fontanella S, Bonhomme S, Brusson JM, Pitteri S, et al. Comparison of biodegradability of various polypropylene films containing pro-oxidant additives based on Mn, Mn/Fe or Co. *Polymer Degradation and Stability*. 2013;98(4):875-884. DOI:10.1016/j.polymdegradstab.2013.01.002

17. Gulmine JV, Janissek PR, Heise HM, Akcelrud L. Polyethylene characterization by FTIR. *Polymer Testing*. 2002;21(5):557-563. DOI:10.1016/S0142-9418(01)00124-6

18. Benítez A, Sánchez JJ, Arnal ML, Müller AJ, et al. Abiotic degradation of LDPE and LLDPE formulated with a pro-oxidant additive. *Polymer Degradation and Stability*. 2013;98(2):490-501. DOI:10.1016/j.polymdegradstab.2012.12.011

19. Amelia RPD, Gentile S, Nirode W, Huang L. Quantitative analysis of copolymers and blends of polyvinyl acetate (PVAc) using fourier transform infrared spectroscopy (FTIR) and elemental analysis (EA). *World Journal of Chemical Education*. 2016;4(2):25-31. DOI:10.12691/wjce-4-2-1

20. Minaeva VA, Minaev BF, Baryshnikov GV, Romeyko OM, Pittelkow M. The FTIR spectra of substituted tetraoxa[8]circulenes and their assignments based on DFT calculations. *Vibrational Spectroscopy*. 2013;65:147-158. DOI:10.1016/j.vibspec.2013.01.001

21. Luo M, Olivier GK, Frechette J. Electrostatic interactions to modulate the reflective assembly of nanoparticles at the oil-water interface. *Soft Matter*. 2012;8(47):11923-11932. DOI:10.1039/C2SM26890F

22. Pablos JL, Abrusci C, Marín I, López-Marín J, et al. Photodegradation of polyethylenes: Comparative effect of Fe and Ca-stearates as pro-oxidant additives. *Polymer Degradation and Stability*. 2010;95(10):2057-2064. DOI:10.1016/j.polymdegradstab.2010.07.003

23. Zapata P, Palza H, Díaz B, Armijo A, et al. Effect of $CaCO_3$ Nanoparticles on the mechanical and photo-degradation properties of LDPE. *Molecules*. 2018;24(1):126. DOI:10.3390/molecules24010126

24. Miyazaki K, Arai T, Shibata K, Terano M, Nakatani H. Study on biodegradation mechanism of novel oxo-biodegradable polypropylenes in an aqueous medium. *Polymer Degradation and Stability*. 2012;97(11):2177-2184. DOI: 10.1016/j.polymdegradstab.2012.08.010

25. Li J, Yang R, Yu J, Liu Y. Natural photo-aging degradation of polypropylene nanocomposites. *Polymer Degradation and Stability*. 2008;93(1):84-89. DOI:10.1016/j.polymdegradstab.2007.10.022

26. Alshammari BA, Alothman OY, Alhamidi A, Jawaid M, Shaikh HM. Effect of accelerated weathering on the thermal, tensile, and morphological characteristics of polypropylene/date nanofiller composites. *Materials.* 2022;15(17):6053. DOI:10.3390/ma15176053

27. Ovchinnikov VA, Abushahmanova ZR, Mastalygina EE, Pantyuhov PV, et al. Kinetic features of oxidative degradation of polyethylene at addition of stearates of various transition metals. *Vse Materialy. Entsiklopedicheskiy Spravochnik = Polymer Science, Series D*. 2024;1:31-36. DOI:10.31044/1994-6260-2024-0-1-31-36 (In Russ.)

28. Antunes A, Popelka A, Aljarod O, Hassan MK, Kasak P, Luyt AS. Accelerated weathering effects on poly(3-hydroxybutyrate-co-3-hydroxyvalerate) (PHBV) and PHBV/TiO_2. *Nanocomposites. Polymers*. 2020;12(8):1743. DOI:10.3390/polym12081743

Information about the authors / Информация об авторах

Dmitrii A. Metlenkin, Engineer, Plekhanov Russian University of Economics, Moscow, Russian Federation; ORCID 0000-0002-7006-2253; e-mail: dametl@mail.ru

Nikolay V. Kiselev, Leading Specialist, Plekhanov Russian University of Economics; Engineer, National University of Science and Technology "MISIS", Moscow, Russian Federation, Moscow, Russian Federation; ORCID 0000-0003-0541-7035; e-mail: nikokisely12345@gmail.com

Bekzod B. Khaydarov, Cand. Sc. (Eng.), Engineer, National University of Science and Technology "MISIS"; Leading Researcher, Plekhanov Russian University of Economics, Moscow, Russian Federation; Moscow, Russian Federation; ORCID 0000-0003-2769-7437; e-mail: bekzod1991@mail.ru

Dmitrii S. Suvorov, Engineer, National University of Science and Technology "MISIS", Moscow, Russian Federation; Laboratory Assistant, Plekhanov Russian University of Economics, Moscow, Russian Federation; ORCID 0000-0002-0358-9987; e-mail: suvorov8225@yandex.ru

Elena A. Boychenko, Researcher, N.N. Semenov Federal Research Center for Chemical Physics RAS; Laboratory Assistant, Plekhanov Russian University of Economics, Moscow, Russian Federation; Engineer, National University of Science and Technology "MISIS", Moscow, Russian Federation; ORCID 0000-0001-9216-7147; e-mail: elena.boychenko.sar@gmail.com

Vasily A. Ovchinnikov, Cand. Sc. (Chem.), Senior Researcher, Plekhanov Russian University of Economics, Moscow, Russian Federation; ORCID 0000-0002-1827-905X; e-mail: OvchinnikovVA@rea.ru

Zubarzhat R. Abushakhmanova, Junior Researcher, Plekhanov Russian University of Economics, Moscow, Russian Federation; ORCID 0000-0002-4848-357X; e-mail: Zubarzhat.Akh@gmail.com

Evgeniy A. Kolesnikov, Engineer, National University of Science and Technology "MISIS", Moscow, Russian Federation; ORCID 0000-0001-7241-6214; e-mail: kolesnikov.ea@misis.ru

Igor N. Burmistrov, D. Sc. (Eng.), Director, Plekhanov Russian University of Economics; Leading Expert, National University of Science and Technology "MISIS", Moscow, Russian Federation; ORCID 0000-0003-0776-2465; e-mail: burmistrov.in@rea.ru

Метленкин Дмитрий Андреевич, инженер, Российский экономический университет имени Г. В. Плеханова, Москва, Российская Федерация; ORCID 0000-0002-7006-2253; e-mail: dametl@mail.ru

Киселев Николай Витальевич, ведущий специалист, Российский экономический университет имени Г. В. Плеханова; инженер, Национальный исследовательский технологический университет «МИСИС», Москва, Российская Федерация; Москва, Российская Федерация; ORCID 0000-0003-0541-7035; e-mail: nikokisely12345@gmail.com

Хайдаров Бекзод Бахтиёрович, кандидат технических наук, инженер, Национальный исследовательский технологический университет «МИСИС»; ведущий научный сотрудник, Российский экономический университет имени Г. В. Плеханова, Москва, Российская Федерация; Москва, Российская Федерация; ORCID 0000-0003-2769-7437; e-mail: bekzod1991@mail.ru

Суворов Дмитрий Сергеевич, инженер, Национальный исследовательский технологический университет «МИСИС», Москва, Российская Федерация; лаборант-исследователь, Российский экономический университет имени Г. В. Плеханова, Москва, Российская Федерация; ORCID 0000-0002-0358-9987; e-mail: suvorov8225@yandex.ru

Бойченко Елена Андреевна, научный сотрудник, Федеральный исследовательский центр химической физики им. Н. Н. Семенова РАН; лаборант, Российский экономический университет имени Г. В. Плеханова; инженер, Национальный исследовательский технологический университет «МИСИС», Москва, Российская Федерация; ORCID 0000-0001-9216-7147; e-mail: elena.boychenko.sar@gmail.com

Овчинников Василий Андреевич, кандидат химических наук, старший научный сотрудник, Российский экономический университет имени Г. В. Плеханова, Москва, Российская Федерация; ORCID 0000-0002-1827-905X; e-mail: OvchinnikovVA@rea.ru

Абушахманова Зубаржат Рафисовна, младший научный сотрудник, Российский экономический университет имени Г. В. Плеханова, Москва, Российская Федерация; ORCID 0000-0002-4848-357X; e-mail: Zubarzhat.Akh@gmail.com

Колесников Евгений Александрович, инженер, Национальный исследовательский технологический университет «МИСИС», Москва, Российская Федерация; ORCID 0000-0001-7241-6214; e-mail: kolesnikov.ea@misis.ru

Бурмистров Игорь Николаевич, доктор технических наук, директор инжинирингового центра, Российский экономический университет имени Г. В. Плеханова; ведущий эксперт, Национальный исследовательский технологический университет «МИСИС», Москва, Российская Федерация; ORCID 0000-0003-0776-2465; e-mail: burmistrov.in@rea.ru

Received 04 April 2024; Accepted 06 May 2024; Published 04 July 2024

Original papers
Materials for energy and environment, next-generation photovoltaics, and green technologies

УДК 621.311 DOI: 10.17277/jamt.2024.02.pp.110-121

Encapsulation of solar cells in a transparent polymer composite material

© Ivan Yu. Dmitriev[a]✉, Artem V. Kochergin[a,c], Sergey A. Yakovlev[a,b], Vladimir S. Levitskii[a], Alexey S. Abramov[a], Eugenii I. Terukov[a,b,c]

[a] *R&D Center of Thin Film Technologies in Energetics, 28, Politekhnicheskaya St., Saint Petersburg, 194064, Russian Federation,*
[b] *Ioffe Physical-Technical Institute of the Russian Academy of Sciences, 26, Politekhnicheskaya St., Saint Petersburg, 194021, Russian Federation,*
[c] *Saint Petersburg Electrotechnical University "LETI", 5, Professora Popova St., Saint Petersburg, 197022, Russian Federation*

✉ I.Dmitriev@hevelsolar.com

Abstract: Lightweight photovoltaic modules are becoming increasingly popular in many technical applications. This study proposes an approach to the production of a glass-filled prepreg encapsulant for solar cells lamination. Lamination of solar cells strings can result in the creation of a transparent and mechanically strong protective composite material. Prototypes of composite photovoltaic modules with high-efficiency HJT solar cells connected using electroconductive adhesive technology were fabricated. The climatic resistance of the obtained samples was estimated. It was found that composite modules pass successfully thermal cycling, UV exposure and hail tests. Damp heat test has revealed increased degradation. Degradation caused by moisture penetration initiates corrosion processes in the layers of transparent conductive oxide ITO or contact metallization mesh. The use of composite polymer material makes it possible to reduce the weight of photovoltaic modules due to the use of sheet glass in their design while maintaining an acceptable level of their climatic resistance.

Keywords: photovoltaic cells; photovoltaic module; heterostructure silicon cells; silicon; solar cells; polymer composite materials; light transmission; thermal cycling; hail resistance.

For citation: Dmitriev IYu, Kochergin AV, Yakovlev SA, Levitskii VS, Abramov AS, Terukov EI. Encapsulation of solar cells in a transparent polymer composite material. *Journal of Advanced Materials and Technologies*. 2024;9(2):110-121. DOI: 10.17277/jamt.2024.02.pp.110-121

Инкапсуляция фотоэлектрических преобразователей в прозрачный полимерный композиционный материал

© И. Ю. Дмитриев[a]✉, А. В. Кочергин[a,c], С. А. Яковлев[a,b], В. С. Левицкий[a], А. С. Абрамов[a], Е. И. Теруков[a,b,c]

[a] *Научно-технический центр тонкопленочных технологий в энергетике, ул. Политехническая, 28, Санкт-Петербург, 194064, Российская Федерация,*
[b] *Физико-технический институт им. А. Ф. Иоффе РАН, ул. Политехническая, 26, Санкт-Петербург, 194021, Российская Федерация,*
[c] *Санкт-Петербургский государственный электротехнический университет «ЛЭТИ», ул. Профессора Попова, 5, Санкт-Петербург, 197022, Российская Федерация*

✉ I.Dmitriev@hevelsolar.com

Аннотация: Легковесные фотоэлектрические модули становятся все более востребованными во многих технических применениях. В работе предложен подход к изготовлению стеклонаполненного инкапсулянта-препрега для ламинирования фотоэлектрических преобразователей. В процессе ламинации матрицы скоммутированных фотоэлектрических преобразователей образуется прозрачный и ударопрочный защитный композиционный материал. Проведена характеристика структуры и свойств композиционного материала с применением спектрофотометрии, инфракрасной спектроскопии и термического анализа. Изготовлены

прототипы композитных фотоэлектрических модулей с высокоэффективными кремниевыми ячейками гетероструктурного типа, скоммутированными с применением клеевой технологии. Проведена оценка климатической стойкости полученных образцов. Установлено, что прототипы композитных фотоэлектрических модулей хорошо проходят испытания на термоциклирование, УФ-воздействие и градостойкость. Испытания композитных модулей выявили относительно высокую деградацию во время воздействия высокой температуры при высокой влажности. Деградация, вызванная проникновением влаги через композиционное покрытие, запускает коррозионные процессы в слоях прозрачного проводящего оксида ITO или контактной металлизационной сетки. Применение композиционного полимерного материала позволяет существенно снизить вес фотоэлектрических модулей за счет ухода от применения листового стекла в их конструкции при сохранении приемлемого уровня их климатической стойкости.

Ключевые слова: фотоэлектрический преобразователь; фотоэлектрический модуль; гетероструктурная технология; кремний; солнечные элементы; полимерные композиционные материалы; светопропускание; термоциклирование; градостойкость.

Для цитирования: Dmitriev IYu, Kochergin AV, Yakovlev SA, Levitskii VS, Abramov AS, Terukov EI. Encapsulation of solar cells in a transparent polymer composite material. *Journal of Advanced Materials and Technologies*. 2024;9(2):110-121. DOI: 10.17277/jamt.2024.02.pp.110-121

1. Introduction

Technical solutions in the development of lightweight photovoltaic modules (PVMs) are in demand in connection with the spread of solar energy in the areas of its integration into architecture, industrial and urban infrastructure, transport, mobile devices, communications equipment, and products for non-civilian use. The reliability of a typical PVM is ensured by the use of front and rear protective glass in its design, which makes a critical contribution to its weight. The specific weight of a glass-to-glass PVM structure is 15–16 kg·m^{-2}, while in a glass-free structure this value is 2–4 kg·m^{-2}. It is obvious that avoiding the use of sheet glass in the design of PVMs while maintaining an acceptable level of their climatic resistance and impact strength is an important practical task. At the scientific and technical center of the Hevel Group of Companies (*LLC Scientific and Technical Center of Thin-Film Technologies in Energy*), semi-flexible lightweight batteries have been developed that can be used to solve a wide range of similar problems. Some examples of implemented projects are shown in Fig. 1.

Fig. 1. Examples of completed projects for the integration of semi-flexible lightweight PVMs in sea, air, and mobile deployable applications

A common approach in the solar energy industry is to produce semi-flexible, lightweight PVMs by replacing the front glass with a protective transparent sheet based on polyethylene terephthalate (PET) or ethylene tetrafluoroethylene copolymer (ETFE). Multilayer PET-based sheets, as well as fiberglass laminates and honeycomb panels are used as the back protective substrate. These structures use polymeric encapsulating materials in a highly elastic state, the same type as in industrial glass-to-glass PVMs or glass-to-protective back sheet structures. Semi-flexible lightweight PVMs based on heterojunction silicon photovoltaic converters (HJT solar cells) have a number of disadvantages: low shock and hail resistance, destruction of busbar jumpers during thermal cycling, the appearance of delamination and increased corrosion of HJT solar cells when exposed to high temperatures and high humidity [1–3].

The climatic and mechanical reliability of PVMs of any design is largely determined by the materials used and their mutual compatibility. The introduction of fiberglass reinforcing materials into the encapsulant can significantly improve the impact resistance of glassless modules [4–7]. This is achieved by immersing a matrix of connected solar cells in a durable, lightweight and optically transparent composite material. Composite PVMs can be made by pouring curable epoxy compounds into interconnected solar cells using Resin Transfer Molding technology. However, a more effective approach involves the production of a glass-filled prepreg encapsulant, which can be used to laminate PVMs in an industrial membrane vacuum laminator. Prepreg contains a hot-melt binder, which, when heated, takes the required shape and vulcanizes, actually turning into a solid aggregate state.

The purpose of this study is to develop a method for encapsulating solar cells into a transparent, impact-resistant composite material and assess the climatic resistance of the resulting samples. To solve the problem, it was proposed to use a polymer thermosetting material of epoxy-acrylic chemical nature. The main feature of the material under development is that it is based on a chemical cross-linkable system capable of processing within technological parameters close to those used in mass production of PVMs (using polyolefin-based film laminations). A separate objective of this study was to compare PVMs made with the new composite technology in terms of reliability with semi-flexible lightweight PVMs of traditional design using front and back protective sheets based on PET and laminating polyolefin films of the POE type.

2. Materials and Methods

2.1. Initial components

The study used silicon heterostructure (*n*-type, HJT technology) five-bar solar cells of M2+ format (157.35×157.35 mm) produced by Hevel. Metallization of the contact mesh was carried out by screen printing using an electrically conductive adhesive. The PV cells were connected to each other on an industrial stringer at the production site of the Hevel Company.

The commercial product, the thermosetting powder composition FREOCRYL Powder Coating PY1005BR999C, manufactured by Freilacke, was used as a polymer binder. This composition was chosen due to the fact that after curing it forms a transparent coating and has a processing temperature that is close to the temperature used in typical PVM lamination technology (about 140–160 °C). The powder composition is a polymer composition of epoxy-acrylic nature; its exact composition is not disclosed by the manufacturer, however, general technological aspects of production are given in [8]. An important difference between the cured polymer is its high glass transition temperature (more than 60 °C), which causes a high rigidity value (the cured polymer is close to plexiglass in mechanical characteristics). The latter circumstance favorably distinguishes the proposed approach from the common lamination technology using film encapsulants, which have a very low glass transition temperature (usually below –40 °C) and are in a highly elastic state under PVM operating temperatures.

Commercial plain weave glass fabric with a density of 80 $g \cdot m^{-2}$ based on EC6-34tex fiber was used as a reinforcing material. Photovoltaic rear protective sheets based on fluorinated polyethylene terephthalate and front ETFE films with corona treatment with a thickness of 50–150 microns were used.

2.2. Methodology for preparing composite PVMs

Composite PVM samples were prepared in two steps (Table 1). The first stage is the production of prepreg – a sheet material consisting of fiberglass with a polymer binder fused to it. To make the prepreg, the glass fabric was placed on a heating table with a set temperature of about 100 °C, and then the polymer powder was manually applied, distributing it along the surface with a spatula, evenly pressing the melting polymer into the glass fabric and cleaning off the non-absorbable excess. Then the material was

Table 1. Sequence of manufacturing PVM samples

Stage 1. Preparation of samples (prepregs)	Stage 2. Lamination of the module with prepregs
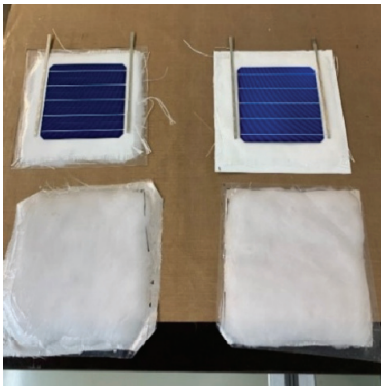	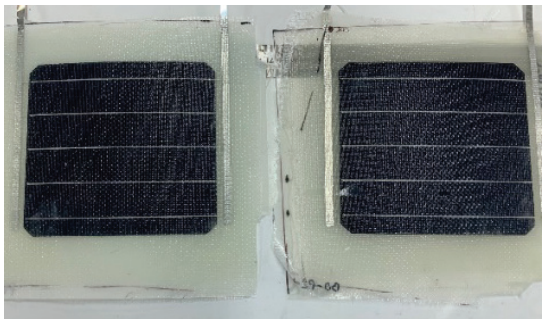

pressed (rolling with a hand roller for 5–15 seconds). The prepreg prepared in this way contained a binder, the content of which was determined by the absorbency of the fiberglass fabric. The weight of the powder in a fiberglass-based prepreg with a density of 80 $g \cdot m^{-2}$ was (632 ± 109) $g \cdot m^{-2}$. The resulting prepreg had a thickness of (420 ± 55) microns.

At the second stage – lamination of the module blank – the prepreg was used as a laminate to bond the solar cell matrix to the front ETFE sheet and the rear PET protective sheet. The PVM samples were prepared using a laboratory membrane vacuum laminator at the following mode: temperature 160 °C, evacuation time 5 min, pressure build-up time 1 min, pressure 500 mbar, pressure application time 25 min. During the lamination process, the workpiece was positioned with its front side facing the heating plate of the laminator. After lamination, the PVM was cooled under load.

Reference semi-flexible lightweight PVMs of traditional design were manufactured from commercial 320 μm PET front and back sheets and 520 $g \cdot m^{-2}$ polyolefin polyolefin films. The PVM assembly was carried out on the same equipment using a technological regime that ensured cross-linking of POE laminates of at least 80 % (measured gel content using the xylene dissolution method).

2.3. Analytical methods and test conditions

A Nicolet 8700 FT-IR spectrometer and an Agilent Cary 5000 spectrophotometer were used to analyze the structure and properties of the encapsulating material.

The thermal properties of the materials were studied by differential scanning calorimetry (DSC) and thermogravimetric analysis (TGA) on a ZH-1000 synchronous analyzer (Shanghai Innuo Precision Instruments Co., Ltd.). The measurements were carried out in the temperature range from 30 to 200 °C, at a scanning speed of 10 $°C \cdot min^{-1}$ in an air atmosphere. Samples were weighed at 15–20 mg.

Climatic tests of the modules for reliability included the following tests according to the conditions of Russian Standard R 56980.2 (IEC 61215-2:2016) - 2020: damp heat test (section 4.10), thermal cycling (section 4.8), test for exposure to ultraviolet radiation with frontal exposure of the sample (section 4.7).

The test for resistance to hail impacts was carried out under standard conditions according to Russian Standard R 56980.2 (IEC 61215-2:2016) – 2020 section 4.14: hail diameter 25 mm, speed 22 $m \cdot s^{-1}$. During testing, two shots were fired - at the center and at the edge of each sample.

Electro- and photoluminescence images of the samples were obtained using LumiSolarCell and MBJ Solutions illumination stands, respectively.

The current-voltage characteristic (short circuit current I_{sc}, open circuit potential V_{oc}, power at maximum point P_{mpp} and FF duty cycle) was measured using a specialized I-V tester under standard conditions (1.5AM, 25 °C).

3. Results and Discussion

3.1 Characteristics of transparent composite material

Figure 2 shows the infrared spectrum of attenuated total internal reflection (ATR) of the binder polymer before and after curing. Table 2 shows the attribution data for the absorption bands observed in the spectrum [9–12]. Based on the data

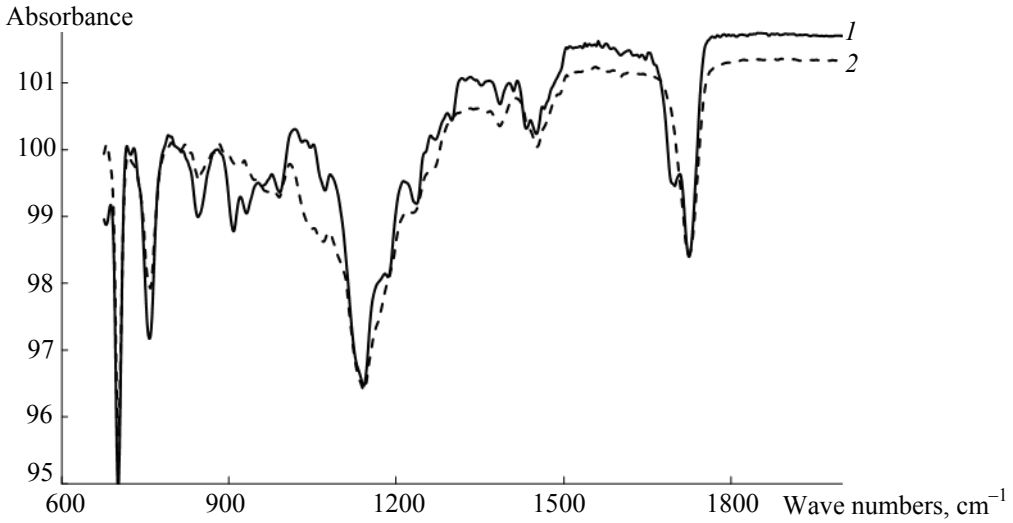

Fig. 2. ATR IR spectra of the binder polymer before (curve *1*) and after (curve *2*) curing

Table 2. Characteristic bands of the ATR IR spectra of the binder and cured composites (according to Fig. 2)

Prepreg	Cured polymer	Attribution
700	700	Flexural deformation of CH groups of monosubstituted aromatic compounds
757	757	Bending vibration of the CH group of the epoxy ring
760	760	Bending vibration of CH groups of epoxy ring
790	–	Stretching vibrations of Si–C bonds
846 907	–	Epoxy ring vibrations (glycidyl methacrylate)
966 990	966 990	Vibrations of Si–O–Si bonds
1030	–	Vibrations of Si–C bonds
1074	1074	Stretching vibrations of C–O bonds of butyl acrylate and glycidyl methacrylate
1147	1147	
1189	1189	
1247	1247	
1238	1238	Bending vibrations of Si–C bonds
1302	1302	Glycidyl methacrylate side chain methyl groups (presumably)
1387	1387	Bending vibrations of C–H bonds
1410 1431	1431	Bending vibrations of groups of CH_2 groups
1452	1452	Aromatic group vibrations
1493	1493	
1600	1600	
1462	1462	Vibrations of C–H bonds of methylene groups of glycidyl methacrylate
1695 1728	1728	Stretching vibrations of carbonyl C=O, C–O, methacrylate groups of butyl and glycidyl methacrylate
2851 2937	–	Asymmetric and symmetric vibrations of CH_2 alkanes groups
3060	3060	C–H vibrations of aromatic groups
3026	3026	

obtained, it can be concluded that the binder is a copolymer containing acrylic comonomers (butyl methacrylate, glycidyl methacrylate), styrene, and grafted silane groups. The intensities of the bands at 845 and 906 cm^{-1}, attributed to vibrations of the epoxy ring [11], differ markedly between the prepreg and the cured polymer. This suggests that curing occurred through the reaction of the crosslinker with the epoxy groups of glycidyl methacrylate. It was found that after curing, the polymer material lost solubility in boiling xylene, with the insoluble residue reaching 95 %. The changes in bonds with Si noted in Table 2 can presumably be attributed to changes in silane additives that act as adhesion promoters. A more detailed analysis of the comonomer composition of the base polymer, the content of functional additives, and the degree of conversion using chromatographic and spectroscopic methods will be presented in a separate study.

During the first heating cycle the DSC curve (Fig. 3) reveals a glass transition transition in the temperature range of 50–70 °C and a melting peak around 118 °C. The crosslinking chemical reaction is detected as a peak at 160 °C. Comparing the thermogram data with IR spectroscopy data, we can conclude that the transition corresponding to the glass transition is associated with the softening of the copolymer of glycidyl methacrylate with butyl methacrylate [14], and the melting observed at 118 °C referred to dodecanedioic acid, which was used as a cross-linker for this group of copolymers [8]. During the second and further cycles of cooling/heating of the sample, the noted melting process is not observed, however, a glass transition transition is detected in the region of 78 °C (Fig. 3, inset).

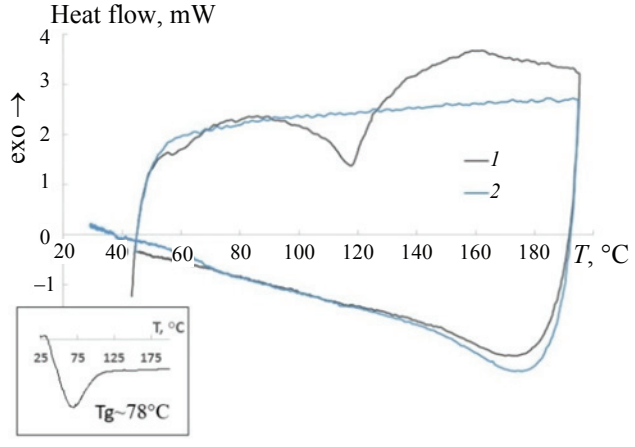

Fig. 3. DSC curve of a polymer binder (*1* – first pass, *2* – second pass); inset – DSC scanning section of the cured composite to determine Tg

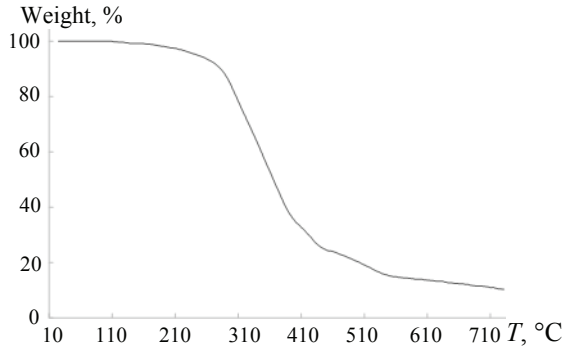

Fig. 4. TGA composite curve

An important feature of this polymer material is that it is based on a chemical cross-linkable system, the thermal behavior of which is close to the behavior of POE or EVA laminating films common in the solar industry. Thanks to this, the composite laminate is capable of processing within technological parameters close to those used in PVM mass production.

The cured composite material shows relatively high thermal stability (Fig. 4). According to thermogravimetry data, it was found that when heated to a temperature of 102 °C, the material lost no more than 0.1 % of its weight; a loss of 1.0 % of weight was observed only when reaching 162 °C, 10 % – at 280 °C, 50 % – at 364 °C. The process of thermal decomposition of the main polymer unit began at a temperature of about 243 °C. After complete burnout of organic residues, the weight of the remaining glass fiber occupied about 10 % of the original weight of the sample.

As can be seen from the light transmission spectra (Fig. 5), the composite prepared by the described method is characterized by a relatively high level of light transmission – the average value in the wave range 400–900 nm was 89.6 %.

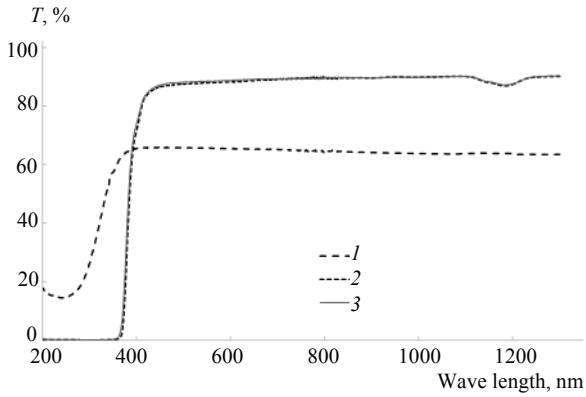

Fig. 5. Light transmittance of glass fabric (*1*), binder (*2*) and cured composite (*3*)

At a wavelength of 360 nm, transmission did not exceed 0.5 %. It is obvious that the polymer binder contains a substance that plays the role of a UV filter. It is significant that the transmission spectrum of the composite and the cured binder are identical, which indicates a good match of the refractive indices of the polymer and glass fabric.

3.2 Climatic testing of composite photovoltaic modules

It is known that silicon HJT solar cells exhibit increased degradation upon UV exposure [13]. UV-induced degradation of a heterostructural solar cell consists of a decrease in the lifetime of charge carriers, usually accompanied by a decrease in the V_{oc} and FF parameters, which is associated with the appearance of bulk defects in the a-Si:H structure and the interface between c-Si and a-Si:H. In practice, it is necessary to provide UV protection to HJT solar cells by introducing a UV absorbent component into the protective encapsulating layers. The behavior of a PVM sample with a UV exposure of at least 60 kW·h·m^{-2} corresponds to one year of operation in a temperate climate [16]. As can be seen from the results obtained (Fig. 6), the level of power degradation (P_{mpp}) of composite PVM samples after a frontal exposure of 60 kWh·m^{-2} slightly exceeded the degradation value of the reference sample prepared by lamination using a commercial POE polyolefin film containing a UV adsorber. Another PVM reference sample laminated to POE film without UV blocker showed noticeably higher (30 %) power degradation. The main contribution to the degradation of composite PVM under UV exposure after exposure to 60 kWh·m^{-2} was associated with a decrease in the I_{sc} parameter. For a reference sample laminated with a commercial POE film without a UV blocker, significant degradation in the I_{sc}, V_{oc} and FF parameters was observed. It is noteworthy that for the reference sample laminated to a commercial lamination film with a UV blocker, degradation was more pronounced for the FF parameter than for the I_{sc} parameter compared to the data for the composite PVM. This circumstance may be associated with different UV adsorbers used by different manufacturers of protective materials [15]. As a UV adsorber, additives based on benzophenones or benzotriazoles were used in combination with antioxidants and HALS stabilizers, and provided cutoff of the UV spectrum. The electroluminescence (EL) image of the composite sample showed no noticeable darkening (Fig. 7).

When testing for exposure to high temperature and high humidity (temperature 85 °C, humidity 85 %), increased PVM power degradation was detected, this exceeded 5 % when reaching 600 hours of experiment (Fig. 8). Degradation was accompanied by the appearance of darkening in EL images. In this case, the greatest contribution to the magnitude of power degradation was made by a decrease in the FF fill factor. Photoluminescence (PL) images of test samples with power degradation of more than 10 % had a uniform color (in contrast to the EL images of the corresponding solar cells).

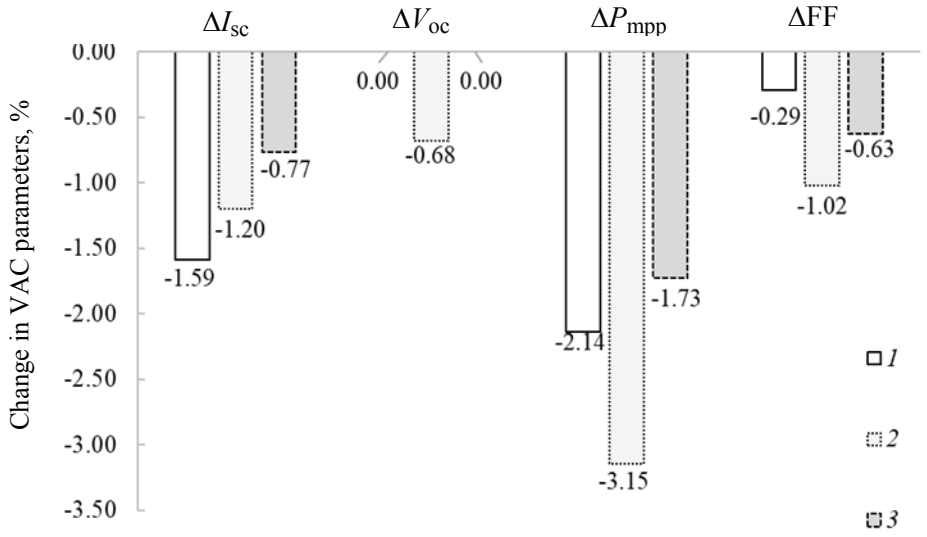

Fig. 6. The degradation value of the current-voltage characteristics (I_{sc}, V_{oc}, P_{mpp} and FF) for a composite PVM after UV exposure of 60 kW·h·m^{-2} (*1*), a reference PVM with a POE laminating film without a UV blocker (*2*) and a reference PVM with a laminating film with a UV blocker (*3*)

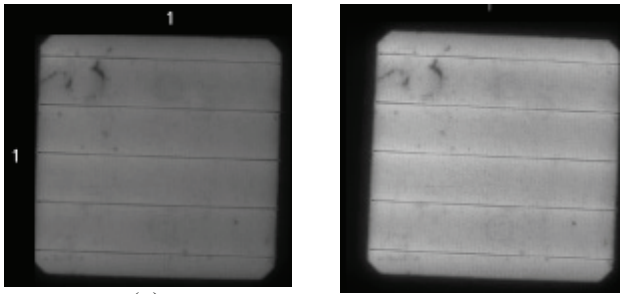

(*a*) (*b*)

Fig. 7. Electroluminescence image of a composite PVM sample before (*a*) and after (*b*) 60 kW·h·m^{-2} UV irradiation of the front side of the PVM

This allows us to conclude that the reduction in power occurred due to corrosion of the current collection system: in the layers of transparent conductive oxide ITO or on the elements of the contact mesh. Increasing the resistance of HJT solar cells to high temperatures and high humidity was a solvable problem and was achievable by using methods for cleaning the solar cell surface from contaminants, modifying the composition of metallizing materials, and also forming additional dielectric protective coatings [17, 18].

To carry out thermal cycling tests, PVMs with dimensions of 2×3 solar cell were manufactured (Fig. 9). The minimodules underwent 200 cycles of transitions between –40 °C – +85 °C with a final power degradation of 0.3 %, which was noticeably better than the results obtained when testing semi-flexible lightweight PVMs of traditional design using polyolefin encapsulating films [3]. Thus, the samples demonstrated high resistance to temperature changes, which was due to the fact that the rigid and glassy composite was capable of forming a frame resistant to thermomechanical effects, which increased the durability of busbars in solar cell chains.

The results of the damp heat and thermal cycling tests of PVMs of PET/POE/POE/PET design are shown in Table 3. The comparison of the results of these tests with the results obtained for composite PVMs (Figs. 6–8) shows that the composite structure is inferior traditional in moisture resistance, but noticeably superior in thermal cycling. The lower resistance of HJT solar cell composite encapsulation

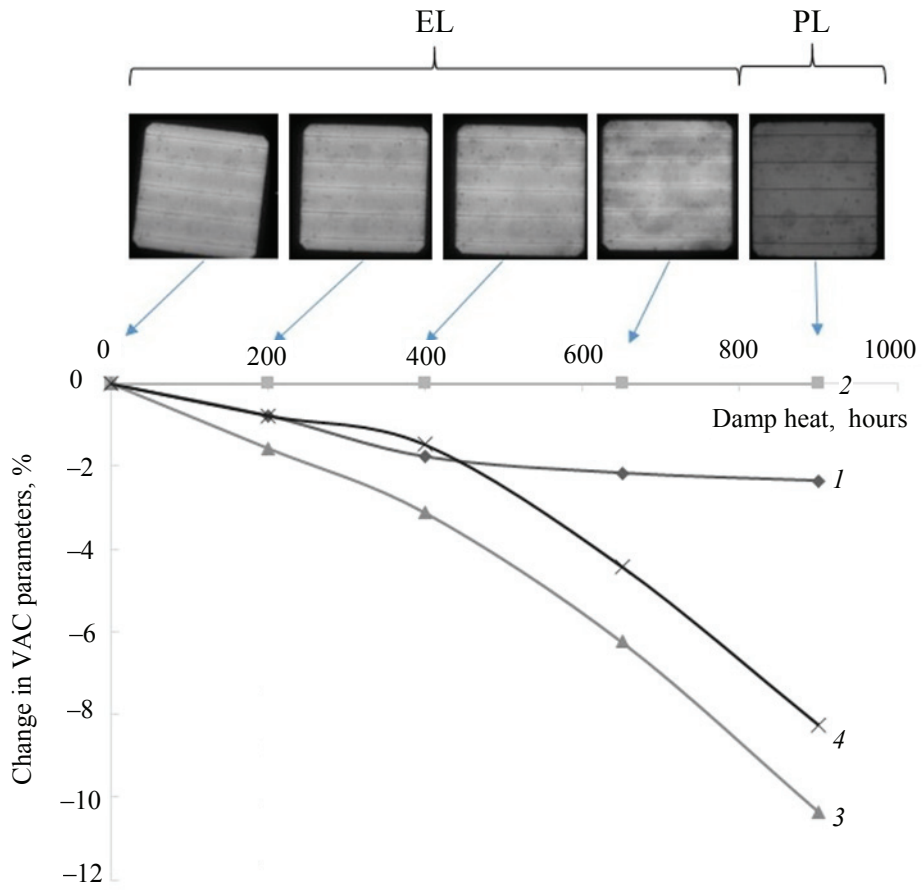

Fig. 8. Changing the values of the current-voltage characteristic parameters (I_{sc} (*1*), V_{oc} (*2*), P_{mpp} (*3*) and FF (*4*)) during damp heat test f a composite PVM, as well as EL and PL images of the corresponding samples

to moisture penetration is associated with the higher vapor transmission coefficient of acrylic polymers compared to polyolefin ones [19]. In addition, it is necessary to take into account the likely degradation of the polymer base during hydrolysis with the release of corrosive by-products of the reaction.

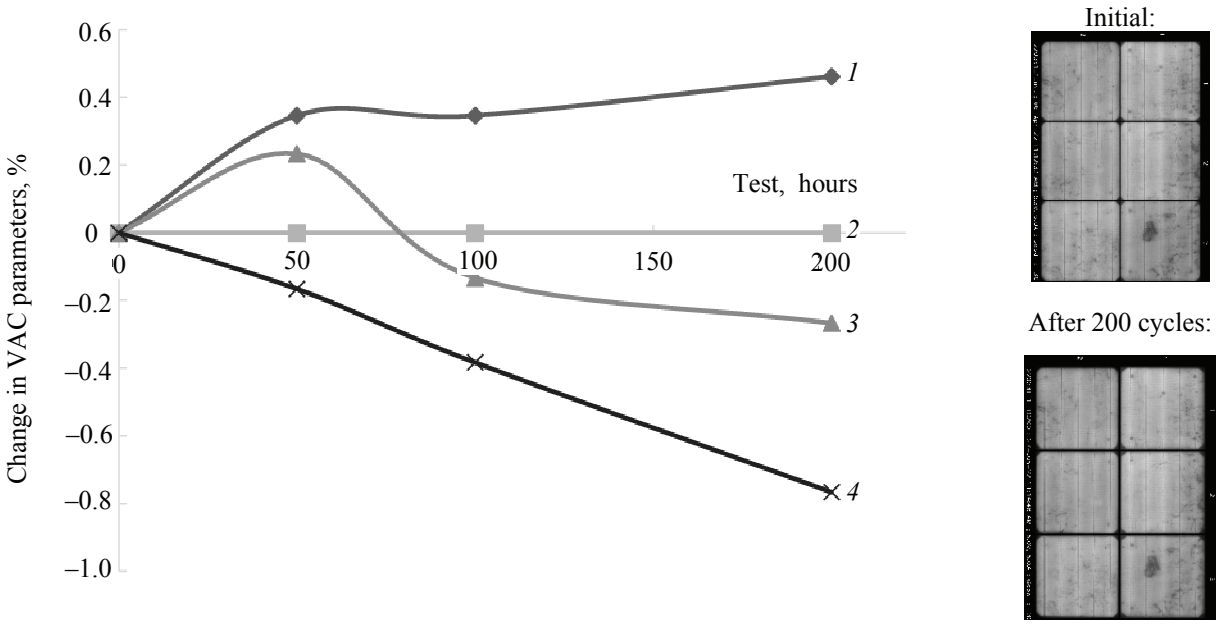

Fig. 9. Relative change in values I_{sc} (*1*), V_{oc} (*2*), P_{mpp} (*3*) and FF (*4*) when testing composite PVMs for thermal cycling and EL images of samples before and after testing (right)

Table 3. Results of damp heat and thermal cycling tests of PVMs of PET/POE/POE/PET design (reference modules)

Test	Results		
	Initial EL	EL after testing	P_{mpp} degradation after test
Exposure to high temperature and high humidity 1000 hours	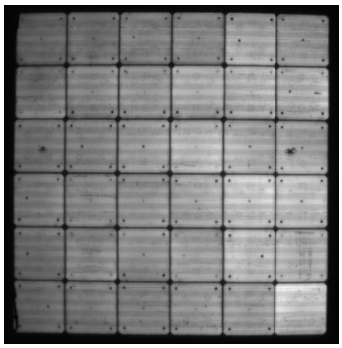	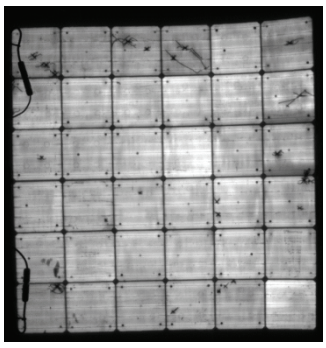	–1,0 %
	Initial EL	EL after testing	P_{mpp} degradation after test
Thermal cycling 200 cycles	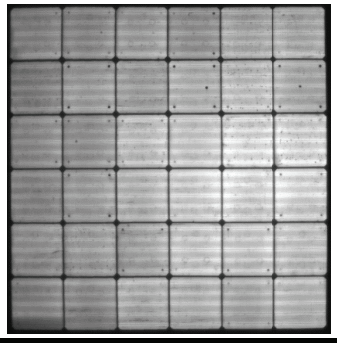	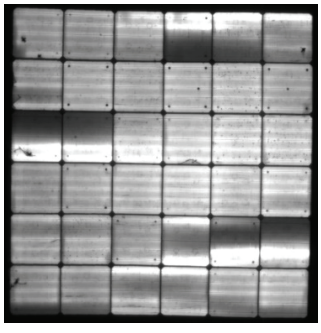	–10.5 %

Table 4. Hail resistance test results (EL images)

Sample	Initial	After being hit by hail Method of fixing PVM on a substrate	
		No gap from the rear	Gap from the rear
PVM composite construction	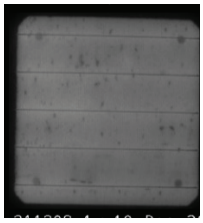	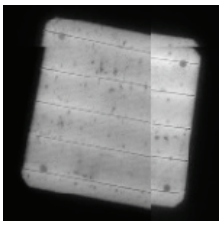	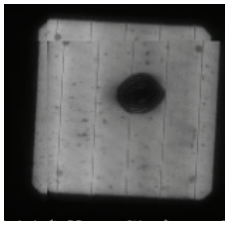
Solar cell lamination in PET/POE/POE/PET structure	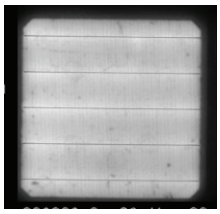	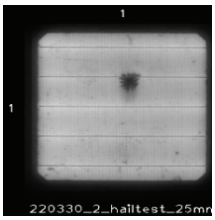	

For hail resistance tests (Table 4), two conditions for attaching samples were considered: 1) PVM fixed on the back side with double-sided tape to a rigid base, and 2) PVM fixed only at the edges in the absence of tight contact of the central part of the sample with the rigid base. It was found that if the back side of the PVM is tightly fixed to a rigid substrate, hail shots do not lead to any damage (Table 4). In case of loose contact with the base, damage remained in the central places of the module, i.e. in places where there is slight bulging of the module from the substrate. Thus, the effect of hail resistance of the modules occurs in conditions when the back side of the solar cell is completely supported by a sufficiently rigid base, which eliminates critical deflection of the fragile photovoltaic plate. The lack of a rigid base only on the back side of the solar cell is the main reason that semi-flexible lightweight PVMs of traditional design are not able to pass the hail test even when tightly fixed to a rigid base, since the back side of the solar cell is located on a viscoelastic, pliable base (polyolefin film) [2] . Thus, traditionally designed semi-flexible lightweight PVMs can be recommended more for deployable and portable solar generation systems with reduced impact requirements.

4. Conclusion

The study proposes to use a polymer thermosetting material of epoxy-acrylic chemical nature for the preparation of a composite laminating material on a fiberglass substrate. The prospects for using the resulting composite material for the lamination of high-performance silicon HJT solar cells and the production of lightweight impact-resistant PVMs have been studied. The general concept for the production of composite modules has been defined and PVM prototypes have been manufactured for reliability testing. Prototypes of composite PVMs with five-bar adhesive solar cells perform well in thermal cycling, UV exposure and hail resistance tests. However, testing of prototype composite modules revealed increased degradation during the damp heat test, which is associated with corrosion when water penetrates between the composite material and the ITO layer or contact mesh. The results obtained open up new prospects for expanding the scope of practical applications of heterostructure technology of silicon solar cells.

5. Funding

This study received no external funding.

6. Conflict of interests

The authors declare no conflict of interest.

References

1. Abramov A, Andronikov D, Emtsev K, Orekhov D, et al. Super lightweight flexible HJT solar panel. (eds.) *35th European Photovoltaic Solar Energy Conference and Exhibition, 23 – 28 September 2018.* USA: WIP - Renewable Energies; 2019. p.1227-1229. DOI:10.4229/35THEUPVSEC20182018-5CV.1.34

2. Yakovlev S, Schebet E, Emtsev K, Andronikov D, et al. Mechanical stability of semi-flexible solar panels. (eds.) *36th European Photovoltaic Solar Energy Conference and Exhibition, 9 – 13 September 2019.*

France: Fraunhofer Institute for Solar Energy Systems ISE; 2019. p.1040-1041. DOI: 10.4229/EUPVSEC20192019-4AV.1.22

3. Yakovlev S, Schebet E, Emtsev K, Andronikov D, et al. Environmental stability of semi-flexible HJT solar panels. (eds.) *37th European Photovoltaic Solar Energy Conference and Exhibition, 7 – 10 September 2020*. France: Fraunhofer Institute for Solar Energy Systems ISE; 2020. p. 1117-1119. DOI:10.4229/EUPVSEC20202020-4AV.2.18

4. Govaerts J, Luo B, Borgers T, Dyck R, et at. Development and testing of light-weight PV modules based on glass-fibre reinforcement. *EPJ Photovoltaics*. 2022;13:1-13. DOI:10.1051/epjpv/2022007.

5. Reinders A, Wit H, Boer A. Design of fibre reinforced pv concepts for building integrated applications. (eds.) *24th European Photovoltaic Solar Energy Conference and Exhibition*, *21 – 25 September 2009*. Germany: WIP - Renewable Energies; 2009. p.3940-3944.

6. Kyritsis A, Roman E, Kalogirou S, Nikoletatos J, et al. Households with fibre reinforced composite bipv modules in southern europe under net metering scheme. *Renewable Energy*. 2019;137(3):167-176. DOI:10.1016/j.renene.2017.09.068

7. Govaers J, Moliya K, Bin L, Borgers T, et al. The potential of glass-fibre-reinforcement: (thermo-) mechanical testing of light-weight PV modules. (eds.) *38th European Photovoltaic Solar Energy Conference and Exhibition*, *6 – 9 September 2021*. Germany: WIP Wirtschaft und Infrastruktur GmbH & Co Planungs KG. DOI:10.4229/EUPVSEC20212021-1AO.3.1.

8. Lu S, Holla R, Morley B. *Resin suitable for powder coating compositions*. United State patent 7,737,238. 15 May 2010.

9. Tzoumani I, Beobide A, Iatridi Z, Voyiatzis G, et al. Glycidyl methacrylate-based copolymers as healing agents of waterborne polyurethanes. *International Journal of Molecular Sciences.* 2022;23(15):8118. DOI:10.3390/ijms23158118

10. Anakabe J, Zaldua Huici AM, Eceiza A, Arbelaiz A. The effect of the addition of poly(styrene- co -glycidyl methacrylate) copolymer on the properties of polylactide/poly(methyl methacrylate) blend. *Journal of Applied Polymer Science*. 2016;133(37). DOI:10.1002/app.43935

11. Abdollahi H, Najafi V, Amiri F. Determination of monomer reactivity ratios and thermal properties of poly(GMA-co-MMA) copolymers. *Polymer Bulletin*. 2021;78:493-511. DOI:10.1007/s00289-020-03123-5

12. Li JL, Xie XM. Reconsideration on the mechanism of free-radical melt grafting of glycidyl methacrylate on polyolefin. *Polymer*. 2012;53(11):2197-2204. DOI:10.1016/j.polymer.2012.03.035

13. Yang P, Razzaq S, Jiao R, Hu Y, Liu L, Tao J. UV Light-induced degradation of industrial silicon HJT solar cells: degradation mechanism and recovery strategies. *Journal of Solar Energy Research Updates*. 2023;10:36-45. DOI:10.31875/2410-2199.2023.10.04

14. Kaya I, Ilter Z, Senol D. Thermodynamic interactions and characterisation of poly[(glycidyl methacrylate-co-methyl, ethyl, butyl) methacrylate] by inverse gas chromatography. *Polymer*. 2002;43(24):6455-6463. DOI:10.1016/s0032-3861(02)00554-2

15. Heidrich R, Barretta C, Mordvinkin A, Pinter G, et al. UV lamp spectral effects on the aging behavior of encapsulants for photovoltaic modules. *Solar Energy Materials and Solar Cells*. 2024;266:112674. DOI:10.1016/j.solmat.2023.112674

16. Tiefenthaler M, Wallner GM, Pugstaller R. Effect of global damp heat ageing on debonding of crosslinked EVA- and POE-glass laminates. *Solar Energy Materials and Solar Cells.* 2024;264:112602. DOI:10.1016/j.solmat.2023.112602

17. Sen C, Wang H, Wu X, Khan M, et al. Four failure modes in silicon heterojunction glass-backsheet modules. *Solar Energy Materials and Solar Cells*. 2023;257:112358. DOI:10.1016/j.solmat.2023.112358

18. Wu X, Sen C, Wang H, Wang X, et al. Addressing sodium ion-related degradation in SHJ cells by the application of nano-scale barrier layers. *Solar Energy Materials and Solar Cells.* 2024;264:112604. DOI:10.1016/j.solmat.2023.112604

19. Call J, Varde U, Konson A, Walters M, et al. Methodology and systems to ensure reliable thin-film PV modules. *Reliability of Photovoltaic Cells*, *Modules, Components, and Systems*. 2008;70480S. DOI:10.1117/12.797103

Information about the authors / Информация об авторах

Ivan Yu. Dmitriev, Cand. Sc. (Phys. and Math.), Lead Process Technologist, R&D Center of Thin Film Technologies in Energetics (R&D Center TFTE), Saint Petersburg, Russian Federation; ORCID 0000-0003-0605-9006; e-mail: I.Dmitriev@hevelsolar.com

Дмитриев Иван Юрьевич, кандидат физико-математических наук, ведущий технолог, Научно-технический центр тонкопленочных технологий в энергетике (НТЦ ТПТ), Санкт-Петербург, Российская Федерация; ORCID 0000-0003-0605-9006; e-mail: I.Dmitriev@hevelsolar.com

Artem V. Kochergin, Postgraduate Student, Saint Petersburg Electrotechnical University “LETI”, Saint Petersburg, Russian Federation; ORCID0009-0005-6670-8508; e-mail: A.Kochergin@hevelsolar.com

Кочергин Артем Владимирович, аспирант, Санкт-Петербургский государственный электротехнический университет «ЛЭТИ», Санкт-Петербург, Российская Федерация; ORCID 0009-0005-6670-8508; e-mail: A.Kochergin@hevelsolar.com

Sergey A. Yakovlev, Cand. Sc. (Phys. and Math.), Lead Process Technologist, R&D Center TFTE, Saint Petersburg, Russian Federation; ORCID0009-0009-3963-8355; e-mail: S.Yakovlev@hevelsolar.com

Vladimir S. Levitskii, Cand. Sc. (Eng.), Lead Measurements Specialist, R&D Center TFTE, Saint Petersburg, Russian Federation; ORCID 0000-0002-7877-1329; e-mail: V.Levitskiy@hevelsolar.com

Alexey S. Abramov, Cand. Sc. (Phys. and Math.), Head of Solar Energy Department, R&D Center TFTE, Saint Petersburg, Russian Federation; ORCID 0000-0003-4310-4478; e-mail: a.abramov@hevelsolar.com

Eugenii I. Terukov, D. Sc (Eng.), Professor, Deputy Director for Science, R&D Center TFTE, Saint Petersburg, Russian Federation; ORCID 0000-0002-4818-4924; e-mail: e.terukov@hevelsolar.com

Яковлев Сергей Александрович, кандидат физико-математических наук, ведущий технолог, НТЦ ТПТ, Санкт-Петербург, Российская Федерация; ORCID 0009-0009-3963-8355; e-mail: S.Yakovlev@hevelsolar.com

Левицкий Владимир Сергеевич, кандидат технических наук, ведущий специалист по измерениям, НТЦ ТПТ, Санкт-Петербург, Российская Федерация; ORCID 0000-0002-7877-1329; e-mail: V.Levitskiy@hevelsolar.com

Абрамов Алексей Станиславович, кандидат физико-математических наук, руководитель отдела солнечной энергетики, НТЦ ТПТ, Санкт-Петербург, Российская Федерация; ORCID 0000-0003-4310-4478; e-mail: a.abramov@hevelsolar.com

Теруков Евгений Иванович, доктор технических наук, профессор, заместитель генерального директора по научной работе, НТЦ ТПТ, Санкт-Петербург, Российская Федерация; ORCID 0000-0002-4818-4924; e-mail: e.terukov@hevelsolar.com

Received 17 April 2024; Accepted 20 May 2024; Published 04 July 2024

Original papers
Materials for energy and environment, next-generation photovoltaics, and green technologies

УДК 66.021:66.081.32 DOI: 10.17277/jamt.2024.02.pp.122-131

A study of adsorption characteristics of activated carbon material for typical organic and inorganic pollutants

© Igor N. Shubin[a]✉, Oksana A. Ananyeva[a]

[a] *Tambov State Technical University,*
Bld. 2, 106/5, Sovetskaya St., Tambov, 392000, Russian Federation

✉ i.shubin77@yandex.ru

Abstract: The paper presents the results of adsorption studies on the developed activated carbon material (AM), obtained by two activation methods – with one (AM1) and two activators (AM2), respectively, as well as its compacted versions (AMK) using polyvinyl alcohol (PVA), polyvinyl acetate (PVAC) and basalt fiber (BF) as binders, with regard to typical pollutants of aquatic environments – organic dyes and heavy metals. The carbon materials sorption capacity was assessed by the ability to remove dye molecules – "methylene blue" (MB) and "sunset yellow" (SY) using spectrophotometric analysis, as well as by the ability to remove heavy metal salts – lead (Pb^{2+}) using X-ray fluorescence spectrometry. As a result of adsorption kinetic studies, the absorption capacity of the starting material, activated and compacted materials was determined. The sorption capacity for lead for the materials carbonisate and AMK1 was 71 and 65 $mg \cdot g^{-1}$, respectively, the optimal sorption time was 30 minutes; for the materials AM1, AM2, AMK1/PVA, AMK1/PVAC and AMK1/BF 65, 66, 49, 45, 42 $mg \cdot g^{-1}$ accordingly, the optimal sorption time was 15 min. For MB and SY dyes, the parameters were 1000 – 2010 $mg \cdot g^{-1}$, 66 – 972 $mg \cdot g^{-1}$ and 15 min, respectively. To analyze the adsorption mechanisms using kinetic relationships and sorption isotherms, empirical equations of pseudo-first and pseudo-second order, Elovich equation and intraparticle diffusion model were used. The presented results show the possibility of using the developed activated carbon material as an effective sorbent of organic and inorganic pollutants from aqueous solutions.

Keywords: activated carbon material; compaction; adsorption; methylene blue; yellow sunset; lead; kinetics.

For citation: Shubin IN, Ananyeva OA. Studies of adsorption characteristics of activated carbon material for typical organic and inorganic pollutants. *Journal of Advanced Materials and Technologies*. 2024;9(2):122-131. DOI: 10.17277/jamt.2024.02.pp.122-131

Исследование адсорбционных характеристик активированного углеродного материала по отношению к типовым органическим и неорганическим загрязнителям

© И. Н. Шубин[a]✉, О. А. Ананьева[a]

[a] *Тамбовский государственный технический университет,*
ул. Советская, 106/5, пом. 2, Тамбов, 392000, Российская Федерация

✉ i.shubin77@yandex.ru

Аннотация: Представлены результаты исследований адсорбционной способности разработанного активированного углеродного материала (АМ), полученного двумя методами активации – с одним (АМ1) и двумя активаторами (АМ2) соответственно, а также его компактированных вариантов (АМК) с использованием в качестве связующих поливинилового спирта (ПВС), поливинилацетата (ПВА) и базальтового волокна (БВ) по отношению к типовым загрязнителям водных сред – органическим красителям и тяжелым металлам. Сорбционная способность углеродных материалов оценивалась по способности удаления молекул красителей – «метиленового синего» (МС) и «желтого «солнечного заката» (СЗ) с помощью спектрофотометрического анализа, а также ионов тяжелых металлов – свинца (Pb^{2+}) с помощью рентгенофлуоресцентной спектрометрии. В результате проведенных адсорбционных кинетических исследований установлена поглотительная способность исходного, активированных

и компактированных материалов. Сорбционная емкость по свинцу для материалов карбонизат и АМК1 составила 71 и 65 мг/г соответственно, оптимальное время сорбции – 30 мин; для материалов АМ1, АМ2, АМК1/ПВС, АМК1/ПВА и АМК1/БВ – 65, 66, 49, 45, 42 мг/г соответственно, оптимальное время сорбции – 15 мин. Для красителей МС и СЗ получены значения емкости: 1000 – 2010 мг/г, 66 – 972 мг/г и 15 мин соответственно. Для анализа механизмов поглощения применялись эмпирические уравнения псевдо-первого и псевдо-второго порядка, Еловича и внутричастичной диффузии. Представленные результаты показывают возможность применения разработанного активированного углеродного материала в качестве эффективного сорбента органических и неорганических поллютантов из водных растворов.

Ключевые слова: активированный углеродный материал; компактирование; адсорбция; метиленовый синий; желтый солнечный закат; свинец; кинетика.
Для цитирования: Shubin IN, Ananyeva OA. Studies of adsorption characteristics of activated carbon material for typical organic and inorganic pollutants. *Journal of Advanced Materials and Technologies*. 2024;9(2):122-131. DOI: 10.17277/jamt.2024.02.pp.122-131

1. Introduction

Nowadays, many regions of Russia, especially the industrialized ones, are facing the problem of environmental pollution, especially water pollution. The development of industrial complexes, technologies and materials is directly related to the emergence of new chemical production facilities, which, as a rule, produce large volumes of wastewater that require proper and high quality recycling or treatment. Failure to comply with disposal requirements has serious consequences for the environment and the ecological situation in general. The most typical representatives of toxic pollutants of water resources are various organic dyes and heavy metals (e.g. methylene blue (MB) and sunset yellow (SY) dyes or heavy metals – Pb^{2+}). They are widely used in a variety of industries and, when present in wastewater, have a detrimental effect on flora and fauna, including humans. Therefore, water needs to be treated to remove these pollutants and research in this direction is relevant [1–3].

One of the most popular methods of water treatment is sorption, which is technologically proven, economically justified and in many cases the most effective [1, 3–5].

The most widely used modern adsorption materials are activated carbons [6–9], silica gels and zeolites [10–14]. These form the basis of industrial sorption materials, but do not always fully meet the ever-increasing demands on their efficiency [1, 7].

The solution to this problem – the creation of an effective sorbent – is seen in the development and research of promising activated carbon materials (AMs), which combine a high specific surface area and significant porosity with a predominance of micro- and mesopores, the presence of sufficiently large transport pores, ensuring rapid diffusion of sorbent substances, chemical inertness and stability in real application conditions. This is confirmed by a number of publications on this subject [1, 6, 9, 15–16].

To obtain such carbon materials, different pre-carbonized carbon sources, such as furfural, hydroquinone, dextrin, urotropine, natural carbons, carbon nanotubes, graphene or their combinations, are activated by various gas- or liquid-phase reagents: different acids or alkalis, steam, etc. [17–24].

In practice, the resulting activated highly porous carbon materials can be used in the form of powders, granules or fibers, which often places additional high requirements on the possibility of their molding for convenience of further use in finished products and improvement of sorption properties. They should also have a high specific surface area and large pore volume, have a hierarchical porous structure, be environmentally safe, economical and highly selective, which makes them promising and in demand materials for use in adsorption of organic and inorganic pollutants from aqueous media, including various heavy metals and dyes, i.e. these materials should have a specific surface area of 500–3000 $m^2 \cdot g^{-1}$ and a porosity of more than 1 $cm^3 \cdot g^{-1}$ [1, 6, 8, 9, 25, 26].

The influence of the technological parameters of activation of the initial carbon raw material and the modes of its subsequent compaction on the sorption properties is studied in [27–31], where the authors note their relationship, as well as the possibility of using the results of laboratory studies in real production conditions.

The relationship between adsorption and structural properties of highly porous carbon materials is assessed in [15, 32, 33], where the importance of research in this direction is pointed out.

The analysis of the literature sources shows the undoubted interest in the research of the adsorption activity of sorbents on typical pollutants, which in various works was in the following ranges: on MB dye – 61–1190 $mg \cdot g^{-1}$ [34–39], on SY dye – 44–333 $mg \cdot g^{-1}$ [40–43] and on lead – 40–413 $mg \cdot g^{-1}$ [41–46].

Thus, taking into account the need and relevance of this research direction - development and research of effective sorbents – the aim of this work was to study the sorption activity of the developed activated carbon material in relation to organic dyes and heavy metals.

2. Materials and Methods

2.1. Reagents and techniques for the preparation of activated and compacted carbon materials

Based on preliminary studies, the authors of the paper developed and studied an activated carbon material obtained by two activation methods and its compacted variants with different binders. The work consisted of several stages.

In the first stage, samples of activated carbon material were obtained using one activator – potassium hydroxide (KOH) and two activators – KOH + H_2O. In general, this process was a high temperature chemical activation of the initial carbonisate with the activator(s) at a temperature of 400–7500 °C for two hours in an inert environment [18]. At this stage, AM was obtained with a specific surface area greater than 2700 $m^2 \cdot g^{-1}$ and a pore volume greater than 1.3 $cm^3 \cdot g^{-1}$ [27].

The second stage of work involved obtaining compacted samples using such binders as polyvinyl alcohol (PVA), polyvinyl acetate (PVAC) and basalt fiber (BF), the main technological and process parameters for obtaining which are considered in [29]. Moreover, at this stage, only carbon material activated with one activator (AMK1) was used for compacting. The binder content in different compacted samples was as follows: basalt fibre (LLC 'Kamenny Vek', Dubna, Russia) in the amount of 5 % (AMK1/BF), polyvinyl alcohol (TC Spektr-Chem, Moscow, Russia) – 20 % (AMK1/PVA), polyvinyl acetate (JSC 'Pigment', Tambov, Russia) – 20 % (AMK1/PVAC).

As a result, a number of samples were prepared for the next (third) stage of the research, including: initial carbonisate, carbon materials activated with one AM1 and two AM2 activators, and carbon materials AMK1/PVA, AMK1/PVAC and AMK1/BF compacted with different binders.

2.2. Adsorption studies

The third stage of the research consisted in determining the adsorption activity of the previously obtained samples on Pb^{2+}, for which batch experiments were carried out in a limited volume. The sorbent weighing 0.01 g was placed in 30 mL of Pb^{2+} solution with $C_0 = 100$ mg·L^{-1} according to Russian Standard 4453-74 at pH = 6. Each tube containing purified solutions and sorbent was shaken continuously for 5, 15, 30 and 60 min on a Multi Bio RS-24 programmable rotator (Biosan, Riga, Latvia). The equilibrium concentration of lead ions was determined by energy dispersive X-ray fluorescence spectrometry (ARLQuant ThermoScientific spectrometer, ThermoScientific, USA).

To study sorption to organic dyes, 30 mL of MB, SY solution with an initial concentration of 1500 mg·L^{-1} at pH = 6 was taken and 0.01 g of sorbent was added. Tubes containing the tested solution and sorbent suspension were placed in a programmable multi-rotator Multi Bio RS-24 (Biosan, Riga, Latvia) and stirred continuously for 5, 15, 30 and 60 min. The optical density of the filtered dye solution was then measured on a PE-5400VI spectrophotometer (Ekroskhim Co., Ltd, St. Petersburg, Russia) at a wavelength of λ = 815 nm for MB and λ = 513 nm for SY.

The static sorption capacity of the sorbents, Q_e, mg/g, was calculated using the formula

$$Q_e = \frac{(C_0 - C_e)V}{m}, \qquad (1)$$

where C_0 and C_e are the initial and final concentrations of the substances in solution, mg·L^{-1}; V is the volume of the solution, L; m is the sorbent weight, g.

3. Results and Discussion

Figure 1 shows the time dependence of lead ion adsorption on the starting material (carbonisate) and the activated materials AM1 and AM2.

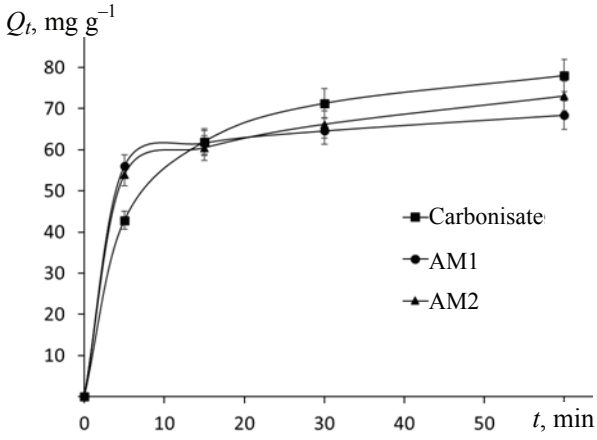

Fig. 1. Kinetic dependence of adsorption of Pb^{+2} ions on carbonisate and the activated materials AM1, AM2

As a result of kinetic studies, carbonisate was found to have an adsorption capacity for the removal of lead ions equal to 71 mg·g^{-1}, with the optimal sorption time being 30 min. The adsorption capacity on lead for activated materials AM1 and AM2 is 65 and 66 mg·g^{-1}, respectively, the optimal sorption time is 15 min.

In order to describe the ongoing processes of lead ion sorption, namely the mechanisms involved in the transfer of sorbent to the surface and inside the structure of sorbents, the equations of known kinetic models (pseudo-first and pseudo-second order, Elovich equation and intraparticle diffusion model) [47] were applied to the obtained experimental data. Table 1 and Figure 2 show the kinetic data for lead and the results of the mathematical processing of the kinetic data for carbonisate, AM1 and AM2 materials.

As a result of the experimental data processing, it was found that the mechanism of the sorption process in the removal of lead ions is well described by the pseudo-first order equation and the pseudo-second order equation. It can be noted that the pseudo-second order model has the highest determination coefficients R^2 for the removal of lead ions (for AM2 $R^2 = 0.9977$; for AM1 $R^2 = 0.9994$; for carbonisate $R^2 = 0.9998$). Based on this, it can be assumed that diffusion limitation (internal and external diffusion) and 'sorbate-sorbate' interaction contribute to the rate of the sorption process. It should also be noted that the Elovich model for AM1 material has a high coefficient of determination – $R^2 = 0.9983$.

Kinetic studies of the compacted carbon materials – AMK1, AMK1/PVA, AMK1/BF, AMK1/PVAC – have also been carried out.

As a result of kinetic studies of sorption capacity of compacted carbon materials (Fig. 3), it was found that the initial AMK1 has an adsorption capacity for removal of lead ions equal to 65 mg·g^{-1}, optimum time of sorption 30 min. With the addition of a binder, the highest sorption capacity is shown by the AMK1/PVA compacted carbon sorbent – 49 mg·g^{-1}, optimum sorption time 15 min. When basalt fibre (AMK1/BF) and polyvinyl acetate (AMK1/PVAC) were used, the adsorption capacity was 45 and 42 mg·g^{-1}, respectively, optimum sorption time 15 min.

Table 1. Parameters of lead ion sorption kinetics on carbonisate, AM1 and AM2 materials

	Pseudo-first order			Pseudo-second order		
	$\log(Q_e - Q_t) = \log Q_e - \frac{k_1}{2.303}t$			$\frac{t}{Q_t} = \frac{1}{k_2 Q_e^2} + \frac{1}{Q_e}t$		
	Q_e	k_1	R^2	Q_e	k_2	R^2
Carbonisate	43.511	0.0523	0.995	84.7458	0.00224	0.9998
AM1	16.319	0.0385	0.995	69.93007	0.0078	0.9994
AM2	28.138	0.0435	0.991	76.3359	0.00399	0.9977
	Elovich equation			Intraparticle diffusion model		
	$Q_t = \frac{1}{\beta}\ln(\alpha\beta) + \frac{1}{\beta}\ln t$			$Q_t = k_{id}t^{0.5} + C$		
	α	β	R^2	k_{id}	C	R^2
Carbonisate	62.4998	0.0699	0.9841	6.1843	33.644	0.9041
AM1	80493.4	0.2025	0.9983	2.1906	52.052	0.9664
AM2	1552.34	0.1307	0.9853	3.4665	46.643	0.9953

* Q_e – amount of adsorbed contaminant on the adsorbent surface at the moment of equilibrium, mg·g^{-1}; Q_t – amount of adsorbed contaminant on the adsorbent surface at time t, mg·g^{-1}; k_1 – pseudo-first order adsorption rate constant, min^{-1}; k_2 – pseudo-second-order adsorption rate constant, g·(mg·min)$^{-1}$; α – adsorption constant, 1·(min·mg/g)$^{-1}$; β – surface coverage and chemisorption activation energy, g·mg^{-1}; k_{id} – internal diffusion coefficient, 1·(mg/g·min)$^{-1}$; C – boundary layer thickness, mg·g^{-1}.

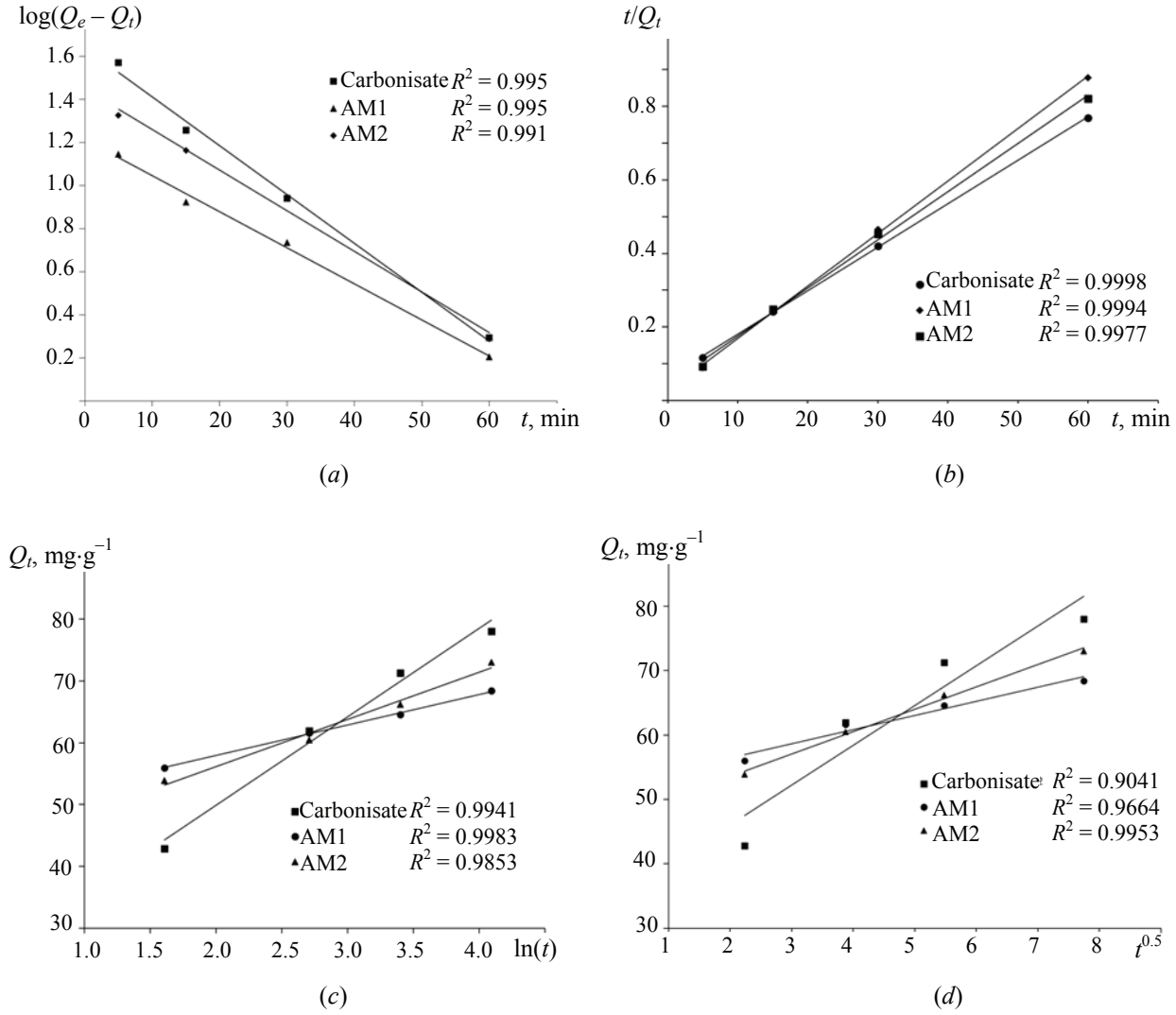

Fig. 2. Results of mathematical processing of the experimental kinetic dependencies using pseudo-first order models (*a*); pseudo-second order models (*b*); Elovich equation (*c*); intraparticle diffusion model (*d*)

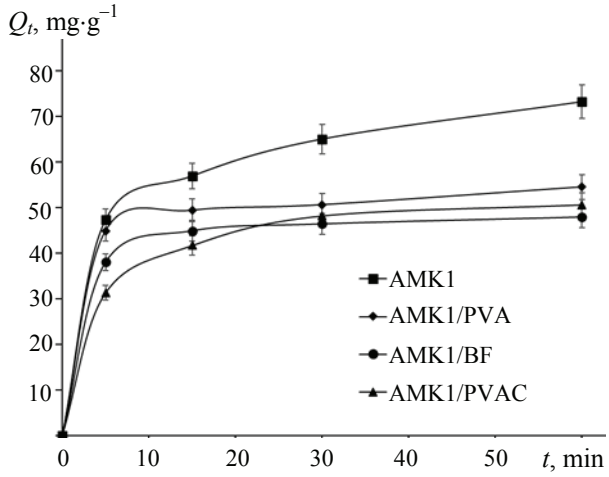

Fig. 3. Kinetic dependences of the adsorption of lead ions on the compacted carbon sorbents AMK1, AMK1/PVA, AMK1/BF, AMK1/PVA

The experimental data obtained for AMK1, AMK1/PVA, AMK1/BF and AMK1/PVAC samples were also processed by the equations of known kinetic models (Table 2, Fig. 4).

The pseudo-second-order model had the highest determination coefficients R^2 for the removal of lead ions (for AMK1 $R^2 = 0.9948$; for AMK1/PVA $R^2 = 0.9988$; for AMK1/BF $R^2 = 1$; for AMK1/PVAC $R^2 = 0.9997$). Accordingly, it can be concluded that the reaction between adsorbate and sorbent functional groups is strictly stoichiometric (one molecule occupies one position on the sorbent), i.e. there is a chemical interaction between Pb^{+2} ions and sorbent functional groups. For the kinetic data for the AM1 material, high coefficients of determination are also observed for the Elovich ($R^2 = 0.9936$) and pseudo-first order ($R^2 = 0.9926$) models.

Table 2. Parameters of lead ion sorption kinetics
on the materials AMK1, AMK1/PVA, AMK1/BF, AMK1/PVAC

	Pseudo-first order			Pseudo-second order		
	Q_e	k_1	R^2	Q_e	k_2	R^2
AMK1	38.318	0.0495	0.9926	78.125	0.00259	0.9948
AMK1/PVA	10.416	0.0299	0.9741	55.56	0.00964	0.9988
AMK1/BF	9.667	0.038	0.9169	49.02	0.01378	1
AMK1/PVAC	25.067	0.0504	0.9656	54.054	0.00475	0.9997
	Elovich equation			Intraparticle diffusion model		
	α	β	R^2	k_{id}	C	R^2
AMK1	178.749	0.0959	0.9936	4.6843	37.938	0.9866
AMK1/PVA	139636	0.2716	0.9741	1.6489	41.861	0.9605
AMK1/BF	14111.3	0.2520	0.9238	1.6675	36.221	0.8022
AMK1/PVAC	86.5644	0.1245	0.9725	3.4523	26.252	0.8829

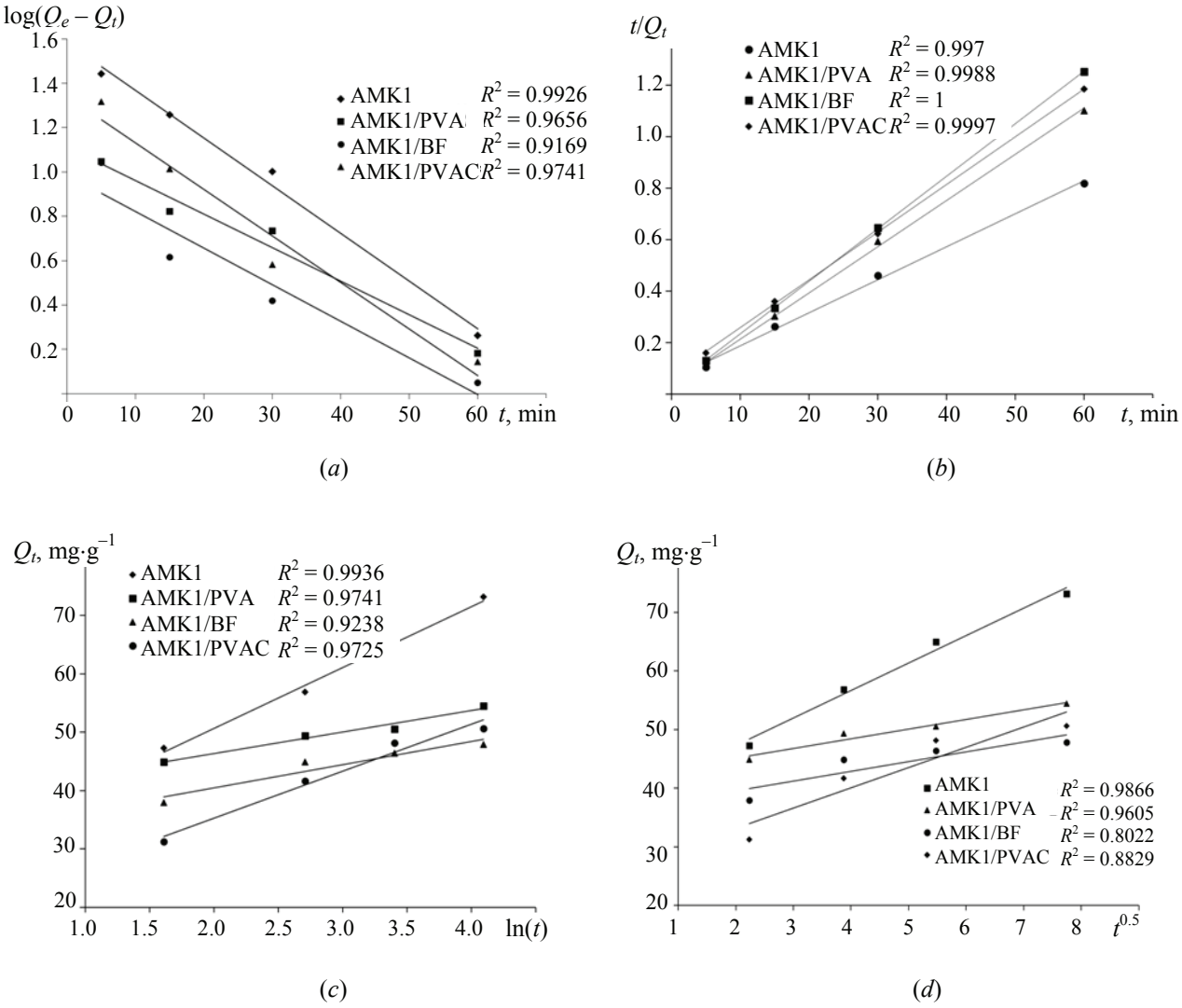

Fig. 4. Results of the mathematical processing of experimental kinetic dependencies using pseudo-first order models (*a*); pseudo-second order (*b*); Elovich equation (*c*); intraparticle diffusion (*d*)

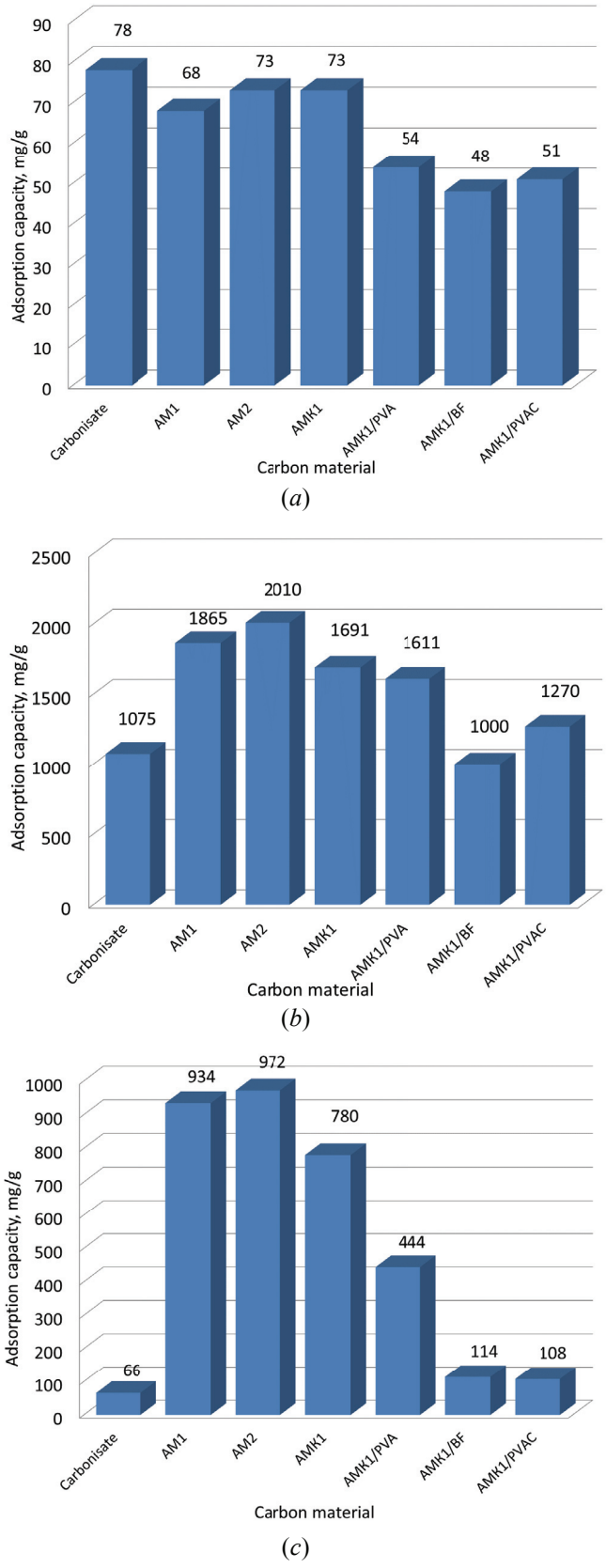

Fig. 5. Comparative results of studies on the adsorption activity of activated carbon materials:
a – on the sorption of lead ions Pb^{2+};
b – MB molecules; *c* – SY molecules

Summarising the studies on the determination of the sorption activity of the developed activated carbon material on typical organic [29, 30] and inorganic pollutants from aqueous solutions (including its compacted variants) (Fig. 5), it can be concluded that the developed material shows comparable or higher adsorption capacities on typical pollutants [34–46].

However, a number of peculiarities can be noted in the course of this study. The activated material obtained shows a rather low sorption activity towards inorganic substances (lead), but in general it is comparable with the results obtained by other authors [42–46]. Moreover, the compacted samples showed slightly worse results, which is explained by the presence of a binder, which is an inert ballast, as well as the formation of a new structure of the material when it is compacted with another.

Analysing the results obtained for dye MB (a typical representative of cationic dyes), it can be seen that the developed activated material, including its compacted variants, shows higher activity in comparison with analogues [34–39] and can be of real practical interest for application in industrial production.

The results for dye SY, an anionic type dye, show a higher efficiency in comparison with the studies of other authors [40, 41], but it can be noted that the sorption activity of the compacted samples also decreases several times with respect to the initial ones.

Thus, the results of the studies on organic dyes MB and SY may indicate a significant influence of the adsorption capacity of the binder used, which can be traced for all the samples studied. At the same time, it should be noted that at this stage of the research, the preferred binder is PVA. Further studies are needed to determine the mechanisms of influence of the technology of obtaining the materials.

4. Conclusion

The paper presents the results of studies of the adsorption activity of the developed carbon material and its compacted variants using different binders. The adsorption capacity of the original, activated and compacted materials was determined. The sorption capacity for lead for carbonisate and AMK1 materials was 71 and 65 $mg \cdot g^{-1}$, respectively, the optimum sorption time was 30 min; for AM1, AM2, AMK1/PVA, AMK1/PVAC and AMK1/BF materials 65, 66, 49, 45, 42 $mg \cdot g^{-1}$, respectively, the optimum sorption time was 15 min. For organic dyes – MB and SY, the capacity was 1000 – 2010 $mg \cdot g^{-1}$,

66 – 972 $mg \cdot g^{-1}$, respectively, at a sorption time of 15 min. The obtained experimental kinetic data were described using known equations of kinetic models (pseudo-first and pseudo-second order, Elovich equation and intraparticle diffusion model). According to the results of the studies, it is possible to note a high sorption activity of the developed carbon material for the extraction of cationic and anionic dyes, as well as similar activity with respect to Pb^{2+} ions, which is comparable with analogues. This may open up prospects for its use in solving a number of environmental problems.

5. Funding

This work was financially supported by the Russian Science Foundation (grant agreement No. 22-13-20074), https://rscf.ru/project/22-13-20074.

6. Conflict of interests

The authors declare no conflict of interests.

References

1. Krasnikova EM, Moiseenko NV. Adsorption and structural characteristics of carbon-containing adsorbents from plant raw material modified with oxidizers. «*Actual physical and chemical problems of adsorption and synthesis of nanoporous materials: All-Russian symposium with international participation, dedicated to the memory of Corresponding Member of the Russian Academy of Sciences V.A. Avramenko. Proceedings of the symposium.* Moscow: IPChE RAS; 2022. p. 219-221. (In Russ.)

2. Razmara RS, Daneshfar A, Sahrai R. Determination of methylene blue and sunset yellow in wastewater and food samples using salting-out assisted liquid–liquid extraction. *Journal of Industrial and Engineering Chemistry*. 2011;17(3):533-536. DOI:10.1016/j.jiec.2010.10.028

3. Auta M, Hameed BH. Coalesced chitosan activated carbon composite for batch and fix-bed adsorption of cationic and anionic dyes. *Colloids and Surfaces B: Biointerfaces*. 2013;105:199-206. DOI:10.1016/j.colsurfb.2012.12.021

4. Ruan X, Liu H, Chang C-Y, Fan X-Y. Preparation of organobentonite by a novel semidry-method and its adsorption of 2,4 edichlorophenol from aqueous solution. *International Biodeterioration & Biodegradation*. 2014;95:212-218. DOI: 10.1016/j.ibiod.2014.06.007

5. Lillo-Ródenas A, Cazoria-Amorós D, Linares-Solano A. Behaviour of activated carbons with different pore size distributions and surface oxygen groups for benzene and toluene adsorption at low concentrations. *Carbon.* 2005;43:1758-1767. DOI:10.1016/j.carbon. 2005.02.023

6. Fomkin AA. *Synthesis, properties and application of carbon adsorbents*. Moscow: Granitsa; 2021. 312 p. (In Russ.)

7. Kadum AHK, Burakova IV, Mkrtchyan ES, Ananyeva OA, Yarkin VO at al. Sorption kinetics of organic dyes methylene blue and malachite green on highly porous carbon material. *Journal of Advanced Materials and Technologies*. 2023;2:130-140. DOI:10.17277/jamt.2023.02.pp.130-140

8. Fenelonov VB. *Porous carbon*. Novosibirsk: Institute of Catalysis SB RAS; 1995. 518 p. (In Russ.)

9. Plaksin GV. Porous carbon materials of sibunite type. *Khimiya v interesakh ustoychivogo razvitiya = Chemistry for Sustainable Development*. 2001;9(5):609-620. (In Russ.)

10. Jafari S, Ghorbani-Shahna F, Bahrami A, Kazemian H. Adsorptive removal of toluene and carbon tetrachloride from gas phase using zeolitic imidazolate framework-8: effects of synthesis method, particle size, and pretreatment of the adsorbent. *Microporous and Mesoporous Materials*. 2018;268:58-68. DOI:10.1016/ j.micromeso.2018.04.013

11. Kucherova AE, Shubin IN, Pasko TV. Perspective sorbents based on zeolite modified with nanostructures for the purification of aqueous media from organic impurities purification of aqueous media from organic impurities. *Nanotechnologies in Russia.* 2018;13(5-6):1-5. DOI:10.1134/S1995078018030096

12. Sui H, An P, Li X, Cong S, He L. Removal and recovery of o-xylene by silica gel using vacuum swing adsorption. *Chemical Engineering Journal*. 2017;316:232-242. DOI:10.1016/j.cej.2017.01.061

13. Popova AA, Shubin IN. Technology for modifying sorbents based on zeolite with carbon nanotubes. *Vestnik tambovskogo gosudarstvennogo tekhnicheskogo universiteta*. 2021;27(4):656-663. DOI:10.17277/vestnik.2021.04.pp.656-663 (In Russ.)

14. Liu F, Jin YJ, Liao HB, Cai L, Tong MP, Hou YL. Facile self-assembly synthesis of titanate/Fe_3O_4 nanocomposites for the efficient removal of Pb^{2+} from aqueous systems. *Journal of Materials Chemistry A*. 2013;1(3):805-813. DOI:10.1039/C2TA00099G

15. Olontsev VF, Farberova EA, Minkova AA, Generalova KN, Belousov KS. Optimization of porous structure of absorbent carbon in the course of technological production. *Vestnik permskogo natsional'nogo issledovatel'skogo politekhnicheskogo universiteta. Khimicheskaya tekhnologiya i biotekhnologiya*. 2015;4:9-23. (In Russ.)

16. Mishchenko SV. *Carbon nanomaterials: production, properties and application*. Moscow: Mashinostroenie; 2008. 320 p. (In Russ.)

17. Dyachkova TP, Tkachev AG. *Methods of functionalisation and modification of the carbon nanotubes.* Moscow: "Spektr" Publ. house; 2013. 152 p. (In Russ.)

18. Shubin IN, Popova AA. Features of implementation options for the process of high-temperature activation of carbon material. *Journal of Advanced Materials and Technologies*. 2023;8(1):041-048. DOI:10.17277/jamt. 2023.01.pp.041-048.

19. Carvalho AP, Cardoso B, Pires J, Carvalho MB. Preparation of activated carbons from cork waste by

chemical activation with KOH. *Carbon*. 2003;41(14): 2873-2876. DOI:10.1016/S0008-6223(03)00323-3

20. Yoon SH, Lim S, Song Y, Ota Y et al. KOH activation of carbon nanofibers. *Carbon*. 2004;42(8-9): 1723-1729. DOI:10.1016/j.carbon.2004.03.006

21. Chesnokov NV, Mikova NM, Ivanov IP, Kuznetsov BN. Synthesis of carbon sorbents by chemical modification of fossil coals and plant biomass. *Zhurnal Sibirskogo federal'nogo universiteta. Khimiya*. 2014;7(1): 42-53. (In Russ.)

22. Dong W, Xia W, Xie K, Peng B at al. Synergistic effect of potassium hydroxide and steam co-treatment on the functionalization of carbon nanotubes applied as basic support in the Pd-catalyzed liquid-phase oxidation of ethanol. *Carbon*. 2017;121:452-462. DOI:10.1016/j.carbon.2017.06.019

23. Raymundo-Pinero E, Azaıs P, Cacciaguerra T, Cazorla-Amoros D at al. KOH and NaOH activation mechanisms of multiwalled carbon nanotubes with different structural organization. *Carbon*. 2005;43(4):786-795. DOI:10.1016/j.carbon.2004.11.005

24. Popova AA, Shubin IN. Investigation of the process of high-temperature alkaline activation of carbon material with additional action of water vapor. *Vestnik tambovskogo gosudarstvennogo tekhnicheskogo universiteta*. 2022;28(3):476-486. DOI:10.17277/vestnik.2022.03.pp.476-486. 9 (In Russ.)

25. Ouyang J, Zhou L, Liu Z, Heng JYY, Chen W. Biomass-derived activated carbons for the removal of pharmaceutical mircopollutants from wastewater: a review. *Separation and Purification Technology*. 2020;253: 117536. DOI:10.1016/j.seppur.2020.117536

26. Han X, Wang H, Zhang L. Efficient removal of methyl blue using nanoporous carbon from the waste biomass. *Water, Air, and Soil Pollution*. 2018;229(2):26. DOI:10.1007/s11270-017-3682-0

27. Shubin IN. Features of hardware and technological process formation in obtaining the compacted carbon materials. *Izvestiya vysshikh uchebnykh zavedeniy. Mashinostroyeniye.* 2024;1:57-67. DOI:10.18698/0536-1044-2024-01-57-67 (In Russ.)

28. Falco C, Marco-Lozar JP, Salinas-Torres D, Morallo´n E at al. Tailoring the porosity of chemically activated hydrothermal carbons: Influence of the precursor and hydrothermal carbonization temperature. *Carbon*. 2013;62:346-355. DOI:10.1016/j.carbon.2013.06.017

29. Shubin IN, Mkrtchyan ES, Ananyeva OA. Promising sorbents based on compacted highly porous carbon materials. *Journal of Advanced Materials and Technologies*. 2023;8(4):270-278. DOI:10.17277/jamt.2023.04.pp.270-278

30. Mkrtchyan ES, Popova AA, Shubin IN. Investigation of promising carbon sorbents obtained by high-temperature activation in the processes of purification of aqueous solutions from dyes. *Perspektivnyye Materialy = Prospective Materials*. 2023;11:28-38. DOI:10.30791/1028-978X-2023-11-28-38 (In Russ.)

31. Zgrzebnicki M, Kałamaga A, Wrobel R. Sorption and textural properties of activated carbon derived from charred beech wood. *Molecules*. 2021;26:7604. DOI:10.3390/molecules26247604

32. Cychosz KA, Thommes M. Progress in the physisorption characterization of nanoporous gas storage materials. *Engineering*. 2018;4:559-566. DOI:10.1016/j.eng.2018.06.001

33. Bahadur J, Melnichenko YB, He L, Contescu CI at al. SANS investigations of CO_2 adsorption in microporous. *Carbon*. 2015;95:535-544. DOI:10.1016/j.carbon.2015.08.010

34. Mukhin VM, Klushin VN. *Production and application of carbon adsorbents: textbook.* Moscow: Mendeleev Russian University of Chemical Technology; 2012. 308 p. (In Russ.)

35. Al-Ghouti MA, Sweleh AO. Optimizing textile dye removal by activated carbon prepar froedm olive stones. *Environmental Technology and Innovation*. 2019;16:100488. DOI:10.1016/j.eti.2019.100488

36. Ji B, Wang J, Song H, Chen W. Removal of methylene blue from aqueous solutions using biochar derived from a fallen leaf by slow pyrolysis: Behavior and mechanism. *Journal of Environmental Chemical Engineering*. 2019;7(3):103036. DOI:10.1016/j.jece.2019.103036

37. Li Z, Hanafy H, Zhanga L, Sellaouid L at al. Adsorption of congo red and methylene blue dyes on an ashitaba waste and a walnut shell-based activated carbon from aqueous solutions: Experiments, characterization and physical interpretations. *Chemical Engineering Journal*. 2020;388:124263. DOI:10.1016/j.cej.2020.124263

38. Canales-Flores RA, Prieto-García F. Taguchi optimization for production of activated carbon from phosphoric acid impregnated agricultural waste by microwave heating for the removal of methylene blue. *Diamond and Related Materials.* 2020;109:108027. DOI:10.1016/j.diamond.2020.108027

39. Wang B, Gao B, Zimmerman AR, Lee X. Impregnation of multiwall carbon nanotubes in alginate beads dramatically enhances their adsorptive ability to aqueous methylene blue. *Chemical Engineering Research and Design.* 2018;133:235-242. DOI:10.1016/j.cherd.2018.03.026

40. Crini G. Non-conventional low-cost adsorbents for dye removal: a review. *Bioresource technology*. 2006; 97(9):1061-1085. DOI:10.1016/j.biortech.2005.05.001

41. Nayeri D, Mousavi SA. Dye removal from water and wastewater by nanosized metal oxides-modified activated carbon: a review on recent researches. *Journal of Environmental Health Science and Engineering*. 2020;18(2):1671-1689. DOI:10.1007/s40201-020-00566-w

42. Mariana M, Khalil AHPS, Mistar EM, Yahya EB, et al. Recent advances in activated carbon modification techniques for enhanced heavy metal adsorption. *Journal of Water Process Engineering*. 2021;43:102221. DOI:10.1016/j.jwpe.2021.102221

43. Sabzehmeidani MM, Mahnaee S, Ghaedi M, Heidari H. Carbon based materials: A review of adsorbents for inorganic and organic compounds. *Materials Advances*. 2021;2(2):598-627. DOI:10.1039/D0MA00087F

44. Han Z, Tang Z, Shen S, Zhao B, at al. Strengthening of graphene aerogels with tunable density and high adsorption capacity towards Pb^{2+}. *Scientific Reports*. 2014;4:5025. DOI:10.1038/srep05025

45. Purnendu SS. Graphene-based 3D xerogel as adsorbent for removal of heavy metal ions from industrial wastewater. *Journal of Renewable Materials*. 2017;5(2):96-102. DOI:10.7569/JRM.2016.634134

46. Wang B, Zhang F, He S, Huang F, Peng Z. Adsorption behavior of reduced graphene oxide for removal of heavy metal ions. *Asian Journal of Chemistry*. 2014;26:4901-4906. DOI:10.14233/ajchem.2014.17024

47. Gautam RK, Chattopadhyaya MC. *Nanomaterials for Wastewater Remediation*. Oxford: Elsevier; 2016. 347 p.

Information about the authors / Информация об авторах

Igor N. Shubin, Cand. Sc. (Eng.), Associate Professor, Associate Professor, TSTU, Tambov, Russian Federation; ORCID 0009-0007-3235-5702; e-mail: i.shubin77@yandex.ru

Oksana A. Ananyeva, Postgraduate Student, TSTU, Tambov, Russian Federation; ORCID 0000-0002-1188-9402; e-mail: oksana.a9993471@gmail.com

Шубин Игорь Николаевич, кандидат технических наук, доцент, ТГТУ, Тамбов, Российская Федерация; ORCID 0009-0007-3235-5702; e-mail: i.shubin77@yandex.ru

Ананьева Оксана Альбертовна, аспирант, ТГТУ, Тамбов, Российская Федерация; ORCID 0000-0002-1188-9402; e-mail: oksana.a9993471@gmail.com

Received 15 April 2024; Accepted 08 May 2024; Published 04 July 2024

Review
Nanostructured, nanoscale materials and nanodevices

УДК 541.64:539.2 DOI: 10.17277/jamt.2024.02.pp.132-151

Polyaniline and its composites with carbon nanomaterials: preparation, properties, application

© Irina V. Gutnik[a]✉, Tatyana P. Dyachkova[a], Elena A. Burakova[a], Evgeniy N. Tugolukov[a], Artem V. Rukhov[a], Georgiy A. Titov[a]

[a] *Tambov State Technical University, Bld. 2, 106/5, Sovetskaya St., Tambov, 392000, Russian Federation*

✉ i.v.gutnik@yandex.ru

Abstract: The increased attention of researchers to electrically conductive polymers, including polyaniline (PANI), is due to the wide possibilities of its use in the production of supercapacitors, energy storage devices, anticorrosive coatings, detectors, sensors, solar cells, antimicrobial materials, sorbents, and coatings that absorb electromagnetic radiation. However, the instability of the PANI properties during operation limits the practical use of the polymer. In this regard, to date, many attempts have been made to stabilize the characteristics and increase the service life of polyaniline. Thus, new composite materials, which combine PANI and one or more other components, including carbon nanomaterials (carbon nanotubes, graphene, graphene oxide, reduced graphene oxide, mesoporous carbon), montmorillonite, metals, chalcogenides, conductive polymers,were developed. The purpose of this study is to summarize the information accumulated to date on electrically conductive polyaniline and its composites with carbon nanomaterials (CNM), as well as to demonstrate their potential and future prospects. The paper describes the structure and properties of the polymer. Chemical and electrochemical approaches to the synthesis of PANI and composites based on it are considered, attention is paid to the influence of synthesis conditions on the structure and properties of the final reaction products. A brief description of the application of polyaniline and its composites with CNM is given.

Keywords: polyaniline; carbon nanotubes; functionalized carbon nanotubes; graphene; composite.

For citation: Gutnik IV, Dyachkova TP, Burakova EA, Tugolukov EN, Rukhov AV, Titov GA. Polyaniline and its composites with carbon nanomaterials: preparation, properties, application. *Journal of Advanced Materials and Technologies*. 2024;9(2):132-151. DOI: 10.17277/jamt.2024.02.pp.132-151

Полианилин и его композиты с углеродными наноматериалами: получение, свойства, применение

© И. В. Гутник[a]✉, Т. П. Дьячкова[a], Е. А. Буракова[a], Е. Н. Туголуков[a], А. В. Рухов[a], Г. А. Титов[a]

[a] *Тамбовский государственный технический университет, ул. Советская, 106/5, пом. 2, Тамбов, 392000, Российская Федерация*

✉ i.v.gutnik@yandex.ru

Аннотация: Повышенное внимание исследователей к электропроводящим полимерам, в том числе к полианилину (ПАНИ), обусловлено широкими возможностями его применения при производстве суперконденсаторов, накопителей энергии, антикоррозионных покрытий, датчиков, сенсоров, элементов солнечных батарей, антимикробных материалов, сорбентов, покрытий, поглощающих электромагнитное излучение. Однако нестабильность свойств ПАНИ в ходе эксплуатации ограничивает практическое применение полимера. В связи с этим к настоящему времени предпринято множество попыток, позволяющих стабилизировать характеристики и увеличить срок службы полианилина. Например, разработаны новые композиционные материалы, сочетающие в себе ПАНИ и один или несколько других компонентов, среди которых углеродные наноматериалы (углеродные нанотрубки, графен, оксид графена, восстановленный оксид графена, мезопористый углерод), монтмориллонит, металлы, халькогениды, проводящие полимеры. Цель исследования – обобщить сведения, накопленные к настоящему времени об электропроводящем полианилине и его композитах с углеродными наноматериалами (УНМ), продемонстрировать их потенциал и будущие перспективы. Даны описания строения и свойств полимера.

Рассмотрены химические и электрохимические подходы к синтезу ПАНИ и композитов на его основе, уделено внимание влиянию условий синтеза на структуру и свойства конечных продуктов реакции. Дана краткая характеристика областей применения полианилина и его композитов с УНМ.

Ключевые слова: полианилин; углеродные нанотрубки; функционализированные углеродные нанотрубки; графен; композит.

Для цитирования: Gutnik IV, Dyachkova TP, Burakova EA, Tugolukov EN, Rukhov AV, Titov GA. Polyaniline and its composites with carbon nanomaterials: preparation, properties, application. *Journal of Advanced Materials and Technologies*. 2024;9(2):132-151. DOI: 10.17277/jamt.2024.02.pp.132-151

1. Introduction

Since the discovery of polyaniline (PANI), which belongs to the class of electrically conductive polymers, to the present time there has been an increase in the number of studies related to this material. This is primarily due to the unique properties of PANI [1]. PANI belongs to the class of conjugated polymers, so it can have conductivity close to metallic. PANI is also distinguished by ease of synthesis and doping with protic acids, environmental stability and low cost [2–4]. However, changes in electrical conductivity during operation, low cyclic stability, mechanical degradation, and processing complexity significantly limit the practical use of the polymer [5, 6]. It is known that charge/discharge processes are accompanied by swelling, shrinkage and destruction of the polymer during doping/dedoping processes, which leads to a decrease in cycle stability. In addition, PANI degradation can occur at relatively high potentials. The consequence of this is the low operating potential of PANI electrodes.

To eliminate the above defects, researchers usually combine polyaniline with other materials (carbon nanotubes (CNTs), graphene (G), graphene oxide (GO), cellulose, montmorillonite, metal oxides). As a result, new materials are obtained, which are characterized by increased capacitive characteristics and high chemical stability [7]. For example, a PANI composite with carbon nanotubes, synthesized for use as an electrode material for a supercapacitor, demonstrates a fairly high specific capacitance of 1266 $F \cdot g^{-1}$, exceeding the capacitance of the original components [8]. It has also been shown that PANI/CNT hybrids exhibit a synergistic effect [9].

On the one hand, the carbon dispersed carrier increases the accessible surface of PANI, on the other hand, it creates an electrically conductive frame, which makes it possible, by increasing electronic and ionic conductivity, to increase the electrical power removed from the electrode. Also, this framework is more rigid than PANI itself, which makes it possible to stabilize the porous structure of the polymer with multiple repetition of charge/discharge.

The possibility of stabilizing the PANI properties by synthesizing composites based on it gives rise to a large number of studies on this topic, the results of which are reflected in both scientific and review articles. However, in the latter, there is mainly a generalization of the results obtained within specific areas of practical application of composites (for example, in supercapacitors, sorbents). With this approach, the effectiveness of the synthesized composites is demonstrated in only one area of application. There is also no systematic information on the dependence of the characteristics of composites on their composition. In this regard, this review summarizes the results accumulated to date in the field of preparation and characterization of PANI composites with carbon nanomaterials. Attention is paid to the influence of the mass composition of composites on their morphological and operational characteristics. A brief description of promising areas of application of these composites is presented. The review also provides information on the structure, properties and methods of producing PANI, which can be used by researchers to select optimal conditions for the synthesis of composites with given parameters.

2. Chemical structure and properties of PANI

PANI has the longest history of research among electrically conductive polymers. This polymer was discovered in the middle of the 19th century [10]. It was then known as “aniline black” (a term in those days used for any product obtained by the oxidation of aniline). The discovery of PANI can probably be considered the experiments of Runge [11]. Later, Fritsche and Leteby continued to study the oxidation process of aniline and discovered a change in the color of the resulting precipitate [12–14]. The results obtained by scientists in the century before last served as a prerequisite for studying the process of obtaining “black aniline”, as well as for studying its redox and acid-base transformations.

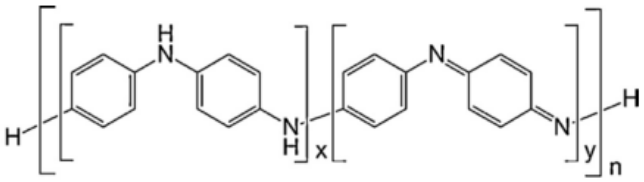

(*a*)

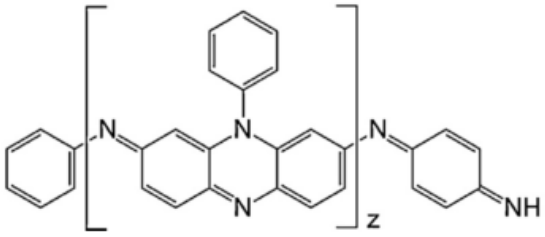

(*b*)

Fig. 1. Molecular structure of various redox forms of linear aniline octamers, proposed at the beginning of the 20th century (*a*: $x + y = 4$, $n = 1$; leucoemeraldine: $x = 4$, $y = 0$; protoemeraldine: $x = 3$, $y = 1$; emeraldine: $x = 2$, $y = 2$; nigranilin: $x = 1$, $y = 3$; pernigraniline: $x = 0$, $y = 4$) and black aniline (*b*: $z = 3$) [15]

The terms emeraldine and nigraniline were coined for the various oxidized/reduced forms of aniline black. At the beginning of the 20th century, the concepts "leucoemeraldine", "protoemeraldine" and "pernigraniline" were introduced to designate linear combinations of aniline octamers with varying degrees of oxidation, i.e. with different numbers of N-phenyl-benzoquinonediimine and 4-aminodiphenylamine fragments in the main chain (Fig. 1*a*) [15].

The molecular weight of PANI in the form of emeraldine is significantly higher than that of octamers, indicating the existence of intermediate oxidation states between leucoemeraldine and emeraldine ($x > y$, $y \geq 1$, Fig. 1*a*), which could be designated as protoemeraldine, corresponding to $x / y \sim 3$, as well as between emeraldine and pernigraniline ($x < y$, $x \geq 1$, Fig. 1*a*), which can be designated as nigraniline, as in the case of $x / y \sim 1/3$ [16].

In 1965, information that emeraldine has high conductivity appeared [17]. At the end of the last century, scientists discovered the possibility of transitioning from one form of PANI to another. For example, emeraldine can be converted from a base to a salt. This process is accompanied by a color change from blue to green (Fig. 2). Based on the results of these studies, a paper was published where it was reported that the transition of emeraldine to this state is accompanied by a sharp increase in conductivity by more than 10 orders of magnitude – up to 1–5 $S \cdot cm^{-1}$ [18].

Multiple studies conducted over the past decades allow us to conclude that the emeraldine salt of PANI (PANI-ES) contains localized/delocalized radical cations (polarons) and dications (bipolarons) in different proportions. Their content depends on the synthesis conditions and isolation procedures [19] (Fig. 2).

The transition of PANI in the form of emeraldine base (PANI-EB) to PANI-ES is carried out using doping, which can be done in two ways: oxidation (p-doping, when the doping component accepts electrons) or reduction (n-doping - the doping component gives up electrons) neutral polymer with a modifying additive [4].

Proton donors, usually acids (hydrochloric, sulfuric, sulfonic acids, etc.) are used to dope PANI. The electrical conductivity of doped PANI can be influenced by a number of factors, including the oxidation state of the polymer, the type of protic acid, the degree of protonation, the moisture content of the polymer, and the morphology of the polymer chain [20].

3. Methods for obtaining PANI

Currently, there are several methods for obtaining PANI. The most common one is the oxidative polymerization of aniline. There are chemical [21–24], electrochemical [25], and enzymatic [26] polymerization.

During chemical synthesis in an acidic environment, the aniline monomer or salt (aniline hydrochloride or sulfate) is converted into a conjugated polymer. Distinctive features of this method are the high yield of the target reaction product (about 90–95 % of the theoretically calculated one), as well as the relatively high electrical conductivity (1–5 $S \cdot cm^{-1}$) of the synthesized material [4].

To date, significant experimental material has been accumulated on the relationship between the properties of PANI obtained by chemical polymerization and synthesis conditions. Among the synthesis parameters that most significantly influence the properties of the final product are the nature of the oxidizing agent, pH, concentration of reagents, and polymerization temperature [27, 28].

It is known that PANI can have different morphologies (nanofibers, nanorods, nanotubes, nanospheres, granules). It has been proven that it depends on the nature of the oxidizing agent or the presence of additives in the reaction mixture [29]. For example, by varying the synthesis conditions, it is possible to obtain PANI with a granular structure [30], and in a weakly acidic environment, PANI is obtained in the form of nanotubular particles [31].

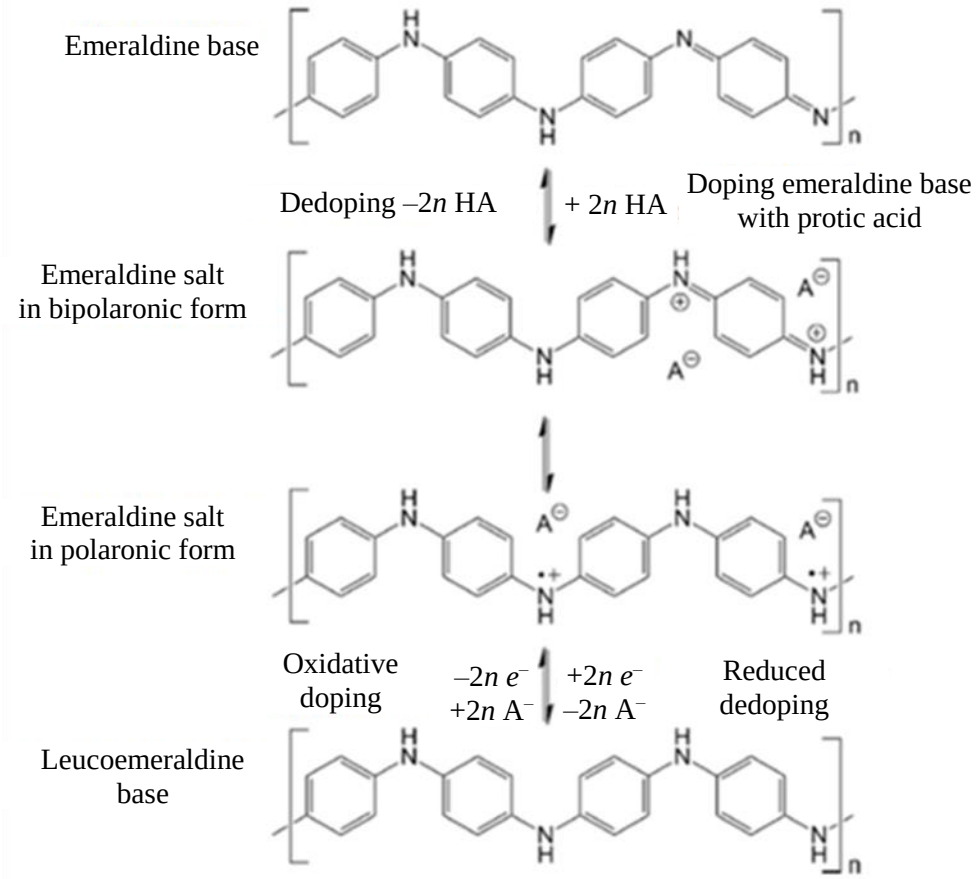

Fig. 2. Oxidative doping of leucoemeraldine base and doping emeraldine base with protic acid; A is anion

Various PANI structures are characterized by a set of morphological features (shape of structural units, specific surface area, pore size), which determine the accessibility of PANI macromolecules to electrolyte ions, and the electronic and redox properties determine the maximum possible power and energy intensity of devices based on it [32–34].

The main methods for carrying out electrochemical synthesis are galvanostatic (at a constant current) [35–37], potentiostatic (at a constant electrochemical potential) [38] and potential cycling modes [39]. The yield, morphology, electrochemical behavior, adhesion to the electrode, optical properties and other characteristics of the PANI film obtained by electrosynthesis are determined by polymerization conditions, such as the type and concentration of the electrolyte, the nature of the electrode, and synthesis modes [35].

Most often, the electrochemical synthesis of PANI is based on the anodic oxidation of aniline at various electrodes. This is due to the possibility of obtaining a purer polymer without oxidizing agent impurities, as well as the possibility of controlling the thickness of the film and observing the process of its formation using various physical and chemical methods (optical, electrochemical, etc.). Moreover, the molecular weight of PANI synthesized by electrochemical polymerization methods is usually lower than that of chemical synthesis [40].

Compared to chemical polymerization, electrochemical synthesis is faster and does not require the use of oxidizing agents and additives. The advantages of the method also include the ability to regulate the conditions (potential and current) of PANI deposition and the almost complete absence of by-products. At the same time, the morphological forms of PANI are not so diverse: nanofibers, nanogranules, or thin films on the surface of the substrate [41–43].

However, the electrochemical method is only suitable for producing polymer in small quantities, while the chemical method allows the production of polymer in large volumes [44].

The processes of converting aniline into PANI during chemical and electrochemical polymerization are similar to each other and occur in several stages (Table 1) [30].

As findings show, the duration of the induction period depends on the synthesis conditions and can increase with a decrease in the initial temperature of aniline oxidation or shorten with increasing acid concentrations [45].

Table 1. Characteristics of the stages of aniline oxidative polymerization

Stage	Observed phenomena	Products formed
Rapid exothermic oxidation of neutral aniline molecules	Increase in temperature, decrease in pH	Non-conducting oligomers
Induction period	Temperature remains virtually unchanged, pH decreases moderately	Aniline trimers
Rapid polymerization of anilinium cations	Rapid heat release is accompanied by the formation of protons	Oligomeric and polymeric products

The induction period also becomes shorter when the reacting mixture contains an inert solid material with a high surface area (carbon nanotubes, graphite) [46]. This is explained by the phenomenon of adsorption of oligomers and the formation of nucleates on such substrates.

The decrease in pH during oxidative polymerization is explained as follows: during the formation of bonds between aniline molecules and oligomers or polymers, hydrogen atoms are eliminated in the form of protons and form sulfuric acid with the persulfate reduction product [47–51].

The course of the reaction and the nature of the final product (structure, physicochemical properties, redox form) are influenced by factors such as the acidity of the medium, the nature and concentration of the oxidizing agent.

Aniline oxidation can be started in an acidic or alkaline environment. In this case, some phases may be absent depending on the initial pH of the reacting mixture. If oxidation begins in an alkaline environment, oligomers quickly form and the reaction mass becomes brown.

Conductive forms of PANI are formed in an acidic environment. In this case, practically no exothermic formation of brown oligomers is observed. A low concentration of neutral aniline molecules slows down the formation of short oligomers (mainly semidine dimers). The light blue color visible at this stage is due to the formation of an oxidized dimer. Semidines subsequently participate in the formation of trimers (nucleates), which become initiation centers for the growth of PANI chains. As a result, the polymer is the main product of the reaction; oligomers are present only in minor quantities [52].

The nature of the oxidizing agent, especially its redox potential, has a significant impact on the morphology and properties of PANI [53]. Persulfates (ammonium persulfate and potassium persulfate [54–58] and iron chloride $FeCl_3$ [59–62] are most often used as oxidizing agents in the synthesis of PANI. However, when using $FeCl_3$, polymerization proceeds at a lower rate, since its redox potential (0.77 V) is lower than that of ammonium persulfate (2.0 V) [63]. However, ammonium persulfate also has disadvantages: it is stoichiometrically consumed in the reaction, which leads to the formation of acidic by-products during the synthesis of the polymer [64]. For environmentally friendly synthesis of PANI, the use of $FeCl_3$ and ozone as a catalyst and oxidizer, respectively, has been proposed [65]. The only byproduct formed during the reaction under these conditions is water.

When ammonium persulfate is used as an oxidizing agent, the molar ratio “aniline: ammonium persulfate” (r) has a different effect on the yield, elemental composition, electrical conductivity and degree of oxidation of the resulting product. At $r \leq 1.15$, the characteristics of PANI are practically independent of the molar ratio. At $r > 1.15$, overoxidation of PANI accompanied by a decrease in the yield of the polymer, its conductivity, and a noticeable change in its morphology [66] is observed. The optimal molar ratio “aniline: ammonium persulfate” is 1 : 1.25 [4]. An increase in the concentration of ammonium persulfate by two times compared to the concentration of aniline leads to the rupture of polymolecular chains, the formation of quinoid compounds and overoxidized forms of PANI. The use of ammonium persulfate in an amount less than half that of aniline causes a decrease in the yield of PANI to 40–50 %. A number of authors believe [22, 67] that ammonium persulfate is involved in the processes of both initiation and growth of chains.

A number of other compounds are also used as oxidizing agents: manganese oxides [68–70], potassium (VI) dichromate $K_2Cr_2O_7$ [71], cerium (IV) sulfate $Ce(SO_4)_2$ [72], copper (II) chloride $CuCl_2$ [73], copper (II) nitrate $Cu(NO_3)_2$ [74], potassium ferricyanide ($K_3(Fe(CN)_6$) [75] and

sodium vanadate ($NaVO_3$) [76]. Compounds of noble metals (Au (II), Pt (IV), Pd (II), Ag (I)) [77], hydrogen peroxide [78, 79], potassium permanganate [80, 81] are also used as oxidizing agents.

In the case of using oxidizing agents such as cerium (IV) sulfate and potassium dichromate at higher concentrations ($r > 1.15$), a complexation reaction probably occurs, which leads to the production of products containing a large percentage of the metal [66].

There is information about the use of a mixture of oxidizing agents, including $FeCl_3$ / H_2O_2 [82] and KIO_3 / NaClO [83]. To accelerate the synthesis of PANI, researchers resorted to the use of catalysts, which are enzymes, for example, horseradish peroxidase [84], enzymes of the oxidoreductase class [85].

A number of researchers propose unconventional methods for the synthesis of PANI: polymerization of aniline under the influence of X-ray irradiation in the presence of nitrate ions [86]; dispersion polymerization in a weak magnetic field [87]; matrix synthesis of PANI on a solid support [88]; oxidation of aniline hydrochloride with ammonium persulfate in non-aqueous media (acetone, methanol, toluene) [89]; plasma polymerization of aniline [90], photoinduced polymerization [91].

4. Preparation and properties of PANI composites with carbon nanomaterials

4.1. PANI / CNT composites

Currently, to obtain nanocomposites of PANI with carbon nanotubes, the method of oxidative polymerization of aniline on the surface of CNTs is most often used [93–99]. This is due to the fact that this approach has a number of advantages over other methods. Thus, the ability to change synthesis conditions opens up prospects for obtaining materials with specified characteristics (specific capacitance, electrical conductivity, specific surface area) for a specific field of practical application. It is also possible to implement this method on an industrial scale [92].

Studies of the morphological features of composites have shown that in composites a layer of polymer, the thickness and roughness of which is determined by the mass fraction of each component, uniformly covers the surface of the CNT [100]. It is noted that, in comparison with emeraldine, PANI deposited on the surface of CNTs has an increased content of quinonediimine fragments. This is explained by stacking interactions between PANI and carbon nanotubes [93].

There is information about the influence of the composition of composites on their characteristics. It has been shown that PANI/CNT composites have higher electrical conductivity compared to the value of this parameter for individual components (PANI and carbon nanotubes) [49]. It has been experimentally shown that the initial PANI has the lowest electrical conductivity; with increasing CNT content in the composite, an increase in electrical conductivity is observed (Table 2). It is assumed that the increase in electrical conductivity is due to the presence of interaction between the amino groups of PANI and CNTs, which facilitates charge transfer between the polymer and carbon nanotubes [100].

Table 2. Electrical conductivity of PANI and its composites with carbon nanotubes, characterized by different mass contents of CNTs

Composite	Electrical conductivity, $S \cdot cm^{-1}$	Source
PANI/CNT (0.2 wt. %)	$0.8 \cdot 10^{-3}$	[100]
PANI/CNT (10 wt. %)	$6.6 \cdot 10^{-2}$	
PANI	$1.0 \cdot 10^{-2}$	[101]
PANI/MWCNT (0.5 wt. %)	$2.9 \cdot 10^{-1}$	
PANI/MWCNT (1 wt. %)	1.10	
PANI	0.18	[102]
PANI/MWCNT (5 wt. %)	0.85	
PANI/MWCNT (15 wt. %)	1.10	
PANI	0.17	[103]
PANI/MWCNT (0.25 wt. %)	0.22	
PANI/MWCNT (8 wt. %)	3.32	
PANI	6.25	[104]
PANI/MWCNT (5 wt. %)	17.54	
PANI/MWCNT (10 wt. %)	20.66	
PANI/MWCNT (15 wt. %)	23.10	
PANI/CNT (1 : 1)	10.00	[105]
PANI/CNT (2 : 1)	6.67	
PANI/CNT (4 : 1)	1.72	
PANI/CNT (8 : 1)	0.41	
PANI	0.028	[106]
PANI/carboxylated CNT (1 wt. %)	0.126	
PANI/carboxylated CNT (6 wt. %)	6.154	
PANI/carboxylated CNT (7 wt. %)	3.349	

Other properties of composites with PANI also depend on the CNT content. A change in the dielectric properties of the material is observed with increasing concentration of single-walled CNTs [107]. The relaxation process, analyzed using the Kohlrausch-William-Watts (KWW) model, is found to occur at lower nanofiller loadings, but gradually decays as the number of SWCNTs increases, yielding relaxation spectra that gradually resemble those of a pure conductor. In addition, the competing processes between the effects of electrical percolation and interfacial capacitance are found to be inherently dependent on the carbon filler content.

In the literature, there are few results of studies of the mechanical properties of PANI composites with carbon nanotubes. Materials testing demonstrated an increase in tensile stress by 150 % and Young's modulus by 110 % when 2 wt. % CNTs were added to the polymer [108]. Huang J. et al. report that the tensile strength of PANI/CNT film composites increases significantly to 232.3 MPa, which is more than twice the tensile strength of carbon nanomaterial (67.2 MPa). The increased tensile strength of the composites can be attributed to the interfacial adhesion between the carbon nanotube film and PANI, promoting more efficient stress transfer [109].

One way or another, obtaining a CNT dispersion is an important stage in the production of PANI/CNT nanocomposite material by chemical polymerization. As indicated in a number of studies, covalent modification of CNTs with carboxyl [110] or sulfo groups [94] allows both to ensure the dispersibility of CNTs in water and to act as a matrix for the polymerization of aniline due to interaction with the monomer and the resulting PANI. In addition, after introducing acid groups, nanotubes can act as a modifying additive for PANI, which allows polymerization to be carried out in water without adding acid. However, it should be noted that polymerization in the absence of an additional modifying additive leads to the production of a nanocomposite material with a low degree of doping and, accordingly, low conductivity (about 10^{-2} S·cm^{-1}) [94].

Pre-functionalized CNTs have been used to prepare PANI composites in other studies. Carboxylated multiwalled CNTs can be used as a dispersed carrier in a composite material demonstrating sensor sensitivity to ammonia [111]. Polyaniline was deposited onto the surface of multiwalled CNTs (MWCNTs) pre-oxidized in a mixture of nitric and sulfuric acids, and it was possible to obtain a composite with a specific surface area of 133.55 $m^2 \cdot g^{-1}$ and a specific capacity of 867 $F \cdot g^{-1}$ [112]. Similarly prepared CNTs were used to obtain ternary CNT/PANI/ZnO composites, which have the ability to effectively absorb gamma radiation [113].

However, CNT functionalization does not always have a positive effect on the properties of composites. There are results indicating that pre-oxidation of CNTs contributes to a decrease in the conductive properties of the material [80]. There is no contradiction in these data, since most studies did not take into account the content of functional groups in CNTs. Dyachkova T.P. and colleagues were the first to analyze the influence of the method and degree of preliminary functionalization of carbon nanotubes on the process of oxidative polymerization of aniline [114]. A correlation has been established between the maximum value on the temperature curve of this reaction and the yield of its target product with the depth of preliminary oxidation of CNTs. The nature of the dependence of the electrically conductive properties of composites and the value of their specific surface area on the degree of preliminary functionalization of CNTs with carboxyl groups is shown. Composites based on carboxylated CNTs with a degree of functionalization of 0.2 mmol·g^{-1} have the best electrical conductivity (3 S·cm^{-1}). Materials with the maximum specific surface area (more than 170 $m^2 \cdot g^{-1}$) were obtained using CNTs oxidized with concentrated nitric acid as a substrate for the deposition of PANI.

Based on the results of calculations obtained by molecular dynamics methods, a mechanism for the modification of carboxylated CNTs with PANI was proposed [115]. It has been shown that phenazine nucleates during the oxidative polymerization of aniline are formed on the surface of nanotubes, desorbed into the bulk of the reaction mixture, where PANI macromolecules then grow.

4.2. PANI / graphene composites

Over the past decade, graphene, which consists of a single layer of sp^2-hybridized carbon atoms linked into a hexagonal two-dimensional crystal lattice, has attracted enormous research attention as a functional material. This is due to its high electrical and thermal conductivity, high mechanical strength and high specific surface area [116–123]. In particular, its structure and unique electron transport properties make graphene in combination with a conducting polymer (for example, PANI) a promising material for the manufacture of electronic, electrochemical and optoelectronic devices [124–126].

Nanocomposites of PANI with graphene and its derivatives can be obtained in various ways, for example, chemical oxidative polymerization [127, 128], electrochemical oxidative polymerization [129, 130], interfacial polymerization [131], by mixing the starting components (polymer and graphene material) [132, 133].

The efficiency and simplicity of the method of chemical oxidative polymerization of aniline on the surface of graphene has made it the most common method for preparing PANI/G nanocomposites. It is reported that when using this approach to improve the electrochemical characteristics of composites and reduce the proportion of PANI in the volume of the reaction mixture, it is advisable to pre-functionalize the surface of graphene materials either with organic molecules or oxygen-containing functional groups. Thus, additional centers for polymer growth will be created on the surface of the carbon material [134]. Synthesis conditions and the percentage of polymer and carbon material in the final product affect the morphology of PANI/G composites. It has been reported that various nanostructures have been obtained: nanospheres [128], nanofibers [135, 136] or nanotubes [137].

The oxidative polymerization method can also be used to coat other carbon nanostructures, for example, mesoporous carbon, with PANI [138].

Methods for electrochemical oxidative polymerization of aniline in the presence of hafen are divided into potentiostatic [139] and potentiodynamic methods [134].

A distinctive feature of interfacial polymerization is that the aniline monomer is dissolved in organic solvents (for example, chloroform, benzene), and the oxidizing agent is dissolved in an aqueous acid solution. After transferring the prepared solutions into the reactor, an organic solvent/water interface is formed, at which the polymerization reaction occurs [131]. As a result of this approach, the PANI/G composite, which comes in the form of a composite film that can be easily separated, is formed at the interface [140].

It is also possible to obtain PANI-graphene composites by mixing and sonicating a dispersion of graphene material with previously prepared PANI [132–134]. The disadvantage of this approach is the instability of composites and their tendency to phase separation [132]. This drawback was eliminated by activating the graphene surface with the formation of acid chloride groups that interact with PANI [132–134].

4.3. Hybrid composites

In addition to binary PANI composites, the preparation of materials combining PANI, CNTs, graphene structures and other types of carbon materials has also been reported. The use of such combinations makes it possible to eliminate the disadvantages of individual dispersed carriers and, in some cases, achieve synergistic effects on various properties.

Graphene/carbon nanotubes/PANI composite can be used as a supercapacitor electrode material, which has a high specific capacitance (1035 $F \cdot g^{-1}$) and retains up to 94 % of the original capacity after 1000 charge/discharge cycles [141].

By combining a mixture of CNTs and graphene oxide with ready-made PANI and subsequent carbonization, a composite is obtained with the specific surface 176 $m^2 \cdot g^{-1}$ and the specific pore volume 0.232 $cm^3 \cdot g^{-1}$ [142].

Based on PANI-modified carbon nanotubes and graphene, a mesoporous airgel with a specific surface area of 289 $m^2 \cdot g^{-1}$ was obtained in a high-pressure autoclave in a supercritical isopropanol environment [143]. In this system, CNTs act as structure formers, preventing the agglomeration of graphene sheets, and PANI astices have a spherical shape. When using reduced graphene oxide and oxidized CNTs to form an airgel, it is possible to obtain a material with a higher specific surface area of 315 $m^2 \cdot g^{-1}$ [144].

Natural carbon materials are often used as one of the components of hybrid composites. For example, the authors of [145] obtained a stable porous sorbent by combining PANI, multi-walled carbon nanotubes and chitosan cryogel. To obtain a flexible composite with a developed surface, porous wood was used, on the surface of which a layer of electrically conductive CNTs was deposited, after which the surface of the material was coated with PANI in situ [146]. A flexible supercapacitor based on this composite has a high specific capacity of 45.89 $F \cdot g^{-1}$ at a current of 0.2 $A \cdot g^{-1}$; after 1000 charge-discharge cycles, about 99% of the capacity is retained; in addition, even when bent by 120°, 62.9 % of capacity is retained. By introducing PANI into a conductive network based on a hybrid material “nanocellulose – multiwalled carbon nanotubes”, a film airgel electrode with a specific capacitance of the order of 2176.3 $mF \cdot cm^{-2}$ was obtained [147].

5. Application of PANI and composites based on it

PANI and its composites are of great interest for various fields of application due to the availability of fairly simple methods for their preparation and the possibility of synergistic effects when combining a dopant and PANI. Recently, most attention has been paid to the production of composites for use as electrode materials for supercapacitors, sorbents, and radiation-absorbing materials (Table 3).

As discussed above, PANI comes in a variety of forms, each with its own properties and applications. Leucoemeraldine, a fully reduced form of PANI, has found applications in electrochromic devices and lithium polymer batteries. Emeraldine salt, which is highly electrically conductive, is used in the sensor industry as an electromagnetic shielding material, in electrochromic devices, and as an electrode material in batteries. Some gas sensors are made using emeraldine salt. Pernigraniline is used in nonlinear optics [160, 161].

Composites based on PANI have high stable electrical conductivity and capacitance (up to 4800 $F \cdot g^{-1}$ [162]) (Table 4). It has also been established that the entire volume of material is involved in storing the charge. This sets this polymer apart from other conductive materials in which charge storage occurs only on the surface. Therefore, composites with PANI can be successfully used as materials for chemical current sources and supercapacitors. For these purposes, binary and three-component composites are being developed that combine PANI, carbon nanomaterials, and metal oxides [163, 164].

The ability of PANI and composites based on it to absorb radiation (due to a combination of magnetic and dielectric properties) opens up prospects for the creation of radio-absorbing [175, 176] and electromagnetic interference shielding materials [177, 178].

PANI and materials containing it can prevent or slow down the oxidation of metal by atmospheric oxygen, which makes it possible to manufacture anti-corrosion coatings [179–181].

The possibility of using PANI in tissue engineering biosensing and targeted drug delivery has been reported [182, 183]. In addition, PANI is considered as a biocidal additive in the production of coatings that protect against viruses [184].

Moreover, composites based on PANI-modified carbon nanotubes can find wide application in electrochemical sensors, solar energy converters, and highly efficient sorbents for heavy metals, bacteria and viruses.

Let us give a number of examples. PANI/CNT composites are proposed to be used in sensors for ammonia detection [185–187]. The detection mechanism is regulated by deprotonation of the emeraldine salt of PANI by NH_3 molecules and conversion to the emeraldine base of PANI, which leads to an increase in electrical resistance. It has been shown that temperature has a strong influence on the performance of sensors. The introduction of CNTs into the composite reduces this effect.

Table 3. Application areas of composites based on PANI and carbon nanomaterials

No.	Composite	Application	Source
1	PANI/ MWCNT	Electrode materials for supercapacitors	[148]
2	PANI/G	Electrode materials for supercapacitors	[149]
3	PANI/GO/G	Electrode materials for supercapacitors	[150]
4	PANI/regenerated exhaust gas	Electrode materials for supercapacitors	[151]
5	PANI/porous carbon microspheres	Electrode materials for supercapacitors	[152]
6	PANI/GO PANI/CNT	Sorbents	[153]
7	PANI/GO/CNT	Sorbents	[154]
8	PANI/regenerated exhaust gas	Sensors for temperature, relative humidity, pesticide detection	[155]
9	PANI/carboxylated CNTs	Biosensors	[156]
10	PANI/ MWCNT/ STARCH	Biosensors	[157]
11	PANI/CNT/Gold nanoparticles	Sensors for detecting zinc, lead and copper	[158]
12	PANI/CNT	Microwave absorbing materials	[159]

Table 4. Specific capacity and stability of PANI and its composites

No.	Composite	Specific capacitance, $F \cdot g^{-1}$	Current ($A \cdot g^{-1}$) or scan rate ($mV \cdot s^{-1}$)	Capacitance conservation	Source
1	PANI/CNT/MoS_2	350	10 $A \cdot g^{-1}$	68 % after 2000 cycles	[165]
2	PANI/GO/MoS_2	815	10 $mV \cdot s^{-1}$	93 % after 100 cycles	[166]
3	PANI/GO/TiO_2	713	10 $mV \cdot s^{-1}$	94 % after 100 cycles	
4	MWCNT	30	0.4 $A \cdot g^{-1}$	–	[167]
5	PANI	210	0.4 $A \cdot g^{-1}$	–	
6	PANI/MWCNT/TiO_2	270	0.4 $A \cdot g^{-1}$	67 % after 6000 cycles	
7	PANI/MWCNT/$Ni(OH)_2$	1917	1.0 $A \cdot g^{-1}$	75 % after 1000 cycles	[168]
8	PANI/polyndol (2:1)	682.4	0.5 $A \cdot g^{-1}$	78.6 % after 1000 cycles	[169]
9	PANI/polyndole/MWCNT (3 wt. %)	895	0.5 $A \cdot g^{-1}$	97.8 % after 1000 cycles	
10	PANI/CNT/graphene	415	3 $A \cdot g^{-1}$	96 % after 5000 cycles	[170]
11	PANI/graphene	310	3	74 % after 5000 cycles	
12	PANI/CNT	215	3	84 % after 5000 cycles	
13	PANI/reduced GO/Fe_3O_4	486.5	1	52.1 % after 2000 cycles	[171]
14	PANI/sulfonated graphene/NiO	1350	1	92.23 % after 5000 cycles	[172]
15	PANI/GO/MWCNT	696	20 $mV \cdot s^{-1}$	–	[173]
16	PANI/GO/$CoFe_2O_4$	781.27	1 $mV \cdot s^{-1}$	79.03 % after 5000 cycles	[174]

PANI composites with reduced graphene oxide have been used to fabricate a VOC sensor that exhibits high sensitivity towards methanol gas [188]. To detect nitrite in tap and rain water, an electrode modified with a reduced graphene oxide/$MnFe_2O_4$/PANI composite was developed [189].

Electrically conductive PANI/CNT composites have found application in the creation of various electrochemical enzyme sensors: sensors for the detection of ascorbic acid [190], glucose [191], phenolic compounds [192], pesticides [193], and cholesterol [194]. A sensor based on PANI and graphene oxide was developed to determine cortisol in human saliva [195].

The possibility of using PANI/CNT composites in solar cells was studied [196, 197]. It was shown that the performance of solar cells increases as a result of using a PANI/CNT composite. The increase in conversion efficiency is explained by more efficient charge transfer due to suppression of the charge recombination process [198].

Composite adsorbents consisting of PANI and carbon nanomaterials are increasingly considered as promising materials for water purification due to their ability to sorb various types of pollutants [199–201]. The prospects for using PANI as an adsorbent are due to the presence of adsorption centers, which are amine and imine groups that interact with pollutants in aqueous solutions [202].

It was shown that PANI/CNT composites can be used for the sorption of copper and nickel ions from water [203]. At the same time, deprotonation of PANI has little effect on this process, and the conversion of the modifying layer of PANI into the leucobase form upon reduction with hydrazine sharply increases the sorption capacity of the material for copper ions. PANI/CNT and PANI/GNP composites can be used for the sorption of various pollutants and pathogenic microorganisms [204], and the successful use of PANI/CNT composites for the extraction of scandium ions from aqueous media has been reported [205].

Hybrid composites based on mixtures of CNTs and graphene materials embedded with PANI demonstrate high sorption capacity with respect to zinc ions (346 $mg \cdot g^{-1}$ at pH 6.5) [142] and lead (350 $mg \cdot g^{-1}$) [143] and others heavy metals [144].

Some sources report quite unusual applications of PANI-based composites. PANI-modified graphene nanoplatelets were used as a reinforcing filler for a composite based on highly oriented ultra-high molecular weight polyethylene (UHMWPE) [206, 207]. It was found that PANI helps to reduce the aggregation of GNP in the polymer matrix and

increase the degree of its crystallinity. The new lamellar crystal structure has high stretchability. The highest tensile strength of 1330 MPa has a composite containing 2 wt. % GNP/PANI filler, and the highest value of Young's modulus of 41 GPa is observed at 1 % content of the modified filler.

6. Conclusion

In this review, we have shown the promise of using PANI and its composites with carbon nanomaterials in various industries due to their unique electrical, physical, chemical, and optical properties. Recent studies show that combining PANI with various substances (carbon nanotubes, graphene, graphene oxide, metal oxides) can improve the performance characteristics of the polymer.

However, despite numerous studies and positive results, many challenges still need to be overcome on the path to commercialization of composites. The analyzed studies are devoted to the development of new materials of complex composition, the study of their properties, and specific proposals for practical use.

A generalization of scientific results shows that the selection of the optimal composition of composites remains relevant in order to find ways to increase their electrical capacity and cyclic stability, increase electrical conductivity and specific surface area. For this purpose, materials are developed that consist of three or more components. And obviously, by varying their mass ratio, fundamentally different materials can be obtained. It has been shown that the properties of composites with PANI depend on the presence of functional groups on the CNM surface. Although such information is available in the literature, it is scattered and requires additional study.

It is assumed that in the near future, composites being developed with PANI may become the basis of many technologies that provide a high-quality standard of living (ecology, energy, safety), but for this it is necessary to continue scientific research. Thus, it is necessary to establish what effect functional groups on the surface of carbon nanomaterials have on the performance characteristics of composites. To evaluate the effectiveness of composites, it is necessary to test them in practice, and for further commercialization it is necessary to develop protocols/recommendations that include a description of methods for obtaining composites with a given structure and properties.

7. Funding

This study received no external funding.

8. Conflict of interests

The authors declare no conflict of interests.

References

1. Li Z, Gong L. Research progress on applications of polyaniline (PANI) for electrochemical energy storage and conversion. *Materials*. 2020;13(3):548. DOI:10.3390/ma13030548

2. Thambidurai S, Pandiselvi K. Polyaniline/natural polymer composites and nanocomposites. In: Visakh PM, Pina CD, Falletta E. (eds.) *Polyaniline blends, composites, and nanocomposites*. Elsevier; 2018, p.235-256. DOI:10.1016/b978-0-12-809551-5.00009-6

3. Stejskal J, Gilbert RG. Polyaniline. Preparation of a conducting polymer (IUPAC Technical Report). *Pure and Applied Chemistry*. 2002;74(5):857-867. DOI:10.1351/pac200274050857

4. Chiang JC, MacDiarmid AG. «Polyaniline»: Protonic acid doping of the emeraldine form to the metallic regime. *Synthetic Metals*. 1986;13(1-3):193-205. DOI:10.1016/0379-6779(86)90070-6

5. Zhang P, Zhai X, Huang H, et al. Capacitance fading mechanism and structural evolution of conductive polyaniline in electrochemical supercapacitor. *Journal of Materials Science: Materials in Electronics*. 2020:31; 14625-14634. DOI:10.1007/s10854-020-04025-y

6. Pawar DC, Malavekar DB, Lokhande AC, et al. Facile synthesis of layered reduced graphene oxide/polyaniline (rGO/PANI) composite electrode for flexible asymmetric solid-state supercapacitor. *Journal of Energy Storage*. 2024;79:110154. DOI:10.1016/j.est.2023.110154

7. Yang J, Liu Y, Liu S, et al. Conducting polymer composites: material synthesis and applications in electrochemical capacitive energy storage. *Materials Chemistry Frontiers.* 2017;1(2):251-268. DOI:10.1039/C6QM00150E

8. Che B, Li H, Zhou D, et al. Porous polyaniline/carbon nanotube composite electrode for supercapacitors with outstanding rate capability and cyclic stability. *Composites Part B: Engineering*. 2019;165:671-678. DOI:10.1016/j.compositesb.2019.02.026

9. Liao G, Li Q, Xu Z. The chemical modification of polyaniline with enhanced properties: A review. *Progress in Organic Coatings*. 2019;126:35-43. DOI:10.1016/j.porgcoat.2018.10.018

10. Nezakati T, Seifalian A, Tan A, et al. Conductive polymers: opportunities and challenges in biomedical applications. *Chemical Reviews*. 2018;118:6766-6843. DOI:10.1021/acs.chemrev.6b00275

11. Runge FF. Über einige Produkte der Steinkohlendestillation. *Annalen der Physik*. 1834;107(5): 65-78.

12. Fritsche J. Ueber das Anilin, ein neues Zersetzungsproduct des Indigo. *Journal fur Praktische Chemie*. 1840;20(1):453-459.

13. Fritzsche J. Vorläufige Notiz über einige neue Körper aus der Indigoreihe. *Journal fur Praktische Chemie*. 1843;28(1):198-204.

14. Letheby H. On the production of a blue substance by the electrolysis of sulphate of aniline. *Journal of the Chemical Society*. 1862;15:161-163. DOI:10.1039/JS8621500161

15. Ciric-Marjanovic G. Recent advances in polyaniline research: Polymerization mechanisms, structural aspects, properties and applications. *Synthetic Metals.* 2013;177:1-47. DOI:10.1016/j.synthmet.2013.06.004

16. Abe M, Ohtani A, Umemoto Y, et al. Soluble and high molecular weight polyaniline. *Journal of the Chemical Society, Chemical Communications*. 1989;(22): 1736-1738. DOI:10.1039/c39890001736

17. Jozefowicz M, Yu LT, Perichon J, et al. Proprietes nouvelles des polymeres semiconducteurs. *Journal of Polymer Science: Part C*. 1969;22:1187-1195. DOI:10.1002/polc.5070220251

18. MacDiarmid AG, Chiang JC, Halpern M, et al. «Polyaniline»: Interconversion of Metallic and Insulating Forms. *Molecular Crystals and Liquid Crystals*. 1985;121:173-180. DOI:10.1080/00268948508074857

19. Do Nascimento GM. Spectroscopy of Polyaniline Nanofibers. In: *Nanofibers*. In Tech; 2010. DOI:10.5772/8162

20. Goswami S, Nandy S, Fortunato E, et al. Polyaniline and its composites engineering: A class of multifunctional smart energy materials. *Journal of Solid State Chemistry*. 2023;317(A):123679. DOI:10.1016/j.jssc.2022.123679

21. Jangid NK, Jadoun S, Kaur N. A review on high-throughput synthesis, deposition of thin films and properties of polyaniline. *European Polymer Journal*. *European Polymer Journal*. 2020;125:109485. DOI:10.1016/j.eurpolymj.2020.109485

22. Gospodinova N, Terlemezyan L. Conducting polymers prepared by oxidative polymerization: polyaniline. *Progress in Polymer Science.* 1998;23(8): 1443-1484. DOI:10.1016/s0079-6700(98)00008-2

23. Sun P, Shen X, Xu P, et al. Conductive polyaniline film synthesized through in-situ polymerization as a conductive seed layer for hole metallization of printed circuit boards. *Applied Surface Science*. 2024;655:159649. DOI:10.1016/j.apsusc.2024.159649

24. Ležaić AJ, Bajuk-Bogdanović D, Ćirić-Marjanović G. In situ Raman spectroscopy study of the oxidative polymerization of aniline in media of different acidity. *Synthetic Metals*. 2024;305:117602. DOI:10.1016/j.synthmet.2024.117602

25. Hussain AMP, Kumar A. Electrochemical synthesis and characterization of chloride doped polyaniline. *Bulletin of Materials Science*. 2003;20:329-344. DOI:10.1007/BF02707455

26. Shan J, Han L, Bai F, et al. Enzymatic polymerization of aniline and phenol derivatives catalyzed by horseradish peroxidase in dioxane(II). *Polymers for Advanced Technologies*. 2003;14(3-5):330-336. DOI:10.1002/pat.316

27. Mohammad RS, Zarrintaj P, Khandelwal P, et al. Synthetic route of polyaniline (I): Conventional oxidative polymerization. In: Mozafari M, Chauhan NPS (eds.) *Fundamentals and Emerging Applications of Polyaniline*, Elsevier, 2019. p. 17-41. DOI:10.1016/B978-0-12-817915-4.00002-6

28. Yılmaz F, Küçükyavuz Z. The influence of polymerization temperature on structure and properties of polyaniline. *e-Polymers*. 2009;9(1). DOI:10.1515/epoly.2009.9.1.48

29. Tran HD, D'Arcy JM, Wang Y, et al. The oxidation of aniline to produce "polyaniline": a process yielding many different nanoscale structures. *Journal of materials Chemistry*. 2011;21:3534-3550. DOI:10.1039/c0jm02699a

30. Stejskal J, Sapurina I, Trchová M. Polyaniline nanostructures and the role of aniline oligomers in their formation. *Progress in Polymer Science*. 2010; 35(12): 1420-1481. DOI:10.1016/j.progpolymsci.2010.07.006

31. Trchová M, Konyushenko EN, Stejskal J, et al. The conversion of polyaniline nanotubes to nitrogen-containing carbon nanotubes and their comparison with multi-walled carbon nanotubes. *Polymer Degradation and Stability*. 2009:94(6):929-938. DOI:10.1016/j.polymdegradstab.2009.03.001

32. Dhawale DS, Dubal DP, Jamadade VS, et al. Fuzzy nanofibrous network of polyaniline electrode for supercapacitor application. *Synthetic Metals*. 2010;160:519-522. DOI: 10.1016/j.synthmet.2010.01.021

33. Mandić Z, Roković MK, Pokupčić T. Polyaniline as cathodic material for electrochemical energy sources. The role of morphology. *Electrochimica Acta*. 2009; 54(10):2941-2950. DOI:10.1016/j.electacta.2008.11.002

34. Qin Q, Tao J, Yang Y. Preparation and characterization of polyaniline film on stainless steel by electrochemical polymerization as a counter electrode of DSSC. *Synthetic Metals*. 2010;160(11-12):1167-1172. DOI: 10.1016/j.synthmet.2010.03.003

35. Lukachova. LV, Shkerin EA, Puganova EA, et al. Electroactivity of chemically synthesized polyaniline in neutral and alkaline aqueous solutions. *Journal of Electroanalytical Chemistry*. 2003;544:59-63. DOI:10.1016/s0022-0728(03)00065-2

36. Sayah A, Habelhames F, Bennouioua A, et al. Capacitance of polyaniline films synthesized by direct and pulse potentiostatic methods. *Journal Marocain de Chimie Hétérocyclique*. 2021;20(2):108-116. DOI:10.48369/IMIST.PRSM/jmch-v20i2.24711

37. Gojgić J, Petrović M, Jugović B, et al. Electrochemical and electrical performances of high energy storage polyaniline electrode with supercapattery behavior. *Polymers*. 2022;14(24):5365. DOI:10.3390/polym14245365

38. Duić L, Mandić Z. Counter-ion and pH effect on the electrochemical synthesis of polyaniline. *Journal of Electroanalytical Chemistry*. 1992;335(1-2):207-221. DOI:10.1016/0022-0728(92)80243-W

39. Abalyaeva VV, Kogan IL. Initiating agents for electrochemical polymerization of aniline on titanium electrodes. *Synthetic Metals*. 1994;63(2):109-113. DOI:10.1016/0379-6779(94)90257-7

40. Lee HT, Chuang KR, Chen SA, et al. Conductivity relaxation of 1-methyl-2-pyrrolidone-

plasticized polyaniline film. *Macromolecules*. 1995; 28:7645-7652. DOI:10.1021/ma00127a009

41. Dhawale DS, Salunkhe RR, Jamadade VS, et al. Hydrophilic polyaniline nanofibrous architecture using electrosynthesis method for supercapacitor application. *Current Applied Physics*. 2010;10(3):904-909. DOI:10.1016/j.cap.2009.10.020

42. Zhang H, Wang J, Wang Z, et al. Electrodeposition of polyaniline nanostructures: A lamellar structure. *Synthetic Metals*. 2009;159(3-4):277-281. DOI:10.1016/j.synthmet.2008.09.015

43. Zhao L, Li X-X, Guo Y-X, et al. Electrochemical Polymerization and Characterization of Polyaniline/Carbon Nanotube Composite Films. *Proceedings of the 2nd Annual International Conference on Advanced Material Engineering (AME 2016).* 2016;281-286. DOI:10.2991/ame-16.2016.47

44. Itoi H, Hayashi S, Matsufusa H, et al. Electrochemical synthesis of polyaniline in the micropores of activated carbon for high-performance electrochemical capacitors. *Chemical Communications*. 2017;53:3201-3204. DOI:10.1039/C6CC08822H

45. Blinova NV, Stejskal J, Trchová M, et al Polyaniline prepared in solutions of phosphoric acid: Powders, thin films, and colloidal dispersions. *Polymer*. 2006;47:42-48. DOI:10.1016/j.polymer.2005.10.145

46. Konyushenko EN, Stejskal J, Trchová M, et al. Multi-wall carbon nanotubes coated with polyaniline. *Polymer*. 2006;47(16):5715-5723. DOI:10.1016/j.polymer.2006.05.059

47. Konyushenko EN, Stejskal J, Šeděnková I, et al. Polyaniline nanotubes: Conditions of formation. *Polymer International*. 2006;55(1):31-39. DOI:10.1002/pi.1899

48. Stejskal J, Sapurina I, Trchová M, et al. The genesis of polyaniline nanotubes. *Polymer*. 2006;47:8253-8262. DOI:10.1016/j.polymer.2006.10.007.

49. Stejskal J, Sapurina I, Trchová M, et al. Oxidation of aniline: Polyaniline granules, nanotubes, and oligoaniline microspheres. *Macromolecules.* 2008;41(10): 3530-3536. DOI:10.1021/ma702601q

50. Ding H, Shen J, Wan M, et al. Formation mechanism of polyaniline nanotubes by a simplified template-free method. *Macromolecular Chemistry and Physics*. 2008;209(8):864-871. DOI:10.1002/macp.200700624

51. Zhang L, Zujovic ZD, Peng H, et al. Structural characteristics of polyaniline nanotubes synthesized from different buffer solutions. *Macromolecules*. 2008;41: 8877-8884. DOI:10.1021/ma801728j

52. Wang J, Zhang D. One-dimensional nanostructured polyaniline: syntheses, morphology controlling, formation mechanisms, new features, and applications. *Advances in Polymer Technology*. 2012;32:E323-E368. DOI:10.1002/adv.21283

53. Anju C, Palatty Sh. Ternary doped polyaniline-metal nanocomposite as high performance supercapacitive material. *Electrochimica Acta*. 2019;299:626-635. DOI:10.1016/j.electacta.2019.01.030

54. Lin K, Hu L, Chen K, et al. Characterization of polyaniline synthesized from chemical oxidative polymerization at various polymerization temperatures. *European Polymer Journal*. 2017;88:311-319. DOI:10.1016/j.eurpolymj.2017.01.035

55. Yashwanth VN, Kariduraganavar MY, Srinivasa HT, et al. Synthesis and characterization of cotton candy-PANI: Enhanced supercapacitance properties. *Journal of the Indian Chemical Society*. 2023;100(3):100944. DOI:10.1016/j.jics.2023.100944

56. Prasutiyo YJ, Manaf A, Hafizah MAE. Synthesis of polyaniline by chemical oxidative polymerization and characteristic of conductivity and reflection for various strong acid dopants. *Journal of Physics: Conference Series*. 2020;1442:012003. DOI:10.1088/1742-6596/1442/1/012003

57. Shaari HAH, Mohtar MN, Rahman NA, et al. Synthesis and functional characterization of conducting polyaniline by oxidative polymerization method. *AIP Conference Proceedings.* 2022;2506(1):030001. DOI:10.1063/5.0084374

58. Zeng F, Qin Z, Liang B, et al. Polyaniline nanostructures tuning with oxidants in interfacial polymerization system. *Progress in Natural Science: Materials International*. 2015;25(5):512-519. DOI:10.1016/j.pnsc.2015.10.002

59. Yasuda A, Shimidzu T. Chemical oxidative polymerization of aniline with ferric chloride. *Polymer Journal*. 1993;25(4):329-338. DOI:10.1295/polymj.25.329

60. Lyu W, Yu M, Li J, et al. Adsorption of anionic acid red G dye on polyaniline nanofibers synthesized by $FeCl_3$ oxidant: Unravelling the role of synthetic conditions. *Colloids and Surfaces A: Physicochemical and Engineering Aspects*. 2022;647:129203. DOI:10.1016/j.colsurfa.2022.129203

61. Bláha M, Riesová M, Zedník J. Polyaniline synthesis with iron (III) chloride – hydrogen peroxide catalyst system: Reaction course and polymer structure study. *Synthetic Metals*. 2011;161:1217-1225. DOI:10.1016/j.synthmet.2011.04.008

62. Ayad M, Amer W, Whdan M. In situ polyaniline film formation using ferric chloride as an oxidant. *Journal of Applied Polymer Science*. 2012;125:2695-2700. DOI:10.1002/app.36584

63. Chiolerio A, Bocchini S, Crepaldi M, et al. Bridging electrochemical and electron devices: fast resistive switching based on polyaniline from one pot synthesis using $FeCl_3$ as oxidant and co-doping agent. *Synthetic Metals*. 2017;229:72-81. DOI:10.1016/j.synthmet.2017.05.001

64. Nestorović GD, Jeremić KB, Jovanović SM. Kinetics of aniline polymerization initiated with iron (III) chloride. *Journal of the Serbian Chemical Society*. 2006;71:895-904. DOI:10.2298/JSC0609895N

65. Yan H, Kajita M, Toshima N. Polymerization of aniline using iron(III) catalyst and ozone, and kinetics of oxidation reactions in the catalytic system. *Macromolecular Materials and Engineering.* 2002;287(8): 503-508. DOI:10.1002/1439-2054(20020801)287:8<503::aid-mame503>3.0.co;2-n

66. Syed AA, Dinesan MK. Review: Polyaniline – A novel polymeric material. *Talanta*. 1991;38(8):815-837. DOI:10.1016/0039-9140(91)80261-w

67. Cao Y, Andreatta A, Heeger AJ, et al. Influence of chemical polymerization conditions on the properties of polyaniline. *Polymer.* 1989;30(12):2305-2311. DOI:10.1016/0032-3861(89)90266-8

68. Jun TS, Kim CK, Kim YS. Vapor phase polymerization of polyaniline nanotubes using Mn_3O_4 nanofibers as an oxidant. *Materials Letters.* 2014;133: 17-19. DOI:10.1016/j.matlet.2014.06.154

69. Li Y, Gong J, He G, et al. Fabrication of polyaniline / titanium dioxide composite nanofibers for gas sensing application. *Materials Chemistry and Physics*. 2011;129(1-2):477-482. DOI:1016/j.matchemphys.2011.|04.045

70. Fei J, Cui Y, Yan X, et al. Controlled fabrication of polyaniline spherical and cubic shells with hierarchical nanostructures. *ACS Nano*. 2009;3(11):3714-3718. DOI:10.1021/nn900921v

71. Yakubu A, Monday M, Tsado MJ, et al. In situ synthesis of polyaniline nanohybrid and formulation of polyaniline/carboxymethyl cellulose/ethylene glycol nanocomposite: study of its conducting and antibacterial properties. *Journal of Materials and Polymer Science*. 2023;3(4):1-9. DOI:10.47485/2832-9384.1041

72. Bláha M, Trchová M, Bober P, et al. Polyaniline: Aniline oxidation with strong and weak oxidants under various acidity. *Materials Chemistry and Physics.* 2017; 194:206-218. DOI:10.1016/j.matchemphys.2017.03.028

73. Ullah R, Bowmaker GA, Laslau C, et al. Synthesis of polyaniline by using $CuCl_2$ as oxidizing agent. *Synthetic Metals*. 2014;198:203-211. DOI:10.1016/j.synthmet.2014.10.005

74. Chuanyu S, Yu W. Synthesis of polyaniline nanotubes through UV light catalytic method. *Materials Science-Poland*. 2015;33(1):193-197. DOI:10.1515/msp-2015-0022

75. Jangid NK, Jadoun S, Kaur N. A Review on high-throughput synthesis, deposition of thin films and properties of polyaniline. *European Polymer Journal*. 2020;125:109485. DOI:10.1016/j.eurpolymj.2020.109485

76. Powar K, Vengurlekar P. Applications of electroactive polymer in electronics and Mechatronics. *International Journal of Scientific & Engineering Research*. 2018;9(2):21-34.

77. Ćirić-Marjanović G. Recent advances in polyaniline composites with metals, metalloids and nonmetals. *Synthetic Metals*. 2013;170(1):31-56. DOI:10.1016/j.synthmet.2013.02.028

78. Gu Y, Tsai JY. Enzymatic synthesis of conductive polyaniline in the presence of ionic liquid. *Synthetic Metals*. 2012;161(23-24):2743-2747. DOI:10.1016/j.synthmet.2011.10.013

79. Guo Z, Hauser N, Moreno A, et al. AOT vesicles as templates for the horseradish peroxidase-triggered polymerization of aniline. *Soft Matter*. 2011;7:180-193. DOI:10.1039/C0SM00599A

80. Ding Q, Qian R, Jing X, et al. Reaction of aniline with $KMnO_4$ to synthesize polyaniline-supported Mn nanocomposites: An unexpected heterogeneous free radical scavenger. *Materials Letters*. 2019;251:222-225. DOI:10.1016/j.matlet.2019.05.076

81. Dyachkova TP, Melezhyk AV, Morozova Zh.G, et al. Effect of the nature of oxidant and synthesis conditions on properties of nanocomposites polyaniline/carbon nanotubes. *Vestnik Tambovskogo gosudarstvennogo tekhnicheskogo universiteta*. 2012;18(3):718-730. (In Russ.)

82. Bláha M, Zedník J, Vohlídal J. Self-doping of polyaniline prepared with the $FeCl_3/H_2O_2$ system and the origin of the Raman band of emeraldine salt at around 1375 cm^{-1}. *Polymer International.* 2015;64(12):1801-1807. DOI:10.1002/pi.4983

83. Garcia-Bernabé A, Gil-Agustí M, Ortega G, et al. On the effect of the oxidative reagents on the conductivity of polyaniline/MMT nanocomposites. *AIP Conference Proceedings*. 2010;1255:273-275. DOI:10.1063/1.3455605

84. Majeed A, Mohammed L, Hammoodi O, et al. A review on polyaniline: synthesis, properties, nanocomposites, and electrochemical applications. *International Journal of Polymer Science*. 2022;2022: 9047554. DOI:10.1155/2022/9047554

85. Carrillo N, León-Silva U, Avalos T, et al. Enzymatically synthesized polyaniline film deposition studied by simultaneous open circuit potential and electrochemical quartz crystal microbalance measurements. *Journal of Colloid and Interface Science*. 2012;369(1):103-110. DOI:10.1016/j.jcis.2011.12.021

86. Felix JF, Barros RA, M. de Azevedo W, et al. X-ray irradiation: A non-conventional route for the synthesis of conducting polymers. *Synthetic Metals*. 2011;161:173-176. DOI:10.1016/j.synthmet.2010.11.017

87. Park JK, Kwon OP, Choi EY, et al. Enhanced electrical conductivity of polyaniline film by a low magnetic field. *Synthetic Metals*. 2010;160:728-731. DOI:10.1016/j.synthmet.2010.01.011

88. Jackowska K, Bieguński AT, Tagowska M. Hard template synthesis of conducting polymers: A route to achieve nanostructures. *Journal of Solid State Electrochemistry*. 2008;12(4):437-443. DOI:10.1007/s10008-007-0453-7

89. Konyushenko EN, Stejskal J, Trchová M, et al. Suspension polymerization of aniline hydrochloride in non-aqueous media. *Polymer International*. 2011;60(5): 794-797. DOI:10.1002/pi.3017

90. Kim JY, Jang H, Lee YR, et al. Nanostructured polyaniline films functionalized through auxiliary nitrogen addition in atmospheric pressure plasma polymerization. *Polymers*. 2023;15(7):1626. DOI:10.3390/polym15071626

91. Sury S, Ulianas A, Aini S. Synthesis of conducting polyaniline with photopolymerization method and characterization. *Journal of Physics: Conference Series*. 2020;1788:012004. DOI:10.1088/1742-6596/1788/1/012004

92. Stejskal J, Riede A, Hlavatá D, et al. The effect of polymerization temperature on molecular weight, crystallinity, and electrical conductivity of polyaniline. *Synthetic Metals*. 1998;96:55-61. DOI:10.1016/S0379-6779(98)00064-2

93. Adams PM, Abell L, Middleton A, et al. Low temperature synthesis of high molecular weight polyaniline using dichromate oxidant. *Synthetic Metals.* 1997;84(1-3): 61-62. DOI:10.1016/s0379-6779(96)03836-2

94. Peng C, Zhang S, Jewell D, et al. Carbon nanotube and conducting polymer composites for supercapacitors. *Progress in Natural Science*. 2008;18(7):777-788. DOI:10.1016/j.pnsc.2008.03.002

95. Wu G, Du H, Cha YL, et al. A wearable mask sensor based on polyaniline/CNT nanocomposites for monitoring ammonia gas and human breathing. *Sensors and Actuators B: Chemical*. 2023;375:132858. DOI:10.1016/j.snb.2022.132858

96. Rodrigues de Souza VH, Oliveira M, Zarbin AJ. Thin and flexible all-solid supercapacitor prepared from novel single wall carbon nanotubes/polyaniline thin films obtained in liquid-liquid interfaces. *Journal of Power Sources*. 2014;260:34-42. DOI:10.1016/j.jpowsour. 2014.02.070

97. Yoo R, Kim J, Song M-J, et al. Nano-composite sensors composed of single-walled carbon nanotubes and polyaniline for the detection of a nerve agent simulant gas. *Sensors and Actuators B: Chemical*. 2015;209:444-448. DOI:10.1016/j.snb.2014.11.137

98. Abdulla S, Lazar T, Pullithadathil M. Highly sensitive, room temperature gas sensor based on polyaniline-multiwalled carbon nanotubes (PANI/ MWCNTs) nanocomposite for trace-level ammonia detection. *Sensors and Actuators B: Chemical*. 2015;21:1523-1534. DOI:10.1016/j.snb.2015.08.002

99. Wang Y, Zhang S, Deng Y. Semiconductor to metallic behavior transition in multi-wall carbon nanotubes/polyaniline composites with improved thermoelectric properties. *Materials Letters*. 2016;164:132-135. DOI:10.1016/j.matlet.2015.10.138

100. Oueiny C, Berlioz S, Perrin F.-X. Carbon nanotube–polyaniline composites. *Progress in Polymer Science*. 2014;39(4):707-748. DOI:10.1016/j.progpolymsci. 2013.08.009

101. Wang Q, Qian X, Wang S, et al. Conductive polyaniline composite films from aqueous dispersion: Performance enhancement by multi-walled carbon nanotube. *Synthetic Metals*. 2015;199:1-7. DOI:10.1016/ j.synthmet.2014.11.007

102. Tan H, Xu X. Conductive properties and mechanism of various polymers doped with carbon nanotube/polyaniline hybrid nanoparticles. *Composites Science and Technology*. 2016;128:155-160. DOI:10.1016/ j.compscitech.2016.03.027

103. Bachhav SG, Patil DR. Synthesis and characterization of polyaniline-multiwalled carbon nanotube nanocomposites and its electrical percolation behavior. *American Journal of Materials Science*. 2015;5(4):90-95. DOI:10.5923/j.materials.20150504.03

104. Xavier PAF, Benoy MD, Stephen SK, et al. Enhanced electrical properties of polyaniline carbon nanotube composites: Analysis of temperature dependence of electrical conductivity using variable range hopping and fluctuation induced tunneling models. *Journal of Solid State Chemistry*. 2021;300:122232. DOI:10.1016/ j.jssc.2021.122232

105. Zhang J, Zhu A. Study on the synthesis of PANI/CNT nanocomposite and its anticorrosion mechanism in waterborne coatings. *Progress in Organic Coatings.* 2021;159:106447. DOI:10.1016/j.porgcoat. 2021.106447

106. Bora A, Mohan K, Pegu D, et al. A room temperature methanol vapor sensor based on highly conducting carboxylated multi-walled carbon nanotube/polyaniline nanotube composite. *Sensors and Actuators B: Chemical*. 2017;253:977-986. DOI:10.1016/ j.snb.2017.07.023

107. Islam R, Papathanassiou A, Chan-Yu-King R, et al. Competing charge trapping and percolation in core-shell single wall carbon nanotubes/polyaniline nanostructured composites. *Synthetic Metals*. 2020;259:116259. DOI:10.1016/j.synthmet.2019.116259

108. Mottaghitalab V, Spinks GM, Wallace GG. The influence of carbon nanotubes on mechanical and electrical properties of polyaniline fibers. *Synthetic Metals.* 2005;152(1-3):77-80. DOI:10.1016/j.synthmet.2005.07.154

109. Huang J, Liu X, Du Y. Highly efficient and wearable thermoelectric composites based on carbon nanotube film/polyaniline. *Journal of Materiomics*. 2024;10(1):173-178. DOI:10.1016/j.jmat.2023.04.014

110. Wu T.-M, Lin Y.-W. Doped polyaniline/multi-walled carbon nanotube composites: Preparation, characterization and properties. *Polymer*. 2006;47(10): 3576-3582. DOI:10.1016/j.polymer.2006.03

111. Snook GA, Kao P, Best AS. Conducting-polymer-based supercapacitor devices and electrodes. *Journal of Power Sources*. 2011;196(1):1-12. DOI:10.1016/j.jpowsour.2010

112. Singh G, Kumar Y, Husain S. Fabrication of high energy density symmetric polyaniline/functionalized multiwalled carbon nanotubes supercapacitor device with swift charge transport in different electrolytic mediums. *Journal of Energy Storage*. 2023;65. DOI:10.1016/ j.est.2023.107328

113. Ali ES, Issa Sh, Zakaly H, et al. Exploration of optical and gamma radiation shielding characteristics of zinc oxide nanoparticles doped functionalized multi-walled carbon nanotubes nanohybrids based polyaniline ternary nanocomposites. *Diamond and Related Materials*. 2024;143:110882. DOI:10.1016/j.diamond.2024.110882

114. Dyachkova TP, Anosova IV, Tkachev AG, et al. Synthesis of composites from functionalized carbon nanotubes and polyaniline. *Inorganic Materials: Applied Research.* 2018;9(2):305-310. DOI:10.1134/ S2075113318020089

115. Gutnik IV, Dyachkova TP, Rukhov AV, et al. Polyaniline/carbon nanotubes composites: kinetic laws of synthesis, morphology and properties. *Advanced Materials and Technologies*. 2018;4:54-68. DOI:10.17277/ amt.2018.04.pp.054-068

116. Geim AK, Novoselov KS. The rise of grapheme. *Nature Materials*. 2007;6(3):183-191. DOI:10.1038/nmat1849

117. Mehmooda Ah, Mubaraka NM, Khalidb M, et al. Graphene based nanomaterials for strain sensor application – a review. *Journal of Environmental Chemical Engineering*. 2020;8:103743. DOI:10.1016/j.jece.2020. 103743

118. Yang Y, Wei Y, Guo Z, et al. From materials to devices: graphene toward practical applications (Review). *Small Methods*. 2022;6(10):2200671. DOI:10.1002/smtd. 202200671

119. Sahoo PK, Kumar N, Jena A, et al. Recent progress in graphene and its derived hybrid materials for high-performance supercapacitor electrode applications. *RSC Advances*. 2024;14(2):1284-1303. DOI:10.1039/ d3ra06904d

120. Avinash K, Patolsky F. Laser-induced graphene structures: From synthesis and applications to future prospects. *Materials Today*. 2023;70:104-136. DOI:10.1016/j.mattod.2023.10.009

121. Nair AS, Sreejakumari SS, Venkatesan J, et al. A novel top-down approach for high yield production of graphene from natural graphite and its supercapacitor applications. *Diamond and Related Materials*. 2024;144:111025. DOI:10.1016/j.diamond.2024.111025

122. Ahmad F, Ghazal H, Rasheed F, et al. Graphene and its derivatives in medical applications: A comprehensive review. *Synthetic Metals*. 2024;304:117594. DOI:10.1016/j.synthmet.2024.117594

123. Nam J, Yang J, Zhao Y, et al. Chemical vapor deposition of graphene and its characterizations and applications. *Current Applied Physics*. 2024;61:55-70. DOI:10.1016/j.cap.2024.02.010

124. Prasannakumar AT, Rohith R, Manju V, et al. Graphene nanoflake-self stabilized dispersion polymerized PANI hybrids as efficient, binder-free electrode materials for high-performance flexible symmetric supercapacitors. *Journal of Electroanalytical Chemistry*. 2024;952:117952. DOI:10.1016/j.jelechem.2023.117952

125. Kerli S, Bhardwaj S, Lın W, et al. Silver-doped reduced graphene oxide/PANI composite synthesis and their supercapacitor applications. *Journal of Organometallic Chemistry*. 2023,995:122725. DOI:10.1016/j.jorganchem.2023.122725

126. Kenesi AG, Ghorbani M, Lashkenari MS. High electrochemical performance of PANI/CdO nanocomposite based on graphene oxide as a hybrid electrode materials for supercapacitor application. *International Journal of Hydrogen Energy*. 2022;47(91):38849-38861. DOI:10.1016/j.ijhydene.2022.09.047

127. Mourya P, Goswami R, Saini R, et al. Epoxy coating reinforced with graphene-PANI nanocomposites for enhancement of corrosion-resistance performance of mild steel in saline water. *Colloids and Surfaces A: Physicochemical and Engineering Aspects*. 2024;687: 133500. DOI:10.1016/j.colsurfa.2024.133500

128. Yan J, Wei T, Shao B, at al. Preparation of a graphene nanosheet/polyaniline composite with high specific capacitance. *Carbon*. 2010;48:487-493. DOI:10.1016/j.carbon.2009.09.066

129. Zhang Q-Y, Yang Y-J, Tang M-Y, et al. Electrochemical preparation and features of newly cross-stacking multi-layered reduced graphene oxide (*r*GO) and polyaniline (PANI) modified carbon-based electrode. *Current Research in Biotechnology*. 2024;7:100196. DOI:10.1016/j.crbiot.2024.100196

130. Okhay O, Tkach A. Polyaniline-graphene electrodes prepared by electropolymerization for high-performance capacitive electrodes: a brief review. *Batteries*. 2022;8(10):191. DOI:10.3390/batteries8100191

131. Ma B, Zhou X, Bao H, et al. Hierarchical composites of sulfonated graphene-supported vertically aligned polyaniline nanorods for high-performance supercapacitors. *Journal of Power Sources.* 2012;215:36-42. DOI:10.1016/j.jpowsour.2012.04.083

132. Jianhua L, Junwei A, Yecheng Z, et al. Preparation of an amide group-connected graphene–polyaniline nanofiber hybrid and its application in supercapacitors. *ACS Applied Materials and Interfaces*. 2012;4:2870-2876. DOI:10.1021/am300640y

133. Umar Ah, Ahmed F, Ullah N, et al. Exploring the potential of reduced graphene oxide/polyaniline (*r*GO@PANI) nanocomposites for high-performance supercapacitor application. *Electrochimica Acta*. 2024;479:143743. DOI:10.1016/j.electacta.2023.143743

134. Huang Z, Li L, Wang Y, et al. Polyaniline/graphene nanocomposites towards high-performance supercapacitors: A review. *Composites Communications*. 2018;8:83-91. DOI:10.1016/j.coco. 2017.11.005

135. Li Y, Zhao X, Yu P, et al. Oriented arrays of polyaniline nanorods grown on graphite nanosheets for an electrochemical supercapacitor. *Langmuir*. 2013;29:493-500. DOI:10.1021/la303632d

136. Wang DW, Li F, Zhao J, et al. Fabrication of graphene/polyaniline composite paper via in situ anodic electropolymerization for high-performance flexible electrode. *ACS Nano*. 2009;3:1745-1752. DOI:10.1021/ nn900297m

137. Huang YF, Lin CW. Facile synthesis and morphology control of graphene oxide/polyaniline nanocomposites via in-situ polymerization process. *Polymer*. 2012;53(13):2574-2582. DOI:10.1016/j.polymer. 2012.04.022

138. Gutnik IV, Dyachkova TP, Burakova EA, et al. Polyaniline/mesoporous carbon composites as promising materials for supercapacitors. *IOP Conference Series: Materials Science and Engineering: 3, Synthesis, Production, and Application*. Tambov. 2019;693:012026. DOI:10.1088/1757-899X/693/1/012026

139. Kumar M, Singh K, Dhawan SK, et al. Synthesis and characterization of covalently-grafted graphene– polyaniline nanocomposites and its use in a

supercapacitor. *Chemical Engineering Journal*. 2013;231:397-405. DOI:10.1016/j.cej.2013.07.043

140. Shen J, Yang C, Li X, et al. High–performance asymmetric supercapacitor based on nanoarchitectured polyaniline/graphene/carbon nanotube and activated graphene electrodes. *ACS Applied Materials and Interfaces*. 2013;5:8467-8476. DOI:10.1021/am4028235

141. Yan J, Wei T, Fan Z, et al. Preparation of graphene nanosheet / carbon nanotube / polyaniline composite as electrode material for supercapacitors. *Journal of Power Sources*. 2010;195(9):3041-3045. DOI:10.1016/j.jpowsour.2009.11.028

142. Ali I, Burakov AE, Burakova IV, et al. Polyaniline modified CNTs and graphene nanocomposite for removal of lead and zinc metal ions: kinetics, thermodynamics and desorption studies. *Molecules*. 2022;27(17):5623. DOI:10.3390/molecules27175623

143. Kuznetsova TS, Burakov AE, Pasko TV, et al. Physico-chemical and sorption properties of nanocomposite aerogels based on modified carbon nanotubes and grapheme. *Izvestiya vysshih uchebnyh zavedenij. Seriya: himiya i himicheskaya tekhnologiya. = ChemChemTech.* 2023;66(3);66-76. DOI:10.6060/ivkkt.20236603.6726 (In Russ.)

144. Kuznetsova TS, Burakov AE, Burakova IV, et al. Preparation of a polyaniline-modified hybrid graphene aerogel-like nanocomposite for efficient adsorption of heavy metal ions from aquatic media. *Polymers*. 2023;15(5):1101. DOI:10.3390/polym15051101

145. Rattanakunsong N, Bunkoed O. A porous composite monolith sorbent of polyaniline, multiwall carbon nanotubes and chitosan cryogel for aromatic compounds extraction. *Microchemical Journal*. 2020;154:104562. DOI:10.1016/j.microc.2019.104562

146. Wang X, Ouyang J, Wang L, et al. Wood shavings combined with polyaniline and carbon nanotube film for flexible high-performance energy storage devices. *Journal of Energy Storage*. 2024;77:109927. DOI:10.1016/j.est.2023.109927

147. Liu Sh, Chen Y, P.-K. Dorsel P, et al. Facile preparation of nanocellulose/multi-walled carbon nanotube/polyaniline composite aerogel electrodes with high area-specific capacitance for supercapacitors. *International Journal of Biological Macromolecules.* 2023;238:124158. DOI:10.1016/j.ijbiomac.2023.124158

148. Lee KS, Park ChW, Phiri I, et al. New design for Polyaniline@Multiwalled carbon nanotubes composites with bacteria doping for supercapacitor electrodes. *Polymer*. 2020;210:123014. DOI:10.1016/j.polymer.2020.123014

149. Yu T, Zhu P, Xiong Y, et al. Synthesis of microspherical polyaniline/graphene composites and their application in supercapacitors. *Electrochimica Acta*. 2016;222:12-19. DOI:10.1016/j.electacta.2016.11.033

150. Zhang Y, Si L, Zhou B, et al. Synthesis of novel graphene oxide/pristine graphene/polyaniline ternary composites and application to supercapacitor. *Chemical Engineering Journal*. 2016;288:689-700. DOI:10.1016/j.cej.2015.12.058

151. Shao F, Niu Y, Li B, et al. Binary nanosheet frameworks of graphene/polyaniline composite for high-areal flexible supercapacitors. *Materials Chemistry and Physics.* 2021;273:125128. DOI:10.1016/j.matchemphys.2021.125128

152. Li B, Li Z, Zhang L, et al. Facile synthesis of polyaniline nanofibers/porous carbon microspheres composite for high performance supercapacitors. *Journal of the Taiwan Institute of Chemical Engineers*. 2017;81:465-471. DOI:10.1016/j.jtice.2017.08.009

153. Zhou J, Sun Y, Zhou Ch, et al. Polyaniline/carbon hybrids: Synthesis and application for alizarin red S removal from water. *Colloids and Surfaces A: Physicochemical and Engineering Aspects*. 2023;676(A):132204. DOI:10.1016/j.colsurfa.2023.132204

154. Ansari MO, Kumar R, Ansari SA, et al. Anion selective pTSA doped polyaniline@graphene oxide-multiwalled carbon nanotube composite for Cr(VI) and Congo red adsorption. *Journal of Colloid and Interface Science.* 2017;496:407-415. DOI:10.1016/j.jcis.2017.02.034

155. Al-Hamry A, Lu T, Bai J, et al. Versatile sensing capabilities of layer-by-layer deposited polyaniline-reduced graphene oxide composite-based sensors. *Sensors and Actuators B: Chemical*. 2023;390:133988. DOI:10.1016/j.snb.2023.133988

156. Aghamiri ZS, Mohsennia M, Rafiee-Pour H-A. Fabrication and characterization of cytochrome c-immobilized polyaniline/multi-walled carbon nanotube composite thin film layers for biosensor applications. *Thin Solid Films*. 2018;660:484-492. DOI:10.1016/j.tsf.2018.06.055

157. Gautam V, Singh KP, Yadav VL. Polyaniline/multiwall carbon nanotubes/starch nanocomposite material and hemoglobin modified carbon paste electrode for hydrogen peroxide and glucose biosensing. *International Journal of Biological Macromolecules*. 2018;111:1124-1132. DOI:10.1016/j.ijbiomac.2018.01.094

158. Shao Y, Dong Y, Bin L, et al. Application of gold nanoparticles/polyaniline-multi-walled carbon nanotubes modified screen-printed carbon electrode for electrochemical sensing of zinc, lead, and copper. *Microchemical Journal*. 2021;170:106726. DOI:10.1016/j.microc.2021.106726

159. Pontes K, Soares BG. Segregated structure of poly (vinylidene fluoride-co-hexafluoropropylene) composites loaded with polyaniline@carbon nanotube hybrids with enhanced microwave absorbing properties. *Synthetic Metals*. 2022;288:117096. DOI:10.1016/j.synthmet.2022.117096

160. Ebrahim S, El-Raey R, Hefnawy A, et al. Electrochemical sensor based on polyanilinenanofibers/single wall carbon nanotubes composite for detection of malathion. *Synthetic Metals*. 2014;190:13-19. DOI:10.1016/j.synthmet.2014.01.021

161. Dhawan SK, Singh N, Rodrigues D. Electromagnetic shielding behaviour of conducting polyaniline composites. *Science and Technology of*

Advanced Materials. 2003;4(2):105-113. DOI:10.1016/S1468-6996(02)00053-0

162. Batool K, Rani M, Osman SM, et al. High electrochemical capacity of novel ternary graphene oxide based PANI/Co_3O_4 nanocomposite as supercapacitor electrode material. *Diamond and Related Materials*. 2024;143:110904. DOI:10.1016/j.diamond.2024.110904

163. Mahato N, Faisal M, Sreekanth TVM, et al. In-situ engineered polycrystalline phases in polyaniline-multiwalled carbon nanotubes composite exhibiting unique mechanism of charge storage. *Materials Letters*. 2023;350:134867. DOI:10.1016/j.matlet.2023.134867

164. Liu S, Chen Y, Dorsel P-KP, et al. Facile preparation of nanocellulose/multi-walled carbon nanotube/polyaniline composite aerogel electrodes with high area-specific capacitance for supercapacitors. *International Journal of Biological Macromolecules*. 2023;238:124158. DOI:10.1016/j.ijbiomac.2023.124158

165. Anukul KTh, Deshmukh AB, Choudhary RB, et al. Facile synthesis and electrochemical evaluation of PANI/CNT/MoS_2 ternary composite as an electrode material for high performance supercapacitor. *Materials Science and Engineering: B*. 2017;223:24-34. DOI:10.1016/j.mseb.2017.05.001

166. Rahman MdM, Shawon MR, Rahman MdH, et al. Synthesis of polyaniline-graphene oxide based ternary nanocomposite for supercapacitor application. *Journal of Energy Storage*. 2023;67:107615. DOI:10.1016/j.est.2023.107615

167. Singu BS, Male U, Srinivasan P, et al. Preparation and performance of polyaniline–multiwall carbon nanotubes–titanium dioxide ternary composite electrode material for supercapacitors. *Journal of Industrial and Engineering Chemistry*. 2017;49:82-87. DOI:10.1016/j.jiec.2017.01.010

168. Thomas L, Pete S, Chaitra K, et al. Facile synthesis of PANI-MWCNT-$Ni(OH)_2$ ternary composites and study of their performance as electrode material for supercapacitors. *Diamond and Related Materials*. 2020;106:107853. DOI:10.1016/j.diamond.2020.107853

169. Zaghloul MMY, Ebrahim Sh, Anas M, et al. Synthesis and characterization of nanocomposites of polyaniline and polyindole with multiwalled carbon nanotubes for high performance supercapacitor electrodes. *Electrochimica Acta*. 2024;475:143631. DOI:10.1016/j.electacta.2023.143631

170. Lu X, Dou H, Yang S, et al. Fabrication and electrochemical capacitance of hierarchical graphene/polyaniline/carbon nanotube ternary composite film. *Electrochimica Acta*. 2011;56(25):9224-9232. DOI:10.1016/j.electacta.2011.07.142

171. Mezgebe MM, Yan Zh, Wei G, et al. 3D graphene-Fe_3O_4-polyaniline, a novel ternary composite for supercapacitor electrodes with improved electrochemical properties. *Materials Today Energy*. 2017;5:164-172. DOI:10.1016/j.mtener.2017.06.007

172. Huang Ch, Hao Ch, Zheng W, et al. Synthesis of polyaniline/nickel oxide/sulfonated graphene ternary composite for all-solid-state asymmetric supercapacitor. *Applied Surface Science*. 2020;505:144589. DOI:10.1016/j.apsusc.2019.144589

173. Hao M, Chen Y, Xiong W, et al. Coherent polyaniline/graphene oxides/multi-walled carbon nanotubes ternary composites for asymmetric supercapacitors. *Electrochimica Acta*. 2016;191:165-172. DOI:10.1016/j.electacta.2016.01.076

174. Verma S, Das T, Pandey VK, et al. Nanoarchitectonics of GO/PANI/$CoFe_2O_4$ (Graphene Oxide/polyaniline/Cobalt Ferrite) based hybrid composite and its use in fabricating symmetric supercapacitor devices. *Journal of Molecular Structure*. 2022;1266:133515. DOI:10.1016/j.molstruc.2022.133515

175. Muhammad Z, Rukhsar A, Sabahat S, et al. Polyaniline-based nanocomposites for electromagnetic interference shielding applications: A review. *Journal of Thermoplastic Composite Materials*. 2021;36(4):089270572110224. DOI:10.1177/08927057211022408

176. Hanifah N, Subadra ST. UI, Hidayat Nl, et al. A novel Fe_3O_4/ZnO/PANI/rGO nanohybrid material for radar wave absorbing. *Materials Chemistry and Physics*. 2024;317:129169. DOI:10.1016/j.matchemphys.2024.129169

177. Souto LFC, Soares BG. Electromagnetic wave absorption, EMI shielding effectiveness and electrical properties of ethylene – vinyl Acetate (EVA)/ Polyaniline (PANI) blends prepared by in situ polymerization. *Synthetic Metals*. 2023;298:117441. DOI:10.1016/j.synthmet.2023.117441

178. Xie Zh, Chen H, Xie M, et al. Electrical percolation networks of MWCNT/Graphene/Polyaniline nanocomposites with enhanced electromagnetic interference shielding efficiency. *Applied Surface Science*. 2024;655(51):159613. DOI:10.1016/j.apsusc.2024.159613

179. Goswami RN, Mourya P, Saini R, et al. Polyaniline-wrapped nitrogen-doped graphene nanocomposites as protective functional fillers in epoxy coatings for remarkable enhancement of corrosion inhibition performance. *Progress in Organic Coatings*. 2024;189:108335. DOI:10.1016/j.porgcoat.2024.108335

180. Kang Y, Wang C, Chen C. Preparation of 2D leaf-shaped and 3D flower-shaped sandwich-like polyaniline nanocomposites and application on anticorrosion. *Journal of Applied Polymer Science.* 2020;138(4):49729. DOI:10.1002/app.49729

181. Yuan T, Zhang ZH, Li J, et al. Corrosion protection of aluminum alloy by epoxy coatings containing polyaniline modified graphene additives. *Materials and Corrosion.* 2019;70:1298-1305. DOI:10.1002/maco.201810549

182. Raj GK, Singh E, Hani U, et al. Conductive polymers and composites-based systems: An incipient stride in drug delivery and therapeutics realm. *Journal of Controlled Release*. 2023;355:709-729. DOI:10.1016/j.jconrel.2023.02.017

183. Liu R, Li A, Lang Y, et al. Stimuli-responsive polymer microneedles: A rising transdermal drug delivery system and Its applications in biomedical. *Journal of Drug*

Delivery Science and Technology. 2023;88:104922. DOI:10.1016/j.jddst.2023.104922

184. Jose A, Bansal M, Svirskis D, et al. Synthesis and characterization of antimicrobial colloidal polyanilines. *Colloids and Surfaces B: Biointerfaces*. 2024;238:113912. DOI:10.1016/j.colsurfb.2024.113912

185. Sun S, Xu Y, Maimaitiyiming X. 3D printed carbon nanotube/polyaniline/gelatin flexible NH_3, stress, strain, temperature. *Reactive and Functional Polymers.* 2023;190(11):105625. DOI:10.1016/j.reactfunctpolym. 2023.105625

186. Wu G, Du H, Cha YL, et al. A wearable mask sensor based on polyaniline/CNT nanocomposites for monitoring ammonia gas and human breathing. *Sensors and Actuators B: Chemical*. 2023;375:132858. DOI:10.1016/j.snb.2022.132858.

187. Matindoust S, Farzi A, Nejad MB, et al. Ammonia gas sensor based on flexible polyaniline films for rapid detection of spoilage in protein-rich foods. *Journal of Materials Science: Materials in Electronics*. 2017;28(11):7760-7768. DOI:10.1007/s10854-017-6471-z

188. Pegu B, Konwar M, Sarma D, et al. Cu nanoparticle anchored highly conducting, reusable multifunctional *r*GO/PANI nanocomposite: A novel material for methanol sensor and a catalyst for click reaction. *Synthetic Metals*. 2024;301:117516. DOI:10.1016/j.synthmet.2023.117516

189. Sahoo S, Sahoo PK, Sharma A, et al. Interfacial polymerized RGO/$MnFe_2O_4$/polyaniline fibrous nanocomposite supported glassy carbon electrode for selective and ultrasensitive detection of nitrite. *Sensors and Actuators B: Chemical*. 2020;309:127763-127763. DOI:10.1016/j.snb.2020.127763

190. Jiang Sh, Zhang H, Li Zh, et al. High-sensitivity integrated detector with nanostructured hydrogel electrode for ascorbic acid determination. *Microchemical Journal*. 2023;189:108510. DOI:10.1016/j.microc.2023.108510

191. Morais JPL, Bernardino DV, Batista BdaS, et al. Conductive polymer blend based on polyaniline and galactomannan: Optical and electrical properties. *Synthetic Metals*. 2023;295:117346. DOI:10.1016/j.synthmet.2023. 117346

192. Chajanovsky I, Cohen S, Muthukumar D, et al. Enhancement of integrated nano-sensor performance comprised of electrospun PANI/carbonaceous material fibers for phenolic detection in aqueous solutions. *Water Research*. 2023;246:120709. DOI:1016/j.watres.2023. 120709

193. Virutkar PD, Mahajan AP, Meshram BH, et al. Conductive polymer nanocomposite enzyme immobilized biosensor for pesticide detection. *Journal of Materials NanoScience*. 2019;6(1):7-12.

194. Gautam V, Singh KP, Yadav VL. Polyaniline/MWCNTs/starch modified carbon paste electrode for non-enzymatic detection of cholesterol: application to real sample (cow milk). *Analytical and Bioanalytical Chemistry*. 2018;410:2173-2181. DOI:10.1007/s00216-018-0880-6

195. Hassan Z, Alsalhi SA, Drissi N, et al. Graphene nanoplatelets-polyaniline composite for the detection of cortisol. *Journal of Physics and Chemistry of Solids*. 2024;191:112031.DOI:10.1016/j.jpcs.2024.112031

196. Charekhah R, Jarrahi Z, Darabi M, et al. Bulk heterojunction solar cells based on polyaniline/multi wall carbon nanotube: from morphology control to cell efficiency. *Journal of Materials Science: Materials in Electronics.* 2019;30:26–36. DOI:10.1007/s10854-018-0169-8

197. Yazdi M, Saeidi H, Zarrintaj P, et al. PANI-CNT nanocomposites. In: Mozafari M, Chauhan N. (eds.) *Fundamentals and Emerging Applications of Polyaniline*. Elsevier; 2019. p. 143-163. DOI:10.1016/B978-0-12-817915-4.00009-9

198. Dawo Ch, Iyer PK, Chaturvedi H. Carbon nanotubes/PANI composite as an efficient counter electrode material for dye sensitized solar cell. *Materials Science and Engineering: B*. 2023;297:116722. DOI:10.1016/j.mseb.2023.116722

199. Maponya TC, Hato MJ, Somo TR, et al. Polyaniline-based nanocomposites for environmental remediation. In: *Trace metals in the environment – new approaches and recent advances*. IntechOpen; 2021. DOI:10.5772/intechopen.82384

200. Mondal S, Rana U, Das P, et al. Network of polyaniline nanotubes for wastewater treatment and oil/water separation. *ACS Applied Polymer Materials*. 2019;1(7):1624-1633. DOI:10.1021/acsapm.9b00199

201. Kumar A, Kumar V, Awasthi K. Polyaniline–carbon nanotube composites: preparation methods, properties, and applications. *Polymer-Plastics Technology and Engineering*. 2018;57:70-97. DOI:10.1080/03602559. 2017.1300817

202. Samadi A, Xie M, Li J, et al. Polyaniline-based adsorbents for aqueous pollutants removal: A review. *Chemical Engineering Journal*. 2021;418:129425. DOI:10.1016/j.cej.2021.129425

203. Dyachkova TP, Melezhyk AV, Morozova ZhG, et al. The study of absorption of copper and nickel ions by polyaniline and its nanocomposite with carbon nanotubes. *Vestnik Tambovskogo gosudarstvennogo tekhnicheskogo universiteta.* 2012;18(4):1067-1073. (In Russ.)

204. Dyachkova TP, Anosova IV, Galunin EV, et al. Synthesis of composites based on polyaniline-modified dispersed nanocarbon supports and prospects of their application as sorbents. *Nano Hybrids and Composites*. 2017;13:135-141. DOI:10.4028/www.scientific.net/ NHC.13.135

205. Wai MA, Marchenko MV, Troshkina ID, et al. Scandium adsorption from sulfuric-chloride solutions by PANI/CNTs Nanocomposite. *Advanced Materials and Technologies*. 2019;4(16):58-65. DOI:10.17277/amt.2019. 04.pp.058-065

206. Dayyoub T, Maksimkin AV, Kaloshkin S, et al. The structure and mechanical properties of the uhmwpe films modified by the mixture of graphene nanoplates with

polyaniline. *Polymers*. 2019;11(1):23. DOI:10.3390/polym11010023

207. Dyachkova T, Gutnik I, Nagdaev V, et al. Studying the surface of UHMWPE films modified with graphene nanoplatelets using a Raman mapping method. *Fullerenes, Nanotubes and Carbon Nanostructures*. 2020;28(7):561-564. DOI:10.1080/1536383X.2020.1724103

Information about the authors / Информация об авторах

Irina V. Gutnik, Cand. Sc. (Eng.), Associate Professor, Tambov State Technical University (TSTU), Tambov, Russian Federation; ORCID 0000-0003-1236-7187; e-mail: i.v.gutnik@yandex.ru

Tatyana P. Dyachkova, D. Sc. (Chem.), Professor, TSTU, Tambov, Russian Federation; ORCID 0000-0002-4884-5171; e-mail: dyachkova_tp@mail.ru

Elena A. Burakova, D. Sc. (Eng.), Associate Professor, TSTU, Tambov, Russian Federation; ORCID 0000-0001-8927-7433; e-mail: elenburakova@yandex.ru

Evgeniy N. Tugolukov, D. Sc. (Eng.) Professor, TSTU, Tambov, Russian Federation; ORCID 0000-0003-1766-3786; e-mail: tugolukov.en@mail.ru

Artem V. Rukhov, D. Sc. (Eng.), Head of the Department "Chemistry and Chemical Technologies", TSTU, Tambov, Russian Federation; ORCID 0000-0001-9194-8099; e-mail: artem1@inbox.ru

Georgiy A. Titov, Student, TSTU, Tambov, Russian Federation; ORCID 0000-0002-3930-0559; e-mail: bombercd1@mail.ru

Гутник Ирина Владимировна, кандидат технических наук, доцент, Тамбовский государственный технический университет (ТГТУ), Тамбов, Российская Федерация; ORCID 0000-0003-1236-7187; e-mail: i.v.gutnik@yandex.ru

Дьячкова Татьяна Петровна, доктор химических наук, профессор, ТГТУ, Тамбов, Тамбов, Российская Федерация; ORCID 0000-0002-4884-5171; e-mail: dyachkova_tp@mail.ru

Буракова Елена Анатольевна, доктор технических наук, доцент, ТГТУ, Тамбов, Российская Федерация; ORCID 0000-0001-8927-7433; e-mail: elenaburakova@yandex.ru

Туголуков Евгений Николаевич, доктор технических наук, профессор, ТГТУ, Тамбов, Российская Федерация; ORCID 0000-0003-1766-3786; e-mail: tugolukov.en@mail.ru

Рухов Артем Викторович, доктор технических наук, профессор, заведующий кафедрой, ТГТУ, Тамбов, Российская Федерация; ORCID 0000-0001-9194-8099; e-mail: artem1@inbox.ru

Титов Георгий Анатольевич, студент, ТГТУ, Тамбов, Российская Федерация; ORCID 0000-0002-3930-0559; e-mail: bombercd1@mail.ru

Received 30 April 2024; Accepted 27 May 2024; Published 04 July 2024

Территория распространения – Российская Федерация, зарубежные страны
Distributed is the Russian Federation and foreign countries

Computer layout: Olga V. Mochalina, TSTU, Tambov, Russian Federation
Компьютерный дизайн и верстка: Мочалина О. В., ТГТУ, Тамбов, Россия

Оригинал-макет подготовлен в Издательском центре ФГБОУ ВО «ТГТУ»,
392032, Тамбовская обл., г. Тамбов, ул. Мичуринская, д. 112А

Подписано в печать 28.06.2024. Дата выхода в свет 04.07.2024.
Формат 60×90/8. Усл. печ. л. 9,38. Уч.-изд. л. 9,75. Тираж 100 экз. Цена свободная. Заказ № 018.
СМИ журнал "Journal of Advanced Materials and Technologies"
(Журнал современных материалов и технологий) выпуск 2024. Том 9, № 2